HEAT TRANSFER ANALYSIS OF COMPONENTS OF CONSTRUCTION EXPOSED TO FIRE

- A THEORETICAL, NUMERICAL AND EXPERIMENTAL APPROACH

A Thesis submitted for

The Degree of Doctor of Philosophy

by

HONG-BO WANG, *MSc, BEng*

Department of Civil Engineering and Construction
University of Salford
Manchester, M5 4WT
England

April, 1995

TABLE OF CONTENTS PAGE

TABLE OF CONTENTS i
ACKNOWLEDGMENT iv
DECLARATION v
ABSTRACT vi

CHAPTER 1: INTRODUCTION

1.1 General Introduction 1
1.2 Scope and Contents 5

CHAPTER 2: FINITE DIFFERENCE MODELLING OF A PANEL

2.1 The Governing Equation 10
2.2 Explicit Formulation of FDM for a Multi-layer Panel 12
2.3 Unexposed Side Heat Transfer Coefficient 18
2.4 Fire Boundary Conditions 21

CHAPTER 3: FINITE DIFFERENCE MODELLING OF A PIPE

3.1 1-D Formulation of FDM for a Multi-layer Pipe 27
3.2 2-D Formulation of FDM for a Multi-layer Pipe 31
3.3 Internal Heat Exchange 34

CHAPTER 4: MODELS FOR POLYMER COMPOSITES AND INTUMESCENT COATINGS

4.1 Introduction 39

4.2	Model for WR Glass Polyester Laminate	43
4.3	Special Treatment for WR Phenolic Laminate	50
4.4	Model to Predict the Thermal Response of GRP Pipes	55
4.5	Model for Intumescent Coatings	60

CHAPTER 5: EFFECTS OF INTRINSIC PROPERTIES OF MATERIALS

5.1	Conventional Thermal Properties	65
5.2	Effects of Moisture Content	69
5.3	Kinetic Parameters for Pyrolysis	78

CHAPTER 6. FIRE TEST RESULTS AND THE VERIFICATION OF NUMERICAL MODELLING

6.1	'Traditional' Fire Resistant Panels	89
6.2	WR Glass-Fibre Reinforced Polyester Laminates	95
6.3	WR Glass-Fibre Reinforced Phenolic Laminates	101
6.4	Glass-Reinforced Plastic Pipes	103
6.5	GRP Pipes with Intumescent Coatings	105
6.6	Conclusions	107

CHAPTER 7: COMPUTER PROGRAM DEVELOPMENT FOR FDM 124

CHAPTER 8. HEAT TRANSFER CALCULATION USING FEM

8.1	Introduction	128
8.2	Finite Element Computer Program Development	129
8.3	Composite Concrete/Steel Deck Slab Exposed to Fire	130
8.3.1	Boundary Conditions	132

8.3.2 Moisture Effects 134
8.3.3 Thermal Properties of Materials 136
8.4 Numerical Results and Comparisons 137

CHAPTER 9. EXPERIMENTAL AND COMPUTATIONAL APPROACHES 148

9.1 Fire Resistance Tests 149
9.2 Computational Approach 152

CHAPTER 10: SUMMARY AND CONCLUSIONS

10.1 Present Study 156
10.2 Future Development 164

LIST OF MAIN REFERENCES 168

SUPPLEMENT: DESCRIPTION OF THE FIRE TEST FACILITIES AND PROCEDURES 176

ACKNOWLEDGMENT

The author wishes to express his grateful thanks to Professor John M. Davies, for his supervision, guidance and encouragement throughout the period of study, also for the review of this thesis.

Sincere thanks are due to Dr. John McNicholas and Dr. Raheef Hakmi for their helpful advice and support.

Acknowledgement is made to the multi-sponsor research programme on "The Cost Effective Use of Fibre-Reinforced Composites Offshore", which is supported by the UK Marine Technology Directorate Ltd, EPSRC and a consortium of companies, for their financial support. These industrial sponsors are: Admiralty Research Establishment, AGIP(UK), Amerada Hess, Ameron bv, Amoco Research, Balmoral Group, Bow Valley Petroleum, BP Exploration, BP Research, Brasoil, British Gas, Ciba-Geigy, Conoco, Defence Research Agency, Dow Rheinmunster, Elf(Aquitaine), Elf(UK), Enichem(SPA), Exxon, Fibreforce Composites, Hunting Engineering Ltd, Kerr McGee Oil(UK) Ltd, MaTSU, Marine Technology Directorate Ltd, Mobil Research and Development, Mobil North Sea Ltd, Norsk Hydro, UK Ministry of Defence(Navy), UK Offshore Supplies Office, Phillips Petroleum, Shell Expro, Statoil, Total Oil Marine, UK Department of Energy, VSEL and Vosper Thornycroft.

Also the author wishes to express his thanks to those members of the technical staff of the Department of Civil Engineering and Construction for their assistance in the preparation of experimental work.

DECLARATION

None of the material contained in this thesis has been submitted in support of an application for another degree or qualification of this or any other university or institution of learning.

Hong-Bo Wang

April 1995

ABSTRACT

This thesis describes a theoretical, numerical and experimental heat transfer study of components of construction exposed to fire.

Within the computational aspects of the work, one and two-dimensional finite difference and finite element methods have been developed to determine the transient temperature distributions in the cross-section of elements of construction subject to furnace fire tests. Either Cartesian or cylindrical polar coordinates can be used in order to conform to the shape of the element to be analyzed. The convective and radiative heat transfer boundary conditions at the exposed and unexposed sides of components can be simulated. Structures may comprise several materials each having thermal properties varying with temperature. They could be made of traditional construction materials, for example steel, concrete, plasterboard, or novel fire-resistant composite materials, for instance Glass-Reinforced Plastics (GRP) or intumescent coatings. The critical role of the thermal properties of materials with respect to the heat transfer rate was reviewed and the factors which significantly affect the heat transmission, such as the moisture content in hygroscopic materials and the decomposition of plastic matrices, have been investigated in considerable detail.

A large number of experimental furnace tests have been conducted in order to

reveal the fire-resistant performance of various materials and to verify the numerical modelling. Both the standard cellulosic and hydrocarbon time/temperature regimes have been used to simulate cellulosic and hydrocarbon fires. The comparison between the computational simulation and experimental measurements is generally excellent. In addition, a number of user-friendly, interactive computer programmes have been developed which may be used to predict the behaviour of building elements exposed to a specified fire environment.

The general issues and relevant problems associated with the experimental and computational approaches to fire safety design are discussed. Some recommendations for the further improvement of the existing fire resistance standards are proposed and further required research in the subject areas are identified.

CHAPTER 1

Introduction

1.1 General Introduction

Once human beings had learned how to create a fire, the struggle to control and fight it was started. Unexpected and uncontrolled fire can hazard our communities in a savage and extensive way, both in terms of its harm to life and its economic impact. Fire can cause fatalities and injuries, property damage, and both direct and indirect losses from fire. Design of the structure against fire attack is therefore of paramount importance in engineering practice. It demands increasing attention as the activities of humankind expand to more harsh circumstances, for example, the creation of offshore oil fields and the exploration of outer space.

There are currently two basic ways for fire fighting: active and passive measures. Active fire fighting is commonly provided by automatic detectors, water sprinklers, deluges and sprays, and the use of fire suppressive foam and gas. Although it is quite efficient in some situations, active fire fighting systems cannot be relied upon fully because the active system could be destroyed by fire or explosion. In addition to the above active measures, passive fire protection is now being increasingly used as the primary element of the overall safety strategy to minimise

the consequences of a fire. Passive fire resistance can be achieved either by the structure itself, or by a cladding, coating or free-standing system that provides fire protection and impedes the spread of fire. The choice between active and passive systems (or their combination), will be influenced by the protection philosophy, the anticipated fire type and duration, the equipment or structure requiring protection, and the time required for evacuation. In some applications, the use of passive fire protection alone will be cost-effective, and in other cases, a minimal residual protection must be provided in case the active systems fail to operate. Since structural engineering design is mainly concerned with passive fire protection, in this thesis, the computational and experimental heat transfer studies were solely concerned with the fire resistance of construction. There is no consideration of active fire fighting.

It is well known that a high temperature caused by fire can lead to the loss of strength and stability of a structure to the extent that structural collapse is possible. Between temperatures of 450°C and 750°C, most structural elements will lose their load-bearing capacity. Furthermore, this is not the only perilous hazard which may be caused by fire. Other potential problems include smoke, toxic gas and heat release, and even possible explosion. Therefore, evaluating the thermal response of structures during fire in order to minimize the hazard is of considerable concern for safety and reliability assessments in both onshore and offshore industries.

Conventionally, the building codes and regulations in the UK and internationally have relied on standardized test procedures[1.1,1.2] to specify fire resistance requirements. The regulations require that, depending upon their use, building

components or structures should conform to given standards of fire safety. The term 'fire resistance' is associated with the ability of an element of building construction to withstand exposure to a standard temperature-time and pressure regime without loss of its fire separating function or loadbearing function or both for a given time (as defined in BS 476:part 20 [1.1]). In general they involve placing a prototype element in a furnace (under load, if appropriate) and subjecting it to a heat onslaught, such that temperatures recorded by thermocouples placed in specific locations within the furnace follow a specified temperature-time relationship through control of the rate of fuel supply (gas or oil). The heat flux usually is not directly measured in such tests. This fire testing concept was first introduced in 1916, based on the observations of the temperatures of wood fires used in early *ad hoc* testing [1.3,1.4].

However, the determination of the fire resistance of a component of construction is a complicated process because of the many variables involved. These variables include fire growth and duration, temperature distributions in the components, alterations in material properties, interaction between the building elements, and the influence of mechanical loads on the structural system. Thus, although the standard test method provides a reasonably simple solution to an otherwise complex problem, its outcome can not be generalized and utilized effectively when there is a lack of an appropriate analytical tool. Furthermore, the design procedure usually involves a process of iterative redesign and testing, and the full-scale test which is required by the standards is extremely costly and time-consuming.

With the rapid increase in computer power and technology, many designers and

product developers look towards computer modelling as an economic method to supplement fire testing as a means of performance verification. Based on heat flow studies and structural analysis, and on the knowledge of the behaviour of materials at elevated temperatures, the computer-generated approach may provide the engineer with a solution of considerable practical value. The development of computational techniques in fire safety engineering has previously been somewhat ignored, but the general level of awareness in the area of numerical modelling is growing. An increasing demand has emerged for better predictive techniques based on sophisticated analysis to determine the fire resistance of the components of construction, especially those incorporating novel composite materials. Currently, non-linear structural analysis techniques are increasingly allowing engineers to predict the structural performance under a given set of time-varying temperature and mechanical loads. This will enable the most sensitive members to be identified. However, if the design is not to be over-conservative, it is necessary to be able to forecast the temperature distribution in all structural members with a reasonable accuracy.

The major part of the current information on the performance of passive fire protection materials and systems has been derived from standard fire tests. Faced with this situation, there has been ongoing research with the aim of analyzing the behaviour of elements of construction in fire by studying their fire resistance in the standard furnace tests and developing adequate techniques for interpolation and extrapolation. As understanding increases, a natural progression is the development of analytical procedures for the optimal design of construction elements to provide a specified fire resistance. This is the main objective of this study.

As a number of issues are investigated in this thesis, the summary of previous research work will not be presented here. Instead, the state of the art will be outlined in each related chapter.

1.2 Scope and Contents

The exposure of a component of construction to transient heating conditions in a furnace results in the exposed surfaces receiving heat at increasing rates by radiation supplemented by convective heat transfer. The increase in the surface temperature of the components causes heat to flow to the interior and leads to physical and chemical changes in the material. Organic materials such as wood and GRP might burn, materials with a low softening temperature melt and others may suffer some physical disruptions; most will be distorted and almost all undergo a reduction in strength. Even for a fire protected structure, the structure will eventually heat up to temperatures which lead to a serious loss in stability.

As specified above, the performance of building components under fire conditions has a critical safety implication. Research and development work continue with the aim of providing the fire engineer with a design tool for obtaining a prescribed level of fire safety based on heat transfer principles. Heat transfer is concerned with the physical processes underlying the transport of thermal energy due to a temperature difference or gradient. The objective of heat transfer analysis in this thesis ~~is~~ was then focused on the determination of the

temperature distribution history within a component of construction exposed to a hostile fire environment. All three distinct heat transfer modes, conduction, convection, and radiation, were given full consideration. Based on the transient temperature profile, other information such as the internal heat flow, thermal expansion/contraction, thermal stresses and potential damage to unexposed portions can be estimated.

A nonlinear transient equation which governs the heat transmission must be solved in order to predict the temperature profile in a component of construction. Since closed solutions for such equation exist only for very simple cases, numerical approaches that incorporate either the Finite Difference Method (FDM) or Finite Element Method (FEM) have generally been employed to address heat transfer problems. It is believed that FEM has advantages when dealing with complex geometry and loading but its formulae and programming are more complicated. The formulae for FDM are relatively simple, and the execution of FDM programmes is rapid. As the configurations of components under investigation are not so complicated, the finite difference method is applied in the main part of this thesis. Nevertheless, a two-dimensional finite element model is also developed.

The materials considered encompass various currently used construction materials and insulation materials, such as concrete, mineral wool, plasterboard, GRP and intumescent coatings. These inorganic and organic materials display diverse behaviour under fire conditions. For example, the heat transfer rate in a hygroscopic material will be influenced significantly by moisture evaporation, while for combustible polymeric material, the rate of decomposition will be crucial.

One or two-dimensional Cartesian or Polar coordinates were used to accommodate various configurations of components. Whereas the thermal response and mechanical behaviour of structures subject to a heating process may be interrelated, this coupling has been neglected in this stage. Initially, it is the accuracy of the thermal modelling which normally presents the major problem.

The finite difference formulation for a multi-layer panel system is derived in Chapter 2. The modelling of the boundary conditions on the unexposed and exposed sides due to radiative and convective heat exchange are established.

In Chapter 3, the one and two-dimensional finite difference equations for multi-layer pipe systems are formulated. The internal heat transfer coefficient is calculated for the case of a pipe filled with flowing fluid. For two-dimensional problems, the formulae for heat exchange in the inside of an empty pipe are also outlined.

The use of polymeric materials in building or construction is steadily increasing. As a consequence, the potential for these materials to be exposed to fire is also increased. Because plastic materials are organic in nature and are inherently combustible, they will decompose or burn in a fire environment. Unfortunately, our knowledge of conduction theory, both theoretical and empirical, is very limited when material decomposition is present. There is, therefore, the necessity for a further understanding of the potential fire hazards and fire behaviour under these circumstances. Chapter 4 provides several extended models for decomposing, expanding glass-fibre reinforced plastic laminates and pipes, and intumescent coatings respectively.

The decisive role of the thermal properties of material relating to the heat transfer rate is reviewed in Chapter 5. These include the conventional thermal properties, moisture content and kinetic parameters of decomposition. Those values which were used in the numerical calculations are enumerated. The significant influence of moisture content on heat transfer is investigated and a new model is developed.

The experimental verification of the FD formulations and the modelling of the fire boundary conditions, moisture effects and decomposition are presented in Chapter 6. In order to reduce the cost and time, a model-scale technique is used. The specimens include traditional construction panels, sandwich panels, GRP laminates, GRP pipes, and GRP pipes with intumescent coatings. Their performances under standard fire tests are obtained and experimental and theoretical results are compared.

Chapter 7 presents a description of the development of user-friendly, interactive computer programmes. The functions and capabilities of these fire-dedicated programmes are also illustrated.

Another powerful and popular numerical method, finite element analysis, is exploited for two dimensional problems in Chapter 8. An excellent agreement is obtained between the computational results and test results on representative examples.

Chapter 9 is devoted to a discussion of the general issues and relevant problems associated with experimental and computational approaches to fire resistant

design. The main aim is to assure the fire safety at a reasonable cost.

The summary and conclusions of thesis are given in Chapter 10. Some recommendations for further investigation are proposed, and the requirements in the subject areas for further research are also identified.

CHAPTER 2

Finite Difference Modelling of a Panel

2.1 The Governing Equation

In order to evaluate the fire resistance performance of a component of construction, it is necessary to know the temperature history of the component during exposure to fire. The natural starting-point for discussion about temperature distribution calculation in a structure is Fourier's Partial Differential Equation for heat flow by conduction. The general unsteady-state equation governing heat conduction in Cartesian coordinates is[2.1]:

$$\rho C_p \frac{\partial T}{\partial t} = \frac{\partial}{\partial x}\left(k(T)\frac{\partial T}{\partial x}\right) + \frac{\partial}{\partial y}\left(k(T)\frac{\partial T}{\partial y}\right) + \frac{\partial}{\partial z}\left(k(T)\frac{\partial T}{\partial z}\right) \qquad (2.1)$$

where

$T(x,y,z,t)$ is temperature (°C);

$k(T)$ is temperature dependent conductivity(W/m°C);

ρ is density (kg/m^3);

Cp is specific heat (J/kg°C);

t is time (sec);

x,y,z are the Cartesian coordinates.

The right hand side of equation (2.1) represents the net heat conduction in a solid, while the left hand term represents the sensible energy accumulated. The materials are assumed to be homogeneous and isotropic. The study of conductive heat transfer is principally concerned with the solution of (2.1). As mentioned above, with complicated geometries and boundary conditions, the solution can be obtained only by an approximate numerical method.

The finite difference method is comparatively simple in conception and inherently suited to the approximate solution of heat conduction through sections subjected to a prescribed rate of heat impact. FDM replaces the derivatives in equation (2.1) with approximations in the form of finite-sized differences between values at particular locations. The following two approaches can be used[2.1] to transfer the governing partial differential equation into the corresponding finite difference equation:

a). Mathematical replacement technique

b). Physical energy balance technique

Both techniques will lead to the same algebraic finite difference equation (FDE) system when thermal conductivity is a linear function of temperature. The energy balance method is employed in this study since it is convenient and easy to apply, especially to variable grids and convective boundary conditions. This method considers a control cell for a particular time-step, and the temperature of the cell is calculated in the time-step by considering both the heat flow into and out of the cell. When this is based on the temperature of the adjacent cells in the last time-step, an explicit scheme is obtained. The change of temperature

of the point is then computed, based on the specific heat and mass of material in a particular cell:

$$\textit{Mass of control cell} \times \textit{Specific heat} \times \textit{Rate of change of node temperature} = \textit{Net heat flow to cell} \qquad (2.2)$$

2.2 Explicit Formulation of FDM for a Multi-layer Panel

The FDM approaches to heat transfer problems can be classed as either explicit or implicit methods. The implicit method has to solve a simultaneous system of algebraic equations at each time step, whilst the explicit method yields the temperature at a given time level directly from previously computed values. The explicit finite difference method provides an especially simple and effective procedure although it suffers from a restriction on the length of the time-step in order to maintain numerical stability. However, this does not cause significant problems in fire resistance analysis as a short time-step is necessary in order to model the very rapid temperature increase of the hot face during fire testing. Furthermore, a short time-step also results in an increase in accuracy when temperature-dependent properties are quasi-linearised.

If the thickness of the panel is small compared to the other dimensions, the problem is one-dimensional (ie the heat flow is perpendicular to the face except

near the edges). The one-dimensional transient governing equation of (2.1) is:

$$\rho C_p \frac{\partial T(x,t)}{\partial t} = \frac{\partial}{\partial x}(k(T)\frac{\partial T(x,t)}{\partial x}) \qquad (2.3)$$

where $0 \le x \le L$, *for* $t > 0$.

It is subject to the boundary conditions on x=0 or x=L for t>0:

$$T = T_g(t) \qquad (2.4)$$

where $T_g(t)$ is the known temperature on the boundary;

Or, if the boundary is losing heat to or gaining heat from an ambient temperature condition[2.1]:

$$k(T)\frac{\partial T}{\partial n} = h(T)(T_\infty - T) + FE\sigma[(T_\infty+273)^4 - (T+273)^4] \qquad (2.5)$$

where

T is the temperature(°C) on the boundary;

T_∞ is the ambient temperature(°C);

$h(T)$ is the surface heat transfer coefficient W/m^{2o}C which is dependent on the condition of problems and this will be discussed later;

F is a geometrical factor;

E is the emissivity;

σ is the Stefan-Boltzmann constant ($5.67 \times 10^{-8} W/M^2K^4$).

The formulation of (2.5) is obtained by the energy balance technique. The first term of (2.5) on the right hand side represents the convection and the second term represents the radiation.

The initial boundary condition is:

$$T = T_0(x) \qquad for\ t = 0 \quad in\ 0 \le x \le L \tag{2.6}$$

where T_0 is the known initial temperature distribution.

Transferring the partial differential equation to a finite difference equation(FDE) in both space and time domains by the energy balance technique results in the explicit FDE for a multi-layer panel. The reason for the consideration of multi-layer construction is that the use of passive fire protection normally leads to a sandwich structure. The advantages of sandwich construction include good fire insulation and corrosion resistance, weight reduction with increased strength and stiffness, substantial cost savings and the more efficient provision of increased safety and reliability.

Three typical FDEs need to be derived, one for the internal nodes on each material layer, one for interface nodes between the two material layers, and one for the boundary nodes. Perfect contact at the interface between two material layers is assumed.

(i) For a typical node m within one material layer:

$$T_m^{i+1} = F_o[\frac{2(k_{m-1,m}T_{m-1}^i + k_{m+1,m}T_{m+1}^i)}{k_{m-1,m}+k_{m+1,m}} + T_m^i(\frac{1}{F_o}-2)] \qquad (2.7)$$

where superscript i indicates the time level and F_o is Fourier number which defined by

$$F_o = \frac{(k_{m-1,m}+k_{m+1,m})\Delta t}{2\rho C_p(\Delta x)^2} \qquad (2.8)$$

To preserve the stability of calculation and in order not to violate thermodynamic principles, the coefficient $(1/F_o-2)$ in equation (2.7) should be greater than zero. Then F_o should be less than 0.5 and this provides a restriction on the time step Δt. The conductivity $k_{m-1,m}$ (and similarly $k_{m+1,m}$) is evaluated for each step as

$$k_{m-1,m} = k(\frac{T_{m-1}^i + T_m^i}{2}) \qquad (2.9)$$

(ii) For an interface node m between two material layers

$$T_m^{i+1} = F_0\ [\ \frac{2(k_1\Delta x_2 T_{m-1}^i + k_2\Delta x_1 T_{m+1}^i)}{k_1\Delta x_2 + k_2\Delta x_1} + T_m^i(\frac{1}{F_0}-2)\ ] \qquad (2.10)$$

where

$$F_0 = \frac{k_1\Delta x_2 + k_2\Delta x_1}{\Delta x_1\rho_1 C_{p1} + \Delta x_2\rho_2 C_{p2}} \times \frac{\Delta t}{\Delta x_1 \Delta x_2} \tag{2.11}$$

and subscripts 1,2 indicate the two materials respectively. This formula can be used for two material layers with different Δx.

(iii) For the boundary node, for instance node 1, when it corresponds to the boundary condition (2.5)

$$\begin{aligned} T_1^{i+1} = {} & 2F_o[T_2^i + \frac{h\Delta x}{K_1}T_\infty + (\frac{1}{2F_o} - 1 - \frac{h\Delta x}{k_1})T_1^i] \\ & + FE\sigma[(T_\infty + 273)^4 - (T_1^i + 273)^4]\frac{2\Delta t}{\rho C_p \Delta x} \end{aligned} \tag{2.12}$$

where

$$F_o = \frac{k_1\Delta t}{\rho C_p(\Delta x)^2} \tag{2.13}$$

The method is explicit as the temperature T at node m at a time step $i+1$ is immediately determined from equations (2.7), (2.10) and (2.12) when the temperature of node m and its neighbouring points at the previous time step i are available. The most critical stability criterion usually occurs in the FDEs for the boundary node, which requires the Fourier number F_o to be restricted by

$$F_o \leq 0.5[1+\frac{h\Delta x}{k_1}+\frac{FE\sigma\Delta x}{k_1}\cdot\frac{(T_1^i+273)^4}{T_1^i}]^{-1} \qquad (2.14)$$

In order to check the above treatment on the *temperature-dependant thermal* properties of material, a typical test problem is solved. It is a designed problem which has been used by some researchers to investigate an efficiency of numerical methods for the solution of nonlinear transient heat conduction problems[2.2,2.3]. The question is to find the temperature distribution along the thickness of a wall with temperature-dependent thermal conductivity. The wall is assumed to be 20cm long, 1cm high, and is initially at 100°C. The temperature of the surface of the left hand end is suddenly raised to 200°C and kept at this value for 10 second, after which it is decreased to 100°C again; the temperature of the surface of the right hand end is kept at 100°C, while the other surfaces are presumed to be insulated. The thermal conductivity is k = 2 + 0.01T W/cm°C and the specific heat capacity is ρC = 8 J/cm^3°C. Two available numerical results were given by the relatively complicated FEM or BEM (Boundary Element Methods) with an iteration process at each time step[2.2,2.3]. The time step for our finite difference analysis is 1 sec and the length of wall is divided by 21 nodes. A comparison of the results obtained using the three alternative numerical methods is shown in Table 2.1. The values in the table are temperature distributions in the wall at time t = 10 sec. The agreement between the results is very good. This demonstrates that, although the explicit FDM is a simple algorithm, it is also an effective method.

Table 2.1 Temperature distribution of the wall at time t = 10 s

x/(cm)	FEM	BEM	*FDM*
0	200.00	200.00	200.00
1	176.16	175.29	176.36
2	153.21	151.48	153.50
3	133.47	131.74	133.68
4	118.60	117.63	118.69
5	108.98	108.94	108.95
6	103.72	104.27	103.64
7	101.29	102.01	101.22
8	100.37	100.97	100.32
9	100.08	100.50	100.06
10	100.01	100.27	100.01

2.3 Unexposed Side Heat Transfer Coefficient

In a general case, an insulating panel has an exposed side subjected to fire and an unexposed side losing heat to an ambient environment. Radiation and convection heat exchanges take place on both sides.

Convective heat transfer results in the movement of whole groups of molecules. It is normally concerned with the heat exchange between a fluid and a solid

surface. When the motion of the fluid is induced by buoyancy forces, such as a hot panel in air, and where a change of density of air near the panel occurs due to temperature increases, the mode of heat transfer is called *free (or natural)* convection. When the motion of the fluid is externally induced, as with flowing water in a pipe, which will be considered in next chapter, then although a small amount of free convection may be present, the mode is called *forced* convection. Since in standard test condition, only free convection is encountered on the unexposed face, the calculation of its heat transfer coefficient is presented here.

For natural convection adjacent to a heated vertical or horizontal panel, the following empirical formula applies[2.4]:

$$h(T) = c\,\frac{k_{air}}{H}(G_{r_H}P_r)^n \qquad (2.15)$$

where for a vertical panel

$c = 0.59$ *and* $n = 0.25$ *for* $10^4 < G_{rH}P_r < 10^9$;

$c = 0.10$ *and* $n = 0.33$ *for* $10^9 < G_{rH}P_r < 10^{13}$.

k_{air} is the conductivity of air which depends on temperature:

H is the height of vertical panel;

$$k_{air} = -1.56\times10^{-8}T^2 + 7.43\times10^{-5}T + 0.023 \qquad (2.16)$$

G_{rH} is the Grashof number defined as

$$G_{r_H} = \frac{gH^3(T-T_\infty)}{\nu^2 T_b} \tag{2.17}$$

where

g is the acceleration due to gravity, 9.8m/s^2;

$T_b = (T_\infty + T)/2$, is the average boundary layer absolute temperature;

ν is the kinematic viscosity of air:

$$\nu = 6.75\times10^{-6}T^2 + 9.55\times10^{-3}T + 1.29 \tag{2.18}$$

P_r is the Prandtl number of air which approximately equals 0.7.

For the upper surface of a heated horizontal panel

$c = 0.54$ and $n = 0.25$ for $10^5 < G_{rL}P_r < 2\times10^7$;

$c = 0.15$ and $n = 0.33$ for $2\times10^7 < G_{rL}P_r < 10^{11}$.

In the above equation, the characteristic length L is defined as L = A/P, where A is the surface area and P is the perimeter of panel.

The properties of air should be evaluated at the average boundary layer temperature. The value of $h(T)$ is increased as the difference between the surface and environment temperature increases. A typical value is around 5 W/m^2°C for a vertical panel with 300×300 mm^2 area.

When the heat transfer coefficient is known, the boundary condition (2.5) can be applied to the unexposed side. The geometrical factor (= 1.0 in most cases) and the emissivity of the surface should also be determined.

2.4 Fire Boundary Conditions

Conventionally, fire can be classified as a 'Cellulosic' or 'Hydrocarbon' fire depending on the type of fuel. The standard cellulosic fire test was developed during the early part of the twentieth century and simulated the type of fire which may be experienced in commercial, residential and general industrial construction, while the fire which may occur in the petrochemical industry is appreciably different. In the latter, the fuel is liquid or gaseous in nature. On the other hand, the cellulosic type of fire is characteristic of a fire fuelled by solid combustible materials which is generally in a contained space with limited air movement. Specifiers in the hydrocarbon processing industry have long recognised that the standard cellulosic fire test is less than effective in predicting the performance of fire resistant materials in large scale hydrocarbon-fuelled fires. Nevertheless, cellulosic fires should not be excluded offshore as cellulosic materials are not insignificant, eg, within an accommodation module.

In actuality, there are many different fire scenarios that can occur in the real world. For instance, hydrocarbon fires, which feature a very rapid initial temperature increase together with fierce burning and a high release of heat flux,

in petrochemical industry may include:

- Jet fire: when a stream of fluids burns with some significant momentum
- Pool fire: when a spill of liquid fuel burns
- Running fire: a fire from a burning liquid fuel which flows by gravity over surfaces.
- Fireball or BLEVE: expanding buoyant ball of flaming gas or a Boiling Liquid Expanding Vapour Explosion caused by a catastrophic failure of a pressure vessel containing liquid or gaseous fuel.

The duration of these different fire types can vary from seconds to days.

The standard fire has been adopted to unify test procedures and to enable materials and construction elements to be compared and classified, although the temperature development described by the currently standard time-temperature curve does not necessarily agree with the temperature development experienced in a real fire.

Currently, there are two basic types of time-temperature curve according to BS476 and AMD 6487[1.1]:

1. Cellulosic time-temperature curve:

$$T = 345 \log_{10}(8t+1) + 20 \qquad \textbf{(2.19)}$$

2. Hydrocarbon time-temperature curve:

$$T = 1100[\ 1 - 0.345\ EXP(-0.167\ t) - 0.204\ EXP(-1.417\ t) - 0.471\ EXP(-15.833\ t)\ ] \quad \textbf{(2.20)}$$

where

T is the mean furnace temperature in (°C);

t is the time (in min) up to a maximum of 360 min.

The graphs of both curves are shown in Fig.2.1. During the first 170 minutes, the defined hydrocarbon curve has a steeper rise and a higher fire temperature. After 170 minutes, although the duration of most tests usually does not last so long, the temperature given by cellulosic curve is higher than that given by the

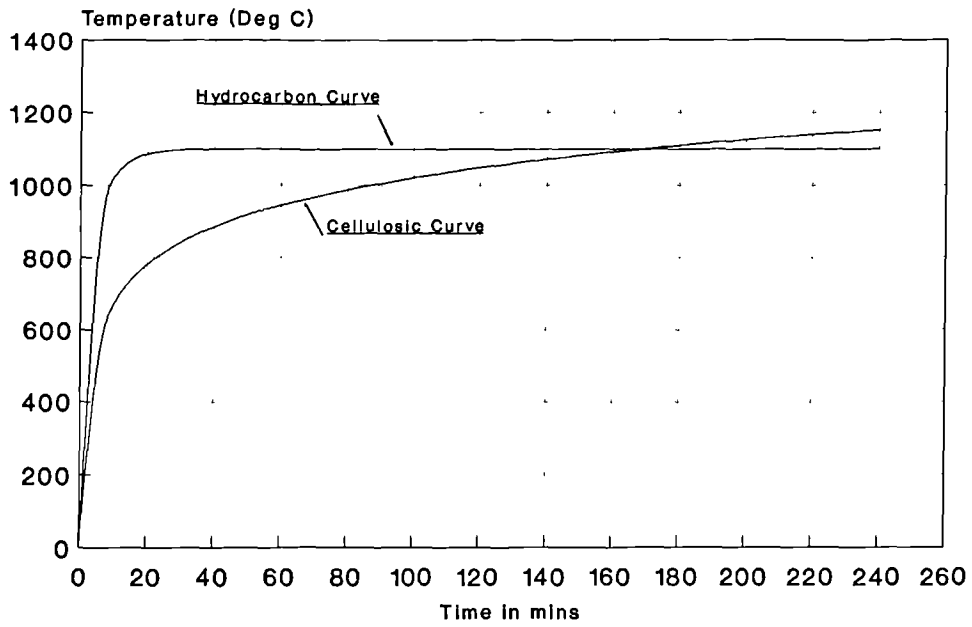

Fig.2.1 The Standard Cellulosic and Hydrocarbon Fire Test Curves [1.1]

hydrocarbon curve.

The expression (2.20) for the representative hydrocarbon fire test, notwithstanding that it is not yet fully accepted by industry, is the most widely recognized curve of this type.

The level of total heat flux could range from 35 KW/m^2 to 400 KW/m^2 under standard tests. Whilst a lot of researches have ignored the convective heat transfer because the radiative heat flux is the dominant component of total heat flux, it is not considered that this is a universally correct approach. For engulfed conditions this may be a reasonable assumption. However, outside the fire, the level of radiation drops away and the assumption becomes less valid. The assumption is also less valid for surfaces that are highly reflective. As the magnitude of the received radiation lowers, then the significance of convection increases and convection may make a considerable difference to the fire endurance of the element.

The heat transfer into a construction on the exposed side depends not only on the temperature of the gas and flames but also on the heat transmission characteristics of both the heating environment and the surface which is receiving heat. The heat transfer and gas temperatures vary strongly during fire exposure. As the phenomena associated with heat transfer in the turbulent environment of a fire are difficult to model exactly, the following alternative schemes are suggested:

i). Direct method: this measures the actual exposed face temperatures of elements during fire test. These measured temperatures can be used in two ways. One is that they can be applied as the Dirichlet boundary

condition (2.4) in numerical modelling. This excludes the uncertainties with regard to the parameters describing the heat transmission from the furnace to the specimens. In the experimental validations of this research, this method is used first to examine the numerical model. Secondly, it can also be used to validate the heat transfer parameters (see following ii).

ii). Heat transfer parameters: although the exact modelling of the heat transfer from fire to specimen is extremely difficult, eventual consideration should be given to the possibility of including the appropriate heat transfer parameters to predict the heat transfer rate from the fire to the specimen. The heat transfer rate from the fire compartment to the panel could be described as a boundary condition using equation (2.5). Here T_∞ should be assumed to be the mean furnace temperature, and E represents the resultant emissivity. The resultant emissivity could be calculated approximately with the equation for radiation between two infinitely large parallel planes[2.4], so that:

$$E = \frac{1}{1/E_f + 1/E_s - 1} \tag{2.21}$$

where

E_f is the emissivity of gases, flames and walls in furnace;

E_s is the emissivity of surface material of specimen.

E_f should be experimentally determined for the furnace. Since this experiment

for the furnaces used in the tests has not been performed, an estimate is made which is based on an educated assumption and a series of calculations. Usually the both the emissivities of the furnace and the heat transfer coefficient are assumed to be constants[2.5]. A considerable error was encountered if this assumption was adopted for the gas-fired furnaces. It was found that the both emissivities of furnace and the heat transfer coefficient should be high at the starting stage, and that they then declined as the temperature increased. The declining trend of E_f is consistent with the research results on the emissivity of gas[2.6], insulating brick[2.7] and ceramic fibre linings[2.8]. For the convective heat transfer coefficient, the reason for the decline is that, at the starting stage of a test, the temperature of the furnace is increased very quickly so that the extent of fire turbulence is high at first.

In the environment of the furnace used for Cellulosic fire test, it is assumed that $E_f = 0.9$ at the beginning of the testing and then linearly declines to $E_f = 0.15$. The average of both values is close to the conventional value of 0.5. The heat transfer coefficient is $h_1 = 60\ W/m^2\ °C$ at beginning of the test and this decreases to $h_2 = 2\ W/m^2\ °C$ at 1000°C. The numerical results based on these parameters give a good correlation with experimental results(see Chapter 6).

For hydrocarbon fires, similar results can be obtained. The slight difference is that at initial stage, the heat transfer coefficient should be higher than with a cellulosic fire.

The experimental verification of the aforementioned formulas will be described in the subsequent chapters.

CHAPTER 3

Finite Difference Modelling of a Pipe

Another extensively used component of construction in onshore and offshore constructions is pipework. A cylindrical polar coordinate model is needed for the heat transfer analysis of pipes under hostile thermal impact. Usually the heat loading is around the outside of the pipe and the following analysis is based on this assumption. Only a slight modification is needed to deal with the reverse case, i.e., heat loading from the inside of a pipe, such as the chimney problem.

3.1 1-D Explicit Formulation of FDM for a Multi-layer Pipe

Assuming that the pipe is subject to a uniform heating condition and that the heat transfer occurs only in the radial direction of the pipe, the general one dimensional heat conduction equation can be written as:

$$\rho C_p \frac{\partial T}{\partial t} = \frac{1}{r}\frac{\partial}{\partial r}\left(k^r(T) r \frac{\partial T}{\partial r}\right) \quad in\ R_1 \le r \le R_2,\ for\ t>0 \qquad (3.1)$$

where

r is the polar coordinate.

k^r is the thermal conductivity in the radial direction.

R_1, R_2 are the inside and outside radii respectively.

The boundary and initial conditions are similar to equations (2.4), (2.5) and (2.6). The boundary condition on $r=R_1$ or $r=R_2$ for $t>0$, is either:

$$T = T_g(t) \qquad (3.2)$$

where $T_g(t)$ is the known temperature given on the inside boundary or outside boundary; Or, if the boundary is losing heat to or gaining heat from an ambient temperature condition:

$$k(T)\frac{\partial T}{\partial n} = h(T)(T_\infty - T) + FE\sigma[(T_\infty+273)^4 - (T+273)^4] \qquad (3.3)$$

The initial boundary condition is:

$$T = T_0(r) \qquad for\ t = 0 \quad in\ R_1 \le r \le R_2 \qquad (3.4)$$

where T_0 is the known initial temperature distribution.

The appropriate explicit finite difference equations for a multi-layer pipe can also be obtained by the energy balance technique. The advantages offered by the use

of sandwich design in pipelines include enhanced insulation capability, double integrity containment and leak or failure protection. The problem requires four different types of FDE to be derived:

a) the interior nodes within one material layer;

b) the interface nodes between two material layers;

c) the external boundary node;

d) the internal boundary node.

(a) For an interior node m within one layer:

$$T_m^{i+1} = T_m^i + \frac{\Delta t}{\rho C_p r_m \delta r^2}[k_{m,m+1}(r_m + \frac{\delta r}{2})(T_{m+1}^i - T_m^i) + k_{m-1,m}(r_m - \frac{\delta r}{2})(T_{m-1}^i - T_m^i)] \quad (3.5)$$

The evaluation of the conductivity $k_{m-1,m}$ or $k_{m+1,m}$ is same as in equation(2.9). The Fourier number is

$$F_o = \frac{[k_{m,m+1}(r_m/\delta r + 0.5) + k_{m-1,m}(r_m/\delta r - 0.5)]\Delta t}{2\rho C_p r_m \delta r} \quad (3.6)$$

(b) For the interface node m between two material layers

$$T_m^{i+1} = T_m^i + \frac{\Delta t}{\rho_1 C_{p1}(r_m - \delta r_1/4)\delta r_1/2 + \rho_2 C_{p2}(r_m + \delta r_2/4)\delta r_2/2} \cdot [k_{m,m+1}$$
$$(r_m/\delta r_2 + 0.5)(T_{m+1}^i - T_m^i) + k_{m-1,m}(r_m/\delta r_1 - 0.5)(T_{m-1}^i - T_m^i)] \quad (3.7)$$

The Fourier number is now

$$F_o = \frac{[k_{m,m+1}(r_m/\delta r_2 + 0.5) + k_{m-1,m}(r_m/\delta r_1 - 0.5)]\Delta t}{\rho_1 C_{p1}(r_m - \delta r_1/4)\delta r_1 + \rho_2 C_{p2}(r_m + \delta r_2/4)\delta r_2} \quad (3.8)$$

where subscripts 1,2 indicate the two materials respectively.

(c) For the outside boundary node m:

$$T_m^{i+1} = T_m^i + \frac{\Delta t}{\rho C_p(r_m - \delta r/4)\delta r/2.}[k_{m-1,m}(r_m/\delta r - 0.5)(T_{m-1}^i - T_m^i) +$$
$$h(T)r_m(T_{fire} - T_m^i) + FE\sigma r_m((T_{fire} + 273)^4 - (T_m^i + 273)^4)] \quad (3.9)$$

where T_{fire} is the furnace temperature. The Fourier number is

$$F_o = \frac{[k_{m-1,m}(r_m/\delta r - 0.5) + hr_m + FE\sigma r_m(T_m + 273)^4/T_m]\Delta t}{\rho C_p(r_m - \delta r/4)\delta r} \quad (3.10)$$

These F_o's should be less than 0.5 in order to preserve the stability of the

calculation.

(d) For the inside surface node 1:

$$T_1^{i+1} = T_1^i + \frac{2\Delta t}{\rho C_p(r_1+0.25\delta r)(\delta r)^2}[k_{1,2}(r_1+0.5\delta r)(T_2^i-T_1^i)+hr\,\delta r(T_a-T_1)] \quad (3.11)$$

where h is inside heat transfer coefficient

T_a is the temperature of inner flow

3.2 2-D Explicit Formulation of FDM for a Multi-layer Pipe

When the heat loading is no longer uniform along the circumferential direction of a pipe, the problem becomes two dimensional. In this case, the general two-dimensional heat conduction equation can be written as:

$$\rho C_p \frac{\partial T}{\partial t} = \frac{1}{r}\frac{\partial}{\partial r}(rk^r(T)\frac{\partial T}{\partial r}) + \frac{1}{r^2}\frac{\partial}{\partial \theta}(k^\theta(T)\frac{\partial T}{\partial \theta}) \quad (3.12)$$

$$\text{in } R_1 \le r \le R_2,\ 0 \le \theta \le 2\pi$$

where

r, θ are the polar coordinates;

k^r is the thermal conductivity in the radial direction;

k^θ is the thermal conductivity in the circumferential direction;

R_1, R_2 are the inside and outside radii respectively.

The boundary and initial conditions are similar to equations (3.2),(3.3) and (3.4). There are four different types of FDE to be derived as well:

a) the interior nodes within one material layer;

b) the interface nodes between two material layers;

c) the external boundary nodes;

d) the internal boundary nodes.

(a) For the interior nodes within one material layer:

$$T'_{i,j} = T_{i,j} + \frac{\Delta t}{\rho C_p r_i \Delta r \Delta \theta}\Big[k^r_{(i,i+1),j}\Delta\theta\left(\frac{r_i}{\Delta r}+0.5\right)(T_{i+1,j}-T_{i,j}) + k^r_{(i-1,i),j}\Delta\theta\left(\frac{r_i}{\Delta r}-0.5\right)(T_{i-1,j}-T_{i,j}) + k^\theta_{i,(j-1,j)}\frac{\Delta r}{r_i\Delta\theta}(T_{i,j-1}-T_{i,j}) + k^\theta_{i,(j,j+1)}\frac{\Delta r}{r_i\Delta\theta}(T_{i,j+1}-T_{i,j})\Big] \quad (3.13)$$

where a prime $'$ denotes the temperature at next time step.

(b) For the interface nodes between two material layers

$$T'_{i,j} = T_{i,j} + 2\Delta t\{[\rho^n C_p^n (r_i - 0.25\Delta r^n)\Delta r^n + \rho^{n+1} C_p^{n+1}$$

$$(r_i + 0.25\Delta r^{n+1})\Delta r^{n+1}]\Delta\theta\}^{-1}\cdot[\, k^{r,n+1}_{(i,i+1),j}\Delta\theta\left(\frac{r_i}{\Delta r^{n+1}} + 0.5\right)(T_{i+1,j} - T_{i,j})$$

$$+ k^{r,n}_{(i-1,i),j}\Delta\theta\left(\frac{r_i}{\Delta r^n} - 0.5\right)(T_{i-1,j} - T_{i,j}) \qquad (3.14)$$

$$+ (k^{\theta,n}_{i,(j,j+1)}\Delta r^n + k^{\theta,n+1}_{i,(j,j+1)}\Delta r^{n+1})\frac{T_{i,j+1} - T_{i,j}}{2r_i\Delta\theta}$$

$$+ (k^{\theta,n}_{i,(j-1,j)}\Delta r^n + k^{\theta,n+1}_{i,(j-1,j)}\Delta r^{n+1})\frac{(T_{i,j-1} - T_{i,j})}{2r_i\Delta\theta}]$$

where the superscripts $n,n+1$ indicate materials.

(c) For nodes on the inside surface:

$$T'_{1,j} = T_{1,j} + \frac{2\Delta t}{\rho C_p(r_1 + 0.25\Delta r)\Delta r\Delta\theta}[\, k^{r}_{(1,2),j}\Delta\theta\left(\frac{r_1}{\Delta r} + 0.5\right)\cdot$$

$$(T_{2,j} - T_{1,j}) + k^{\theta}_{1,(j-1,j)}\frac{\Delta r}{2r_1\Delta\theta}(T_{1,j-1} - T_{1,j}) + k^{\theta}_{1,(j,j+1)} \qquad (3.15)$$

$$\frac{\Delta r}{2r_1\Delta\theta}(T_{1,j+1} - T_{1,j}) + r_1\Psi\Delta\theta]$$

where Ψ is the unit net heat flux due to radiation and convection. The evaluation of Ψ will be presented in section 3.3.

(d) For outside boundary nodes:

$$T'_{ij} = T_{ij} + \frac{2\Delta t}{\rho C_p (r_i - 0.25\Delta r)\Delta r \Delta\theta}[k^r_{(i,i+1)j}\Delta\theta(\frac{r_i}{\Delta r} - 0.5)(T_{i-1,j} - T_{ij}) + k^\theta_{i,(j-1,j)}\frac{\Delta r}{2r_i\Delta r}(T_{ij-1} - T_{ij}) + k^\theta_{i,(j,j+1)}\frac{\Delta r}{2r_i\Delta\theta}(T_{ij+1} - T_{ij}) + h(T)r_i\Delta\theta(T_{fire} - T_{ij}) + F\sigma\varepsilon r_i\Delta\theta((T_{fire}+273)^4 - (T_{ij}+273)^4)] \quad (3.16)$$

3.3 Internal Heat Exchange

For one-dimensional analysis, if the inside of pipe is empty, eg, the pipe is filled with air, the heat capacity of air can be neglected due to the small mass of air inside. If the pipe is filled with flowing water, forced convective heat dissipation is encountered. For a flow inside a circular tube, the rate of heat transfer depends on the type of flow, ie, laminar or turbulent flow. When the flow through the pipe is streamlined and in consequence little mixing takes place, the heat transfer is relatively poor. When the flow becomes turbulent and there is very rapid mixing action, much higher convection rates then take place.

The Reynolds number, defined as $R_e = u_m D \nu$ is used as a criterion for defining the change from laminar to turbulent flow[3.1]. In this definition, u_m is the mean flow velocity, D is the inside diameter of pipe, and ν is the kinematic viscosity

$$T'_{i,j} = T_{i,j} + \frac{2\Delta t}{\rho C_p (r_i - 0.25\Delta r)\Delta r \Delta\theta}[k^r_{(i,i+1),j}\Delta\theta(\frac{r_i}{\Delta r} - 0.5)(T_{i-1,j} - T_{i,j}) + k^\theta_{i,(i-1,j)}\frac{\Delta r}{2r_i\Delta r}(T_{i,j-1} - T_{i,j}) + k^\theta_{i,(i,j+1)}\frac{\Delta r}{2r_i\Delta\theta}(T_{i,j+1} - T_{i,j}) + h(T)r_i\Delta\theta(T_{fire} - T_{i,j}) + F\sigma\varepsilon r_i\Delta\theta((T_{fire}+273)^4 - (T_{i,j}+273)^4)] \quad (3.16)$$

3.3 Internal Heat Exchange

For one-dimensional analysis, if the inside of pipe is empty, eg, the pipe is filled with air, the heat capacity of air can be neglected due to the small mass of air inside. If the pipe is filled with flowing water, forced convective heat dissipation is encountered. For a flow inside a circular tube, the rate of heat transfer depends on the type of flow, ie, laminar or turbulent flow. When the flow through the pipe is streamlined and in consequence little mixing takes place, the heat transfer is relatively poor. When the flow becomes turbulent and there is very rapid mixing action, much higher convection rates then take place.

The Reynolds number, defined as $R_e = u_m D \nu$ is used as a criterion for defining the change from laminar to turbulent flow[3.1]. In this definition, u_m is the mean flow velocity, D is the inside diameter of pipe, and ν is the kinematic viscosity

of the fluid. The range of R_e value in the transition stage is around $2000 < R_e < 4000$. Since in most practical cases the values of R_e are greater than 4000, turbulent flow inside the pipe is assumed. The empirical formula which was proposed by Nusselt is employed to calculate the internal heat transfer coefficient $h(T)$ [2.4]:

$$h(T) = 0.036 R_e^{0.8} P_r^{1/3} (D/L)^{0.055} \frac{k}{D} \qquad for\ 10 < \frac{L}{D} < 400 \qquad (3.17)$$

where

L is the length of the pipe;

D is the inside diameter of the pipe;

k is the conductivity of the fluid;

P_r is the Prandtl number of the fluid.

The fluid properties are evaluated at the bulk mean fluid temperature. A typical illustration of the influence of fluid speed on the inside temperature rise in a GRP pipe under the standard hydrocarbon fire test is shown in Fig.3.1.

If the pipe is filled with stagnant water, the problem will be more complicated because a mixture of conduction and convection occurs. At low temperature, the heat transfer through the water may be considered to be by conduction only, while, as the water temperature increases rapidly in a fire environment, convection will occur.

For the two dimensional analysis of an empty pipe, the heat exchange between

the different parts of the inside surface should be taken into account. Although many construction components and assemblies enclose voids, no general procedure which may be used to calculate heat exchange by radiation and convection through a void has been available[3.2]. Thus some simplifying assumptions are normally needed. One of these is to consider the conduction and specific heat of the internal air to be negligible. The inside curved surface is replaced by a finite number of discrete straight zones. The convective heat transfer to an enclosure boundary is written as

$$q_c = \beta(T_i - T_{air})^{\gamma} \qquad (3.18)$$

where

β,γ are the convection factor and convection power;

T_i is the surface temperature of the *zones;*

T_{air} is the fictitious inner air temperature.

The air temperature is assumed to be uniform over the inside of the void and there is presumed to be no flow of air either in or out of the void. The total heat transfer to the air from the enclosure surfaces must be zero at any given time in order to conserve the energy. The total heat transfer to the enclosed air is

$$\psi_{c_{tot}} = \sum_{i=1}^{N} q_{c_i} A_i = 0 \qquad (3.19)$$

where

N is the number of zones;

q_{ci} is the heat flux per unit area;

A_i is the area of zone i.

If all of the temperatures T_i are known, T_{air} can readily be computed by iteration and the local heat transfer to zone i can be calculated.

Regarding radiation, only diffuse-grey surfaces are considered. This means that the directional spectral emissivity and absorptivity do not depend on either angle or wavelength, but only on surface temperature. Although most materials are not truly diffuse-grey, this assumption simplifies enclosure radiation theory and is often made. The inside surface of the pipe is divided into a number of zones. The temperature and heat flux of each zone are assumed to be uniform. The Hottel's crossed-string method[3.3] may then be employed to calculate view factors for the two-dimensional configuration. Radiation heat flow and absolute surface temperature for an enclosure with N zones can be related by the following expression[3.4]

$$\sum_{j=1}^{N}\left(\frac{\delta_{kj}}{\epsilon_j} - F_{kj}\frac{1-\epsilon_j}{\epsilon_j}\right)\frac{\Psi_{r_j}}{A_j} = \sum_{j=1}^{N}(F_{kj}-\delta_{kj})\sigma T_j^4 \qquad (3.20)$$

where, corresponding to each zone surrounding the enclosure, k is one of the values 1,2,...,N, Ψ_{rj} is radiative heat transfer, F_{kj} are view factors and δ_{kj} is the Kroneker delta. When the surface temperatures are specified, the right hand side of Eq.(3.20) is known and there are N simultaneous equations for the unknown Ψ_r. The sum of Ψ_c and Ψ_r will be the required Ψ in the Eq.(3.15).

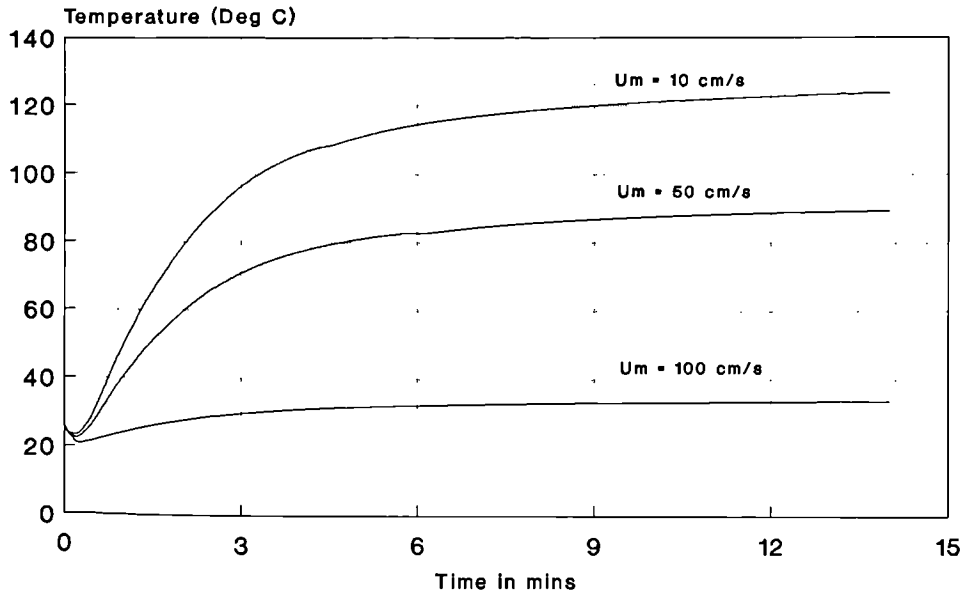

Fig.3.1 Inside Surface Temperature Rise in a GRP Pipe (5mm) with Flowing Water Hydrocarbon Fire, Computer simulations

CHAPTER 4

Models for Polymeric Composites

4.1 Introduction

The use of fibre reinforced polymer composites, and in particular Glass-fibre Reinforced Plastics (GRP), is increasing now owing to their inherent advantages in material characteristics, such as good corrosion resistance, low weight and cost, long service life and low thermal conductivity, typically 1/100 of steel. However, because plastic materials are organic in nature and are inherently combustible, one of the key problems which needs to be overcome before they are accepted for wider use relates to the need for improved understanding and quantitative evaluation of their behaviour in fire. Accurate knowledge of the thermal response of GRP at high temperature is therefore essential for the reliable and economical design of composite structures in hostile fire environments such as may be encountered on offshore oil platforms.

Let us look at what will happen when a typical GRP panel is exposed to fire. When one surface of the GRP panel is exposed to an incident heat flux, the initial temperature rise is a function of the rate of heat conduction into the material and the boundary conditions. As heating continues, the surface

temperature reaches a certain level (usually around 200-300°C) beyond which decomposition begins to occur and the resin components degrade to form gaseous products at a measurable rate. These gaseous products, initially trapped within the composite matrix owing to its low permeability, attain very high internal pressures and induce the solid matrix to expand. Once the decomposition process begins, the thermal behaviour of the material is altered by the chemical reactions, thermochemical expansion and variable thermal and transport properties. Meanwhile, a considerable amount energy will be required in order to break the constituent chemical bonds. As thermal decomposition proceeds, a residual char layer then builds up as the pyrolysis front moves further into the virgin solid. An advantage of thermosetting resins (which are generally used in GRP) is that usually they do not melt when heated owing to their highly cross-linked chemical structures. Initially, the char layer provides an increasing thermal resistance between the exposed surface and the pyrolysis front as a consequence of its low thermal conductivity and because it can only be ignited with difficulty at normal oxygen concentrations. This is the one reason why GRP can provide a useful fire barrier performance, despite it being an organic material. However, after this initial phase, at a certain stage in the heating process, a network of fissures develops in the carbonaceous char layer due to the release of high pressure gasses. At very high temperatures, the char is then gradually oxidized and erodes away. Then the heat resistance of char layer will be totally lost and the glass-fibre remains alone. Under extremely strong heat flux, such as is experienced in a hydrocarbon fire, even the woven roving glass plies will crimp and eventually crumble away.

This problem exhibits some differences with the ablation problem experienced in the

aerospace industry, which is usually associated with rocket nozzles or missile reentry situations. Their major concern is the total energy which must be absorbed into the surface body rather than a heat transfer rate. Another consideration is that in their situation, a portion of surface body exposed to the hot, high speed fluid flow is allowed to melt and rapidly blow away.

Over the past 50 years, several analytical models have been proposed which consider heat transfer in decomposing materials [4.1 to 4.9]. All of these procedures were basically a transient heat conduction calculation in conjunction with the effect of decomposition. The differences existed in their assumptions, approximations, the phenomena included and the property data used. Although most of these studies were concentrated on wood, they provided a theoretical basis for further investigation of the fire performance of other combustible materials.

There are two basic ways to tackle the decomposition of materials: implicit and explicit approaches. The implicit methods[4.4,4.9] include the effects of decomposition by artificially increasing the specific heat for the temperature range in which pyrolysis occurs. The author does not think that this is very appropriate for such a complex problem. The comprehensive explicit methods[4.3,4.6,4.8] model the decomposition as an exponential kinetic rate equation. The conservation of mass and heat of reaction are therefore included. The diffusion of volatiles is also considered. It is believed that this is a better approach.

Arising from the mathematical models proposed by Kung[4.3], Henderson *et al*[4.6,4.8] presented a numerical model for the thermal response of polymer

composite materials together with an experimental verification. Most of the essential processes relating to the temperature development in the process of decomposition were included in the model. But, probably because of the test assembly used, the fact that only a relatively low constant heat flux was imposed, and due to the particular material used in their test, the profile of measured rate of increase of temperature did not display as much variation as we have observed in standard fire testing of GRP panels.

In this study, the solution of a more realistic problem is attempted, namely that of a glass-fibre reinforced plastic panel and pipe exposed to the time-temperature regime of a standard fire test. For the associated tests, the furnace temperature was controlled by computer to follow the standard BS476 cellulosic fire or hydrocarbon time-temperature curve[1.1].

The fire tests revealed that if the empty GRP pipes were exposed directly to a hydrocarbon fire, they can only survive for a few minutes. Therefore it is necessary to add additional protection to the plain GRP pipes. One method is to use a polymer based flame-retardant intumescent coating.

In a fire, an intumescent coating undergoes several chemical changes in order to act as a thermal barrier between the heat source and the substrate. Generically, three main ingredients are necessary for this process: a catalyst, a carbonic (char-former), and a spumific(blowing agent). The catalyst promotes decomposition of the carbonific compound. Initially, an inert gas is liberated to provide transpirational cooling at the surface. As the fire continues, other ingredients of intumescence break down, expand and absorb heat. A low density carbonaceous

char then forms and this is expanded by the spumific agent which provides a good insulating blanket due to its low thermal conductivity. These reactions combine to make intumescent coatings into a most efficient fireproofing material although the labour involved and cost are relatively high.

To date, only a few mathematical models have been based on the fundamental chemical or physical processes occurring in a complex intumescent coating system such as heat transfer, kinetics, and swelling[4.10 to 14]. The various physical processes were considered in mass and energy control volumes. Expansion has been accounted for by assuming it to be a function of mass loss.

With the combination of the above models and the treatment which was originally developed by J.B.Henderson and T.E.Wiecek[4.8] to predict the thermal response of a polymer composite simultaneously undergoing decomposition and thermochemical expansion, an analysis of the heat transfer problem associated with intumescent coatings under hydrocarbon fire is carried out in this paper. The accuracy of the model was evaluated by comparing predicted and experimental temperature distributions in the intumescent coated GRP pipes.

4.2. Model for WR Polyester Laminate

The first GRP component to be used for the experimental and numerical fire resistance study was the woven roving glass-fibre reinforced polyester laminate. Because of their low cost, ease of processing and good performance

characteristics, unsaturated polyesters are the most extensively used type of thermosetting resin. Woven Roving (WR) cloth is a popular fabric to produce high directional strength characteristics. Bidirectional roving cloth laminate, which was used in the present study, has high strength properties in two directions at right angles to each other. The WR glass/polyester laminates were made using a hand lay-up technique with a ply angle of zero. The thin thermocouples (K type) were embedded (during making up process) inside the central area at different locations to measure the temperature profile history across the cross-section of the laminates (Fig.4.1).

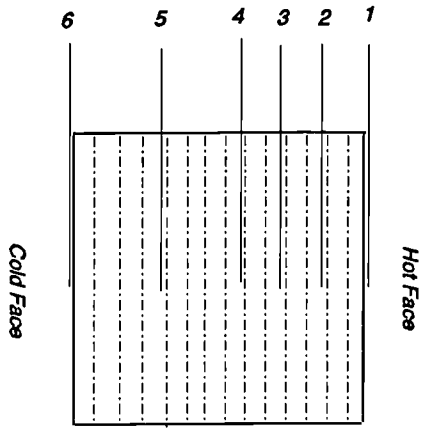

Fig.4.1 The layout of laminate and the location of thermocouples

Since the physical and chemical processes are concurrent, the problem of interpreting and predicting the observed results is a task of awesome complexity. It is considered that main task at present is not to attempt to form a 'complete' model owing to the almost total absence of information concerning

most of the material parameters involved. The most promising approach is to form a mathematically viable but relatively simple model which can capture the main features of the pyrolysis process and the consequent heat transfer behaviour. Therefore, several idealizations are made:

a). The GRP material is assumed to be homogeneous and the transport of heat and mass is perpendicular to the face of panel so that the problem is assumed to be one dimensional.

b). The rate of decomposition is assumed to conform to a mean reaction which is described by a single first-order Arrhenius function.

c). There is thermal equilibrium between the decomposition gases and the solid material and there is no accumulation of these volatile gases in the solid material.

d). The feedback of heat released by the flame of the combustible volatile back to the panel in a small scale furnace test is neglected owing to its relatively small contribution compared with the enormous heat flux created by the furnace. However, it is anticipated that in large or full scale fire tests, or in the case of sustained combustion after removal of the heat source, its contribution may not be ignored.

The governing principles on which the analytical model has been developed are a combination of the principles of conservation of mass and conservation of energy. The one-dimensional energy equation in a panel undergoing thermal

decomposition expresses a balance between the transient energy accumulation rate, with the sum of the rates of conduction, pyrolysed convection, and the energy sink due to decomposition[4.6]

$$\frac{\partial}{\partial t}(\rho h) = \frac{\partial}{\partial x}(k\frac{\partial T}{\partial x}) - \frac{\partial}{\partial x}(m'_g h_g) - Q\frac{\partial \rho}{\partial t} \qquad (4.1)$$

where

ρ	is density (kg/m^3)
h	is the enthalpy (J/kg) of solid
t	is time (s)
T	is the temperature (°C)
k	is the thermal conductivity (W/m°C)
x	is the spatial variable (m)
h_g	is the enthalpy of gas(J/kg)
m'_g	is the mass flux of gas (kg/m^2-s)
Q	is the heat of decomposition (J/kg)

The specific enthalpies of the solid and volatile are

$$h = \int_{T_0}^{T} C_p dT, \quad h_g = \int_{T_0}^{T} C_{pg} dT \qquad (4.2)$$

where T_o is the ambient reference temperature.

Equation (4.1) must be solved simultaneously with the equations for the rate of decomposition and the mass flux of the gas. The rate of decomposition of resin

in GRP is assumed to conform to a mean reaction which is described by a single first-order Arrhenius function

$$\frac{d\rho_r}{dt} = -A\,\rho_r exp(-E_A/RT) \qquad (4.3)$$

where ρ_r is the instantaneous density of partially pyrolysed resin, E_A is the activation energy (J/mol), R is the gas constant (8.314J/K.mol) and T is the temperature (K). The constant A is known as the pre-exponential factor and has unit of s^{-1}. The relationship between the ρ and ρ_r is:

$$\rho = \rho_r v + \rho_g(1-v) \qquad (4.4)$$

where ρ_g is the density of glass-fibre and v is the volume fraction of glass-fibre. The glass-fibre is assumed to be intact in the time zone of interest under fire.

Here, the resin pyrolysis is assumed to be a continuous process until it is totally consumed. Some investigators have included the final density of the char in the expression (4.3). This will cause two problems in practical application. One is that the precise definition of the final char status is difficult to define. Another point is that yet another expression for char pyrolysis will be then required if it commences its final breakdown in the time zone of interest. Although much research has been carried out into the thermal decomposition of polymers, in view of the chemical complexity involved, combined with problems of interpreting data from a variety of sources and experimental assemblies, the available data is still very limited and not in a form suitable for warranting improvements to the

above relatively simple treatment.

Another facet which shows the complexity of the problem is the determination of the heat of decomposition (sometimes called the heat of pyrolysis or heat of reaction). It was reported that its value for wood, for instance, varies greatly[4.15]; and that not only the magnitude but the actual sign of this property has been the subject of debate for many years[4.16,4.17]. We prefer the allegation which declares that the decomposition process itself is endothermic overall. The exothermicity often noticed in the burning of wood and plastics is a result of the reaction between the outflowing volatiles and oxygen. A minor exothermic reaction might happen within the extremely complicated competing reactions, or a local exothermic phenomenon appears due to the change of specific heat. However, in most circumstances, the endothermic reaction is believed to be dominant in the decomposing process for polymeric materials.

If the accumulation of gases and the effect of expansion on density change are ignored, the conservation of mass may be written as:

$$\frac{\partial m'_g}{\partial x} = -\frac{\partial \rho}{\partial t} \qquad (4.5)$$

and the mass flux, m'_g, at any spatial location and time can be calculated by integration of Equation (4.5).

Equation (4.1) is modified to its final form by expanding the first three terms, substituting in the specific heat and the continuity equation, and rearranging. This results in[4.6]

$$\rho C_p \frac{\partial T}{\partial t} = k\frac{\partial^2 T}{\partial x^2} - m'_g C_{pg}\frac{\partial T}{\partial x} - \frac{\partial \rho}{\partial t}(Q + h - h_g) \qquad (4.6)$$

where

C_p is the specific heat of material (J/kg°C);

C_{pg} is the specific heat of gas (J/kg°C).

Equations (4.3), (4.5) and (4.6) form a set of non-linear partial differential equations which may be solved simultaneously for ρ, m'_g and T respectively.

The boundary conditions on the exposed and unexposed surfaces of a panel could be either a prescribed temperature or a radiation and convection boundary condition. To exclude the uncertainties of the heat transmission rate from the fire to the samples under test, the measured temperature can be used as the boundary condition at the exposed side. On the unexposed side, equation (2.5) is again applied.

The initial conditions for $0 \le x \le L$ at $t = 0$ are

$$T = T_i;\ \rho = \rho_0;\ m'_g = 0\ . \qquad (4.7)$$

where

T_i is the initial temperature (°C);

ρ_o is the initial density (kg/m^3).

The comparison of the measured and calculated results shows a good correlation (see Chapter 6). It is shown that the above scheme can be straightforward to

apply to the epoxy and vinyl ester systems. However, for phenolic resin laminates, a more complex behaviour was observed. This requires a special treatment which will be discussed in the next section.

4.3 Special Treatment for WR Phenolic Laminate

Phenolic (phenol-formaldehyde) resins, whose development was once superseded by that of polyesters and epoxies, have experienced a recent recovery in popularity which is mainly attributable to their good fire resistance and low smoke emission (about 10% that of polyester-based GRP).

The test samples of woven roving glass/phenolic laminate were made in a similar manner to the WR polyester laminates as shown in Fig.4.2.

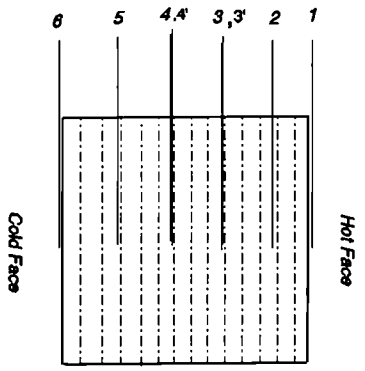

Fig.4.2 The Phenolic laminate with the location of the thermocouples

The resin which was used for fire tests was Cellobond FRP liquid phenolic resole resin J2027L which was supplied by BP Chemicals. According to the supplier, this material has a high degree of fire resistance and excellent high temperature mechanical properties with minimal smoke or toxic fume emission. In order to obtain more information, there were two embedded thermocouples within the layers at the same nominal depth below the surface. After curing, the flat samples were clamped in a vertical position over an opening cut into the door of the fire testing furnace and were exposed to ambient air on the other face. The size of each panel was 380×380 mm^2 with an area of 250×250 mm^2 exposed within the furnace. A typical hydrocarbon fire test result of WR phenolic laminate is shown in Fig.4.3.

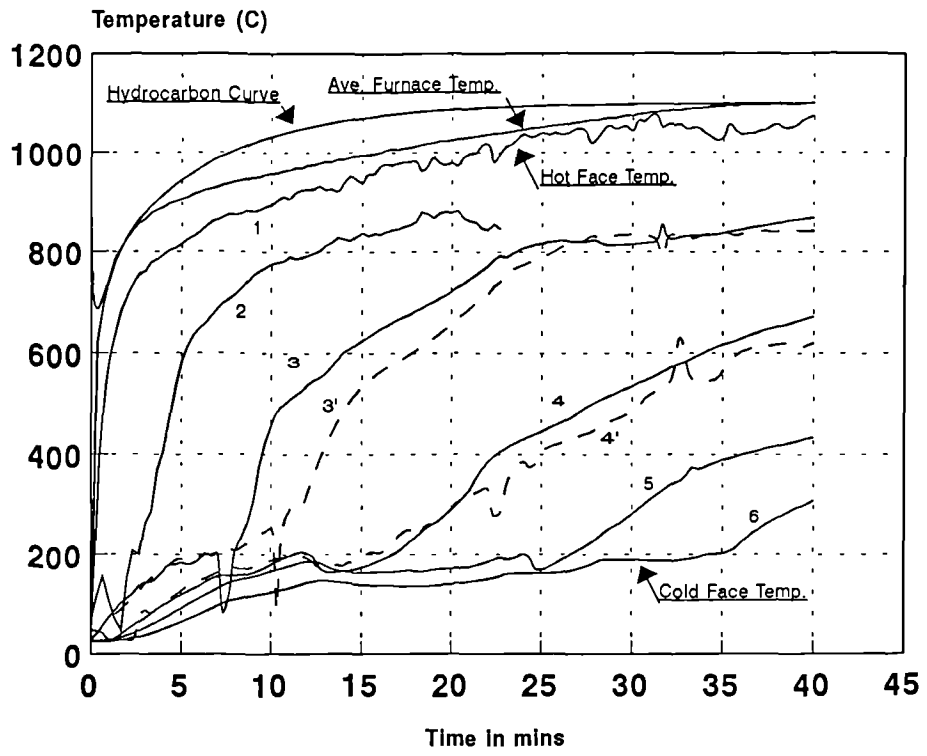

Fig.4.3 Experimental Results of Temperature Profile Hydrocarbon Fire Test of WR Phenolic Laminate I (12.6mm)

A first impression of Fig.4.3 suggests that the temperature response inside the phenolic laminate was quite erratic. In the initial stages of the test, the temperature rose at a moderate rate. Then, at about 200°C, there was a sudden drop of temperature at most locations. After this sudden drop, the temperature at each location concerned increased rapidly again. It was found that this unusual behaviour is due to the delamination of the laminate.

Consider, for example, the output of measured temperature given by two thermocouples at position 3 (see Figs.4.2 and 4.3, where 3 and 3' refer to two different thermocouples in the same layer). Before the temperature reaches 200°C, both thermocouples indicated almost identical temperature values. Then, at 200°C, the reading of one thermocouple suddenly dropped to 80°C. This indicates that the cooler air was drawn into the interstice when a delamination abruptly occurred. After delamination, the outcome of measured temperature will be strongly dependent on the location of the thermocouple which introduces a random element into the measurements. As illustrated by Fig.4.4, if the thermocouple is attached to the surface B, its reading will be high. If the thermocouple is attached to the surface B', its reading will be low. Evidently, if the thermocouple is remote from the region of delamination, an intermediate reading will be obtained. Furthermore, in volatile turbulence, the reading given by a thermocouple in the region of a delamination is unlikely to remain completely stable. This is illustrated by curve 4' in Fig.4.3.

The delamination is also demonstrated by observations made during the progress of the tests. A lot of loud 'bang' sounds were heard which emanated from the laminate during the fire test. This violent delamination is believed to be caused

by the vaporization of intrinsic water (by-product of polymerisation[4.18]) in the resin over 100°C. The water vapour, initially trapped within the composite matrix owing to its low permeability, attains very high internal pressures as heating continues. At about 200°C, a sudden release of high pressure tears the laminate. A subsequent examination of the tested sample also reveals the appearance of deaminations.

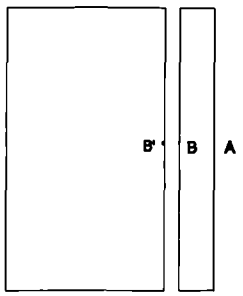

Fig.4.4 Heat transmission through a delaminated surface

Although delamination causes a detrimental effect on the structural integrity of the laminate, it may be beneficial in term of heat resistance as shown by cold face temperature curve 6 in Fig.4.3. Due to the creation of a delamination in the hotter part of the laminate, the mechanism of heat transfer from the hot side to the cold side will be altered. Before the appearance of a delamination, the internal heat transmission is mainly by conduction, whereas, within the interstice caused by the delamination, radiation and convection will be dominant. Initially, for example at point B' in Fig 4.4, the amount of heat transferred by radiation and convection will be lower than that transferred by conduction. Then, following the appearance of a discontinuity in the heat conduction path, the

temperature at that point declines. It is clear that the heat transfer by conduction is disturbed by delamination. This is one of reasons why the cold face temperature of WR phenolic laminate can remain at a low and fluctuating level for quite a long time. Another reason is the energy sink caused by the decomposition of the resin as described for polyester resin in the previous section.

The fundamental equations for this problem are the same as those formulated in section 4.2. However, a particular heat transmission equation will now be established for the delaminated interfaces.

As shown in Fig.4.4, it is assumed that the layer AB is detached from the main body of the laminate. Then an additional term should be included in the energy conservative equation for points B and B' to take account of the heat transmission by radiation and convection between B and B'. If these are assumed to be on two infinitely large flat surfaces, the equation for the magnitude of heat flow G is

$$G = E_r\sigma[(T_B+273)^4 - (T_{B'}+273)^4] + H(T_B - T_{B'}) \qquad (4.8)$$

where

E_r is the resultant emissivity;

H is the heat transfer coefficient.

On the right hand side of equation (4.8), the first term represents the radiation and second term represents convection.

Since both the theoretical prediction and the explicit experimental measurement

of above two parameters are difficult, they are determined by finding a reasonable fit between the model and the observed results. In the final analyses, E_r is set as 0.9 and H is given the value 20 W/°C. It is found that the radiation energy provides the major component of G.

By introducing this equation, a good agreement between the experimental and computational results was obtained (see chapter 6). It demonstrates that a good explanation has been given for the bewildering outcome of the measured temperature development in WR glass/phenolic laminate in a fire.

4.4 Model to Predict the Thermal Response of GRP Pipes

In the offshore industry, it is necessary to design key components of the installation to withstand the effects of fire. One such component is the fire-water system which supplies a deluge of water in the event of a fire-related emergency. Traditionally, fire-water systems have used steel pipework but there is considerable interest in replacing steel with GRP because of its corrosion resistance and lighter weight[4.19]. In order to prove the viability of GRP dry riser pipes in this context, it is necessary to demonstrate that they can withstand the effect of the fire on the empty pipe until the pipe is full of water and the deluge system is in operation.

This problem has been approached by a combination of fire testing and numerical

analysis. A one-dimensional analytical model for GRP pipes subjected to a prescribed time-temperature history applied by the furnace was developed. The explicit finite difference method was employed to solve the transient heat conduction equation in polar coordinates. The performance of GRP pipes under fire condition is quite similar to that of GRP laminates. The two possible differences could be

1. Although some blisters may be observed on the inside of the pipe at the final stage of a fire test, wholesale delamination in GRP pipes can not happen because the glass-fibre reinforcement is wound helically into the cylindric shape.

2. The loss of heat from the cold face, i.e., the inside of pipe, is restricted in the empty pipe. This means that the temperature increase in the pipe will be more rapid.

The fundamental assumptions and principles described in above sections are still applicable for pipe problems. The only thing that is required is to recast the equations in a polar coordinate system. The transport of heat and mass is assumed to be only in the radial direction of the cross-section.

Using the same principles that were used with the polymeric composite panels, an analytical model for the pipe problem is developed. The one-dimensional energy equation in a pipe undergoing thermal decomposition, expressed as a balance between the transient energy accumulation rates, with the sum of the rates of conduction, pyrolysed convection, and the energy sink due to pyrolysis

and the heat feedback by volatile combustion is now

$$\frac{\partial}{\partial t}(\rho h) = \frac{1}{r}\frac{\partial}{\partial r}(k_r(T) r \frac{\partial T}{\partial r}) - \frac{\partial}{\partial r}(m'_g h_g) - \phi\frac{\partial \rho}{\partial t} \qquad (4.9)$$

in which $R_1 \leq r \leq R_2$, for $t > 0$.

Where

ρ is the density (kg/m^3)

h is the solid enthalpy (J/kg)

t is time (s)

r is the polar coordinate (m)

T is the temperature (°C)

k_r is the thermal conductivity in the radial direction(W/m°C)

h_g is the enthalpy of gas(J/kg)

m'_g is the mass flux of gas (kg/m^2-s)

ϕ is the heat of reaction (J/kg).

R_1 and R_2 are the inside and outside radii respectively. Probably due to the pipe samples being enclosed inside the furnace during testing, it is found that the influence of heat release by the combustion of volatiles is now significant. The heat of reaction ϕ is therefore defined as the offset of the endothermic heat of decomposition and the heat feedback by volatile combustion.

Equation (4.9) must be solved simultaneously with the equations for the rate of decomposition and the mass flux of the volatile. The formula for the rate of decomposition is the same as equation (4.3).

If the accumulation of gases and the effect of expansion on density change are ignored, the conservation of mass can be written approximately as:

$$\frac{\partial m'_g}{\partial r} = -\frac{\partial \rho}{\partial t} \qquad (4.10)$$

The mass flux, m'_g, at any spatial location and time can be calculated by integration of equation (4.10).

Equation (4.9) is modified to its final form by expanding the first three terms, substituting in the specific heat and the continuity equation and rearranging. This results in

$$\rho C_p \frac{\partial T}{\partial t} = \frac{1}{r}\frac{\partial}{\partial r}(k_r(T) r \frac{\partial T}{\partial r}) - m'_g C_{pg} \frac{\partial T}{\partial r} - \frac{\partial \rho}{\partial t}(\phi + h - h_g) \qquad (4.11)$$

where

C_p is the specific heat of the material (J/kg°C);

C_{pg} is the specific heat of gas (J/kg°C).

Equations (4.3),(4.10) and (4.11) form a set of non-linear partial differential equations in polar coordinate which may be solved simultaneously for ρ, m'_g and T, respectively.

The boundary conditions on the exposed and unexposed sides of a pipe may be

a prescribed temperature or radiative and convective boundary condition. As previously, in order to exclude the uncertainties of the heat transmission rate from the fire to the samples, the measured temperature was used at the exposed outer surface. While for the unexposed inside, an adiabatic surface is assumed due to the heat capacity of the inside air being negligible.

The equation (4.11) was solved by a simple and effective numerical scheme, namely the 1-D explicit finite difference method. By using the energy balance technique, the finite difference equation for an interior node can be obtained:

$$T_m^{i+1} = T_m^i + \frac{2\Delta t}{\rho C_p[(r_m-\delta r_1/4)\delta r_1+(r_m+\delta r_2/4)\delta r_2]}\cdot[k_{m,m+1}$$
$$(r_m/\delta r_2+0.5)(T_{m+1}^i-T_m^i)+k_{m-1,m}(r_m/\delta r_1-0.5)(T_{m-1}^i-T_m^i)] \qquad (4.12)$$
$$-\delta\rho(\phi+h-h_g)/\rho C_p$$

Since the thermal expansion is required to be included into the model, the spatial interval between the nodes will change according to the temperature, despite the nodes being initially uniformly spaced. Six mesh nodes across the thickness of pipe were used. It is assumed that the inside surface does not move during expansion at high temperature. The second term on the right hand side of equation (4.11) can be ignored under the powerful heat impingement on the pipe experienced during a furnace fire test.

For node 1 on the inside surface,

$$T_1^{i+1} = T_1^i + \frac{2k_{1,2}(r_1 + 0.5\delta r)\Delta t}{\rho C_p (r_1 + 0.25\delta r)(\delta r)^2}(T_2^i - T_1^i) - \frac{\delta\rho(\phi + h - h_g)}{\rho C_p} \qquad (4.13)$$

4.5 Model for the Intumescent coatings

As described above, the heat transfer analysis for the intumescent coating GRP pipe under fire is a complex task due to the physical and chemical processes are concurrent. Therefore, several idealizations were made:

1). The intumescent material is assumed to be homogeneous and the transmission of heat and mass is only in the radial direction of the cross-section. Then, for a straight pipe, the problem is one dimensional.

2). There is thermal equilibrium between the decomposition gases and the solid material and there is no accumulation of these volatile gases in the solid material.

3). The fissures that occur in the residual char are ignored in the model. Only the average performance was taken into considered.

Based on these assumptions, a one-dimensional energy equation in a coated pipe undergoing thermal decomposition is formulated which expresses a balance

between the transient energy accumulation rate, with the sum of the rates of conduction, pyrolysed convection, and the energy sink due to pyrolysis and the heat released by volatile combustion

$$\frac{\partial}{\partial t}(mh) = \frac{1}{r}\frac{\partial}{\partial r}(k_r r\frac{\partial T}{\partial r})\Delta r\Delta A - \frac{\partial}{\partial r}(m'_g h_g) - \phi\frac{\partial m}{\partial t} \qquad (4.14)$$

in which $R_1 \leq r \leq R_2$, for $t > 0$.

Where

m	is the mass (kg)
h	is the solid enthalpy (J/kg)
t	is time (s)
r	is the polar coordinate (m)
T	is the temperature (°C)
k_r	is the thermal conductivity in radial direction(W/m°C)
h_g	is the enthalpy of gas(J/kg)
m'_g	is the mass flux of gas (kg/m^2-s)
ϕ	is the heat of reaction (J/kg).
R_1,R_2	are the inside and outside radii respectively.

The mass of intumescent material is assumed to be composed of two parts

$$m = m_a + m_c \qquad (4.15)$$

where m_a is mass of active material and m_c is the mass of residual char.

The rate of decomposition of the active material is assumed to conform to a mean reaction which is described by a single first-order Arrhenius function

$$\frac{\partial m_a}{\partial t} = -A m_a exp(-E_A/RT) \qquad (4.16)$$

If the accumulation of gases is ignored, the conservation of mass is given by

$$\frac{\partial m}{\partial t} = \frac{\partial m_a}{\partial t} = -\frac{\partial}{\partial r}(m'_g)\Delta r \Delta A \qquad (4.17)$$

Following the treatment of [4.11], the amount of expansion of the intumescent coating is associated with the mass loss:

$$\Delta r = \Delta r_0 [1 + (E_{max} - 1)(\frac{m_0 - m}{m_0 - m_c})^n] \qquad (4.18)$$

where

m_0 is the original mass

m_c is the char mass

m is the current mass

E_{max} is the maximum expansion factor

n is the exponent which describes the dependence of expansion on the change in mass from m_0.

Equation (4.14) is modified to its final form by expanding the terms, substituting in the specific heat and the continuity equation, and rearranging. This results in

$$mC_p\frac{\partial T}{\partial t} = \frac{\partial}{\partial r}(k_r\frac{\partial T}{\partial r})\Delta r\Delta A + \frac{k_r}{r}\frac{\partial T}{\partial r}\Delta r\Delta A$$
$$-m'_g C_{pg}\frac{\partial T}{\partial r}\Delta r\Delta A - [\phi + h - h_g]\frac{\partial m}{\partial t} \qquad (4.19)$$

where

C_p is the specific heat of material (J/kg°C);

C_{pg} is the specific heat of gas (J/kg°C).

The initial conditions for $R_1 < r \leq R_2$, at t = 0 are

$$T = T_i; \quad m = m_0; \quad m'_g = 0 . \qquad (4.20)$$

where T_i is initial temperature (°C);

Equations (4.16) to (4.19) form a set of non-linear partial differential equations which may be solved simultaneously for m, m'_g and T respectively.

The boundary conditions on the exposed outer side of a pipe could be either a prescribed temperature or a radiation and convection boundary condition. To exclude the uncertainties of the heat transmission rate from the fire to the samples under test, the measured temperature was used as the boundary condition at exposed side. While for the unexposed inner surface, the adiabatic condition is assumed because the ends of pipe were blocked and the specified heat capacity of the inside air is negligible.

The equation (4.19) was solved by a simple and effective numerical scheme, namely the explicit finite difference method. By using the energy balance technique, the finite difference equation for a typical interior node i in the intumescent layer can be obtained:

$$T'_i = T_i + [\, k_{i-1,i}\Delta\theta(r_i/\Delta r_{i-1}-0.5)(T_{i-1}-T_i) + k_{i,i+1}\Delta\theta(r_i/\Delta r_i+0.5)(T_{i+1}-T_i) - \dot{m}_g C_{pg}\Delta\theta r_i(T_{i+1}-T_{i-1})/2 - (\phi+h-h_g)\frac{\Delta m_i}{\Delta t}]\frac{\Delta t}{m_i C_p} \qquad (4.21)$$

where a prime $'$ denotes the temperature at the next time step.

CHAPTER 5

Effects of Intrinsic Properties of Materials

5.1 Conventional Thermal Properties

To understand the thermal response of the components of construction to the high temperatures experienced in a fire, it is important to have a knowledge of the thermal properties of materials and their changes with temperature. The difference in performance of insulation materials is mainly determined by their capability to attain a high surface temperature without conducting significant heat into the substrate. For simple systems it may be adequate to say that it is the rate of deterioration of the material properties which determines the fire resistance that the construction is capable of providing. It is well known that the values of the thermal properties of the constituent materials play a crucial role in the numerical modelling of heat transfer in a construction element. A knowledge of the variations of thermal properties with temperature and other circumstances is essential for the prediction of the rate of heat transfer into the construction. The conventional thermal properties which will be considered in this section refer to *thermal conductivity*, *specific heat* and *emissivity*. For most materials, these properties are temperature-dependent. Among them the thermal conductivity of the material has the most significant effect on heat conduction. It is found

that even a relatively slight variation of the conductivity can cause a substantial change in the predicted temperatures.

Heat transmission solely by conduction can take place only in non-porous, non-transparent solids. In porous solids (most construction materials) the mechanism of heat transmission is a combination of conduction, radiation and convection. The thermal conductivity for such solids is, in a strict sense, merely a convenient empirical factor that makes it possible to describe the heat transfer process with the aid of the Fourier law. In this sense, the thermal conductivity is sometimes called the *effective (or apparent)* thermal conductivity. The effective thermal conductivity of most materials is a sensitive property relating to many factors. These factors could be the temperature, the density, its gradient, the moisture content, the degree of crystallinity, the average grain size, the mix proportions for heterogeneous materials and the conductivities of its constituents, the porosity of porous materials, and the type of fluid within its pores, etc. Therefore, in spite of the many efforts that have been devoted to the determination of the effective thermal conductivity of various materials under different circumstances for about a century, total success has yet to be achieved[5.1-3]. It is easy to understand why there are so many existing diverse and disparate data for some materials.

The surface emissivity of the material is also important as this will determine how much heat will be gained from or lost to surrounding environment. It may also vary with temperature and material physical state. Some materials can achieve their effectiveness against certain types of fire by reflecting most of the fire radiation. For instance, aluminium can survive well in non-engulfed conditions and will stay cool for a longer time.

In order to determine the values of thermal properties directly and explicitly, various delicate experimental techniques are demanded. Since the direct experimental measurement is complicated and time-consuming (it is even necessary to make a distinction between conduction studies under steady state conditions and those under transient conditions), the current situation is that there is very little information available regarding the actual values to be used in analysis. It is therefore necessary to regard the determination of the material properties to be used in the analysis as an important part of this study.

An attractive possible solution to this problem is to extract material properties by numerical techniques through *systematically fitting the results given by* computation to the results of standard fire tests. The strategy which has been adopted here is that, at first, approximate thermal properties are assumed. These may be *derived form the literature or from the values provided by the* manufacturer. These are then refined in order to take into account variations with temperature, moisture, decomposition etc and to achieve a good correlation between the numerical model and the test results. Once the thermal properties under varying circumstances have been determined and agreed, the thermal behaviour of this material under a variety of environments and configurations can be modelled.

This prediction-correction method has been proved to be a successful procedure and is an important application of numerical techniques as practical results can be obtained at low cost and with remarkable speed.

The first material which was tested was mineral wool sheet. Mineral wool is

manufactured from long, non-combustible rock fibres bonded with a high performance binder. Mineral wool slabs are easy to handle, cut and install and incorporate high levels of thermal efficiency. The manufacturer, Pilkington[5.4] only supplied the values of thermal conductivity up to 300°C for the sheet used, namely type LR80 with a density of 80kg/m^3. The actual thermal conductivity which was derived from the test results is shown in Table 5.1 for temperature up to 1000°C. The values at other temperatures that are not listed in Table 5.1 are assumed to vary linearly between the two nearest temperatures given in the table. The specific heat is assumed to be 1000 J/kg°C.

The second material to be considered was Supalux, a Calcium-Silicate board reinforced with selected fibres and fillers. It is the product of the Cape Boards Limited. The manufacturer only supplies one value of thermal conductivity, namely 0.17 W/m°C[5.5]. It was found that the numerical simulation can not provide a satisfactory result when based on this constant conductivity. For this material, the piece-wise linear variation with values of 0.16 W/m°C at 10°C, 0.18 W/m°C at 500°C and 0.3 W/m°C at 800°C was found to give the best fit. The specific heat of calcium silicate board was chosen to be 1300 J/kg°C at 10°C and 800J/kg°C at 800°C. The moisture content in the tested sample was small and negligible. The emissivity of the surface was chosen to be 0.6.

The thermal properties of hygroscopic materials and combustible materials will display more complex patterns and they are discussed in the following sections.

5.2 Effects of Moisture Content

Most practical construction materials contain some water and this has a significant influence on the heat transfer mechanism and thermal properties. However, the mechanism of the combination of heat and moisture transfer in elements of construction is quite complicated. The process strongly depends on the temperature, moisture distributions, chemical reactions, multiphase mass transfer, permeability and nonlinear material properties[5.6]. Over past decades, several studies have been carried out which try to take the influence of moisture into account. Both sophisticated[5.9-10] and simple analytical models[5.11-12] have been proposed. Sophisticated models consider the convective and diffusive heat and mass transfer on the basis of an evaporation-condensation mechanism driven by pore pressure and moisture concentration gradients. Despite the much important work that has been done, there is still not a comprehensive and satisfactory theory of the subject, and the existing theories (to the best of the authors' knowledge) have not yet been able to find application in practice. The simple engineering approaches, which mainly concentrate on heat transfer and disregard mass flow and moisture pressure build-up, simulate the influence of moisture by considering the energy demand of evaporation. They are easier to apply and have the potential to yield an acceptable solution for the heat conduction problem. However, if these models were not set up or used properly, significant errors between prediction and experiment were often found at a temperature range of about 90°C to 150°C[5.7,5.8] for hygroscopic components exposed to fire.

During the heating of a hygroscopic material, a process of dissociation

(dehydration), vaporization and migration of moisture takes place. For the moisture to be evaporated, a certain amount of energy is needed, thus suppressing the temperature increase. The moisture content in the materials could be in the form of chemically or physically trapped water. The extra energy needed to vaporize the moisture then comprises two parts: the heat absorbed in dehydration process for chemical bonded water and the energy needed to drive off the water (including physically absorbed free water) from the material. Under atmospheric conditions, the heat of vaporization of water is 2.25×10^6 J per kg of water[5.13]. For most previous investigators this value was the only extra energy needed to get rid of the water. Since they neglected the energy needed to dissociate the chemically combined water and the additional energy consumed in the evaporation-condensation cycle, noticeable errors were incurred.

In combination with the finite difference and finite element technique, an improved engineering approach was developed in this thesis. As a example, Redland gypsum plasterboard[5.14] was considered first, in which the gypsum (calcium sulphate dihydrate, $CaSO_4\cdot2H_2O$) is of about 95% purity. Gypsum-board is one of the cheapest fire protection materials available, and normally has a high moisture content (more than 15% crystalline water and a small amount of absorbed free water). As gypsum is heated to temperatures in excess of about 95°C it begins to undergo a chemical reaction known as calcination, in which the chemically bonded water dissociates from the crystal lattice. The chemical equation for first the step is[5.15]

$$CaSO_4\cdot 2H_2O \rightarrow CaSO_4\cdot 1/2H_2O + 3/2H_2O \qquad (5.1)$$

Calcium sulphate hemihydrate ($CaSO_4 \cdot 1/2H_2O$) is commonly known as plaster of Paris. The energy absorbed in the this process is approximately 100KJ per kg of gypsum[5.15]. With further continued heating, the remaining water in the plaster is released as the hemihydrate undergoes dehydration to form anhydrous calcium sulphate, $CaSO_4$. Then an extra 50KJ per kg is further consumed. By the time the material reaches a temperature of around 155°C calcination in the board is usually complete.

According to the proposed approach, it is assumed that the moisture evaporation takes place during a temperature range, for example 95°C to 155°C at each point in the gypsum, and the latent heat energy of evaporation is then added into the specific heat of material. The average additional specific heat is obtained by

$$DC_p = \frac{2.25 \times 10^6 e}{\Delta T} \cdot \Lambda \quad (J/kg\,°C) \qquad (5.2)$$

where:

DC_p is the average additional specific heat

e is the moisture content expressed as a fraction by weight

ΔT is the magnitude of the given temperature interval

Λ is a correction factor.

Then for example, assuming the gypsum contains 20% water by mass, the energy needed to vaporize this water according the heat of vaporization (2.25MJ per kg water) is 450KJ per kg of gypsum. The additional energy required in the dissociation reaction (5.1) is 150KJ per kg of gypsum. According to this, Λ = 1.33 is established. The numerical analysis showed that although the result is

better than that with Λ = 1.0, the demanded energy is still under-estimated. Actually, it is found that the results with Λ = 1.8 give a satisfactory correlation to the experimental results. This means that extra energy is required for the moisture evaporation-condensation migration under high pressure.

In order to conform with the experimental measurement of the apparent specific heat[5.15] and in order to keep the numerical stability, a triangular variation of the additional specific heat is adopted as shown in Fig.5.1. Nevertheless, the total energy which is needed to evaporate the moisture, in fact, is not altered.

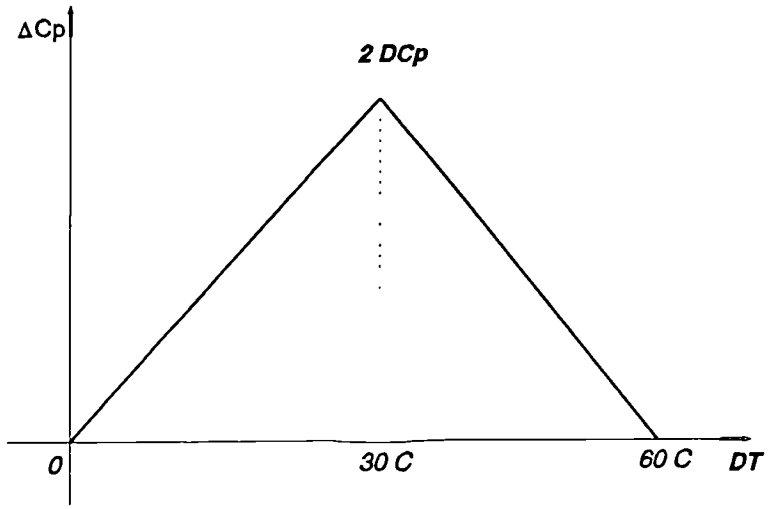

Fig.5.1 The variation of ΔCp in a temperature interval 60°C

In equation (5.2), the value of the temperature interval ΔT should be selected based on experiment. However, the most important parameter for the successful modelling is the total amount of absorbed energy and the final temperature development of modelling is not very sensitive to the value of ΔT.

Following this treatment, the rate of increase of temperature will be suppressed (but not halted as in traditional models) in the range of temperature ΔT, and a gradual increase of temperature during vaporization can be simulated.

No value of specific heat is given by Redland for their plasterboard. However reference[5.15] gave 950 J/kg°C for the specific heat of plasterboard with 3.4% free water of the mass of the gypsum specimens and 14.6% water of crystallization. Normally, the specific heat of a heterogeneous material can be weighted by the fractional extent of each component

$$C_p = \Sigma_{i=1}^{n} F_i C_{pi} \qquad (5.3)$$

where F_i is the weight fraction of each component and $\Sigma F_i = 1$.

Then according to formula (5.3), with specific heat of water taken as 4200 J/kg°C, the specific heat of dried plasterboard is 237 J/kg°C. This value is obviously too low for dried plasterboard. It can be concluded that a modification of (5.3) should be imposed for the chemical bonded water. Half of the weight fraction of the chemically trapped water is tried. Then the specific heat of totally dried plasterboard is set to be 629 J/kg°C.

Since the presence of moisture also has a significant effect on the thermal conductivity, the determination of the thermal conductivity of moist materials under fire is complicated. The thermal conductivity of building materials rises considerably when the materials are even slightly damp. It is not only because that some of the gaps in the solid matrix bridged by water, which is a better

conductor of heat than air, but also because additional heat can be transferred by the migration of moisture. The general expression for thermal conductivity and moisture content can be

$$k(M) = k(0) \cdot \Gamma(M) \qquad (5.4)$$

where $k(M)$ is the thermal conductivity at a moisture content M percentage by volume and $\Gamma(M)$ is the proportion factor.

The relationship between the proportion factor and the moisture content is not a linear one, but an empirical formula can be derived to adjust the measured k-value of masonry materials to an appropriate moisture content M based on a relationship recommended by Jakob[5.16]:

$$\Gamma = 1.0819 + 0.17675 \times M - 8.7812 \times 10^{-3} \times M^2 + 1.7617 \times 10^{-5} M^3 \qquad (5.5)$$

To reduce the error of Γ, the value $\Gamma = 1$ when $M = 0$ is not used in curve fitting.

The thermal conductivity, therefore, at an arbitrary moisture content can be determined by a simple mathematic algorithm manipulating equations (5.4) and (5.5) in the case where one reference thermal conductivity is known at a certain moisture content.

Three types of Redland plasterboard were examined[5.14]. They are Wallboard Type 1, Firecheck Type 5 and Firecheck Coreboard Types 4. Redland

plasterboard consists of a gypsum plaster core bonded between two strong liner pulp boards. The thermal conductivity of Wallboard provided by the manufacturer[5.14] is 0.20 W/m°C. The Firecheck plasterboard consists of a gypsum plaster core with glass fibres and fillers. The thermal conductivity of Firecheck according to the manufacturer is 0.24 W/m°C. Redland Firecheck coreboard consists of a gypsum plaster core with glass fibres and moisture resistant liner boards. The value of the thermal conductivity is 0.22 W/m°C. This has been confirmed by the measurements conducted recently by Dr. A.Simson in S t rd university. The values of these thermal conductivities are close to those quoted by another source[5.17] which gave the value of thermal conductivity between 0.15 - 0.27 W/m°C.

Nevertheless, these are the values of conductivities at room temperature. In fact the thermal conductivity will increase with increasing temperature at a certain moisture content[5.2]. On the other hand, the total moisture content is gradually reduced as heating proceeds during a fire. Therefore the final value of apparent conductivity should be the resultant of both effects. For the r plasterboard, it is found by numerical analysis that the effective thermal conductivity only displays a slight increase with temperature when in the moist state.

The thermal conductivity of a material in a dried state at room temperature could also be derived from (5.4) and (5.5). For dried materials, the fire resistance capacity usually degrades at elevated temperature. Then the value of conductivity will increase with increasing temperature. For the problem analyzed, a linear variation of thermal conductivity with temperature is considered as a reasonable assumption. Hence, for dried plasterboard, it is found that

$$k(T) = k(0) + 1.1 \times 10^{-4} \times T \ (W/m\,°C) \tag{5.6}$$

gave the best fit with the test data.

An interesting observation is that the values of thermal conductivity of gypsum board extracted by above analysis and numerical procedure, which was mainly done in 1993[5.18], is quite consistent with the results which were discovered later in reference [5.15] (1994) by using a commercially available thermal conductivity meter, as shown in Fig.5.2. The capability and potential of the computational technique is astonishingly exhibited in this representative example.

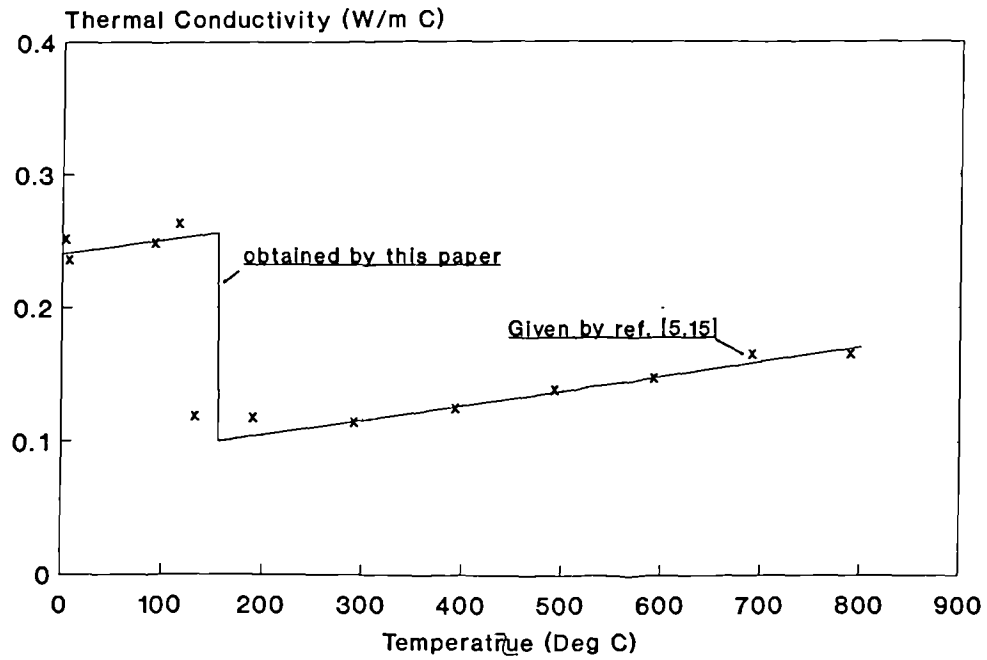

Fig.5.2 The Comparison of Thermal Conductivity of Gypsum Board

The plasterboard is usually covered by paper so that surface emissivity selected should be the value for liner boards manufactured from long fibre pulp. The value 0.8 is chosen[3.1] for the unexposed face. On the exposed side, the value of 0.4 is assumed due to the board burning away during fire exposure. The density of plasterboard was measured before the test(see Table 5.2). The numerical program calculates the new density automatically as water is driven off.

Based on the above-mentioned treatment and properties, a good correlation with the experimental results was obtained (for details, see Chapter 6).

The second material which was tested is concrete. A two-dimension model based on the finite element method for the concrete deck slabs will be described in Chapter 8. For the present studies, only simple flat panels with low moisture are considered. These were made from a mixture of ordinary Portland cement, normal aggregate and febspeed by an undergraduate student. Before fire testing, the concrete panels were dried in an oven to remove most of the moisture. However there was still a small residual water content which was measured to be 0.9% by weight. Quite similar to the behaviour of gypsum, the hydrated cement contains free calcium hydroxide which loses its water at high temperature, leaving calcium oxide. Therefore extra heat for dewatering and dehydration is needed. According to the guidelines given by the ECCS[2.5], the thermal conductivity of concrete (with 0.9% moisture content) is chosen to be 1.5 W/m°C at room temperature and approaches 1.02 W/m°C at high temperature. The values for the completely dried concrete are 1.09 to 0.85 W/m°C. The specific heat is between 900 - 1300 J/kg°C and surface emissivity is 0.8. An excellent agreement between theory and test was again obtained (see Chapter 6).

Another material which we tested with moisture content is Salford Voidfill. The constituent materials are those known to have good fire resistance: namely perlite and high alumina cement. Mixtures of 40% perlite filler, 60% cement and water have been used to cast 50mm thickness samples which were fired up to 1125°C. Because the thermal properties of this material are initially unknown, a systematical calculation was conducted to determine these values. It was found that the conductivity is around 0.07 W/mK with 10.6% water content at room temperature and its maximum value is 0.24 W/mK at high temperature. While the range of conductivity is 0.04 - 0.18 W/mK in a totally dried state. The specific heat of dry material is 1000 J/kg°C approximately.

It should be noticed that the correction factor Λ may have a slight variation under different circumstances. According to the previous explanation, the constituents of the material and the configuration of the component may affect its magnitude.

Based on this modified treatment and chosen properties, reasonable agreements with test results even at high levels of moisture content(up to 20% by weight) have been obtained (see Chapter 6).

5.3 Kinetic Parameters for Pyrolysis

The thermal response of an organic material is significantly sensitive to the stage of decomposition and the rate of density change. This is to be expected since the rate of energy consumption and the thermal and transport properties of the

material are functions of the constituents and the rate of decomposition. The values of kinetic parameters A and E_A in equation (4.3) will determine the intensity and duration of decomposition corresponding to a given intensity of heat flux. Since the in-situ measurement of parameters A and E_A under the desired thermal condition is intricate, the current practice is to use estimated values which give good agreement between simulation and experiment. It is found that A and E_A depend on the rate of heating dT/dt. Therefore, for better modelling without making the model unnecessarily complicated, two sets of values of A and E_A are assumed for inner hot and outer cold sections of panel respectively, as shown in Table 5.3 and 5.4. The values of activation energy are generally consistent with the results for plastic resin quoted by Samuel L. Madorsky in his book[5.21].

Despite the fact that the parameters A and E_A have their own meaning, altering either A or E_A can give a similar result for mass loss rate, as shown in Figs.5.3-5. As an example, the initial values A and E_A are set as A = 800/s and E_A =58000 J/mol (Fig.5.3). Then either by changing the A to 400/s or E_A to 62000 J/mol, almost identical results are obtained (Figs.5.4 and 5.5).

In reference[4.5], Henderson *et al* employed a distinct approach in which they separated the pyrolysis ratings into two separate regions according to the ratio of m/m_o where m is the remaining mass and m_o is the initial mass.

The variation of thermal conductivity will also display a rather more complicated pattern because it will be changed with temperature and the stage of decomposition. It also depends on the type of resin used and the ratio of resin

and glass for GRP material. One reference[5.19] gave the values of thermal conductivity of GRP from 0.2 to 0.3 W/m°C. Another reference[5.20] gave the values of conductivity from 0.25 W/m°C at 20°C to 0.35 W/m°C at 1200°C. The general expression for thermal conductivity is assumed to be a linear function of temperature here

$$k = k_o + \alpha T \qquad (5.7)$$

for different stages of decomposition. For a tested GR polyester panel, from the starting of the test to the point where the char was consumed, the value of k_o is 0.26 W/m°C and α is -1.356×10^{-4} W/m°C^2. The negative value of α indicates that the thermal conductivity deceases due to the low conductivity of the char. As heating continues, the char will be oxidized and eroded away, leaving the glass-fibre alone. During this phase, k_o will retain its value at the end of the last stage and $\alpha = 2.0\times10^{-3}$ W/m°C^2. The conductivity will now increase as the temperature increases due to the char being lost and the crumbling of the glass mat.

For phenolic laminate, the thermal conductivity is fixed as 0.28 W/m°C until the char is totally consumed. After that, the thermal conductivity follows equation (5.7) with $\alpha = 1.8\times10^{-3}$ W/m°C^2.

The actual variation of thermal conductivity is unknown and might be more complicated, but for simplicity, it is assumed to be a linear function of temperature during each stage.

One reference[5.19] gave the specific heat of GRP as 950 J/kg°C and the emissivity as 0.9. The specific heat of WR polyester laminate is also assumed to be a linear function of temperature here: $C_p = 1000 + 0.8 \times T$ (J/kg°C). The heat of decomposition is -2.5×10^6 J/kg and the emissivity of the panel is 0.8. The specific heat of WR phenolic laminate is: $C_p = 1300 + 0.3 \times T$ (J/kg°C). The heat of decomposition is -1.6×10^6 J/kg and the emissivity of the laminate is 0.85. The thermal expansion coefficient is chosen as 4×10^{-4} (1/°C) for both of them. These data have been estimated on the basis of information either found in the literature or by experiment.

For Ameron glass-reinforced epoxy 2000M pipes, the kinetic parameters which were used in the calculation were: $A = 800\ s^{-1}$, $E_A = 56{,}000$ J/mol for cellulosic fire and $A = 1200\ s^{-1}$, $E_A = 52{,}000$ J/mol for hydrocarbon fire. The thermal conductivity is set as 0.24 W/m°C, until the char is totally lost. Then the conductivity will follow the equation

$$k = 0.24 + 1.2 \times 10^{-3} T \quad W/m\,°C \tag{5.8}$$

The increase of conductivity in this stage is due to the char being lost and the cracking of wound glass-fibre. The glass-fibre content in the pipe by volume is about 41%. The variation of specific heat with temperature is

$$C_p = 1270 + 0.230 \times T \quad (J/kg\,°C) \tag{5.9}$$

The heat of reaction Q is chosen as -3×10^4 J/kg and the thermal expansion

coefficient is 5×10^{-4} (1/°C).

The second type of GRP pipe which we tested were BP phenolic pipe. The kinetic parameters which were used in the calculation were: A = 1500 s^{-1} and E_A = 50,000 J/mol. The conductivity is found to be 0.3 W/m°C until the char is totally lost. Under hydrocarbon fire condition, the char will be oxidized and consumed quickly, and leave wound glass-fibre alone. Then from that point, in equation (5.7), the value of k_o will be 0.3 W/m°C, and α will be 1.6×10^{-3} W/m°C^2.

The glass-fibre content in the pipe by volume is estimated to be 57%. The specific heat of GR phenolic material is also assumed to be a linear function of temperature:

$$C_p = 1115 + 0.484 \times T \quad (J/kg\,°C) \qquad (5.10)$$

The heat of reaction Q is chosen as -5×10^4 J/kg and the thermal expansion coefficient is 4×10^{-4} (1/°C).

For intumescent materials, both the famous Pitt-Char and reinforced Pitt-Char were tested. Pitt-Char is an epoxy based material and is sometimes reinforced with glass fibre. From above analysis, it can be seen that the thermophysical and kinetic properties of intumescent materials have a significant influence on the heat transfer rate. Unfortunately, most of these data are not available. One possible solution for this problem is to undertake the direct experiment measurement individually for each parameter. However, from the work described in reference[4.10], one conclusion is, although the authors tried to determine all

thermophysical and kinetic properties of intumescent materials by experimental measurement, the final results of temperature development given by the theoretical analysis was still unsatisfactory. The problem might be caused by the fact that these parameters are very sensitive to the heating rate, configuration and ambient environment, and it is almost impossible to copy these conditions in measurements recorded during real fire tests. Therefore, estimated values were used and refined which can give good agreement between the experimental and numerical results. The adopted thermophysical parameters which were used in numerical calculation for Pitt-Char and reinforced Pitt-Char are listed in Tables 5.5 and 5.6.

The numerical simulations which were based on above quoted parameters all present a satisfactory correlation with the experimental outcomes (see Chapter 6).

Table 5.1 Thermal conductivity of mineral wool

Temperature (°C)	Conductivity (W/m°C)
10	0.034
50	0.037
150	0.054
200	0.066
250	0.080
300	0.097
350	0.108
400	0.113
450	0.150
550	0.320
600	0.520
650	0.820
700	1.000
1000	1.200

Table 5.2 Data for plasterboard specimens

Sample	Thickness (mm)	Density (kg/m^3)	Moisture Content (%) (by weight)	Conductivity (moist state) (W/m°C)
1a	12.5	836.4	17.5	0.20
2b	15.0	825.2	20.2	0.24
3c	25.0	856.4	19.4	0.22
4c	25.0	726.2	6.4	0.164†

† Calculated by equ.(5.4) based on the reference conductivity 0.22W/m°C

Table 5.3 Kinetic parameters of GR Polyester panel

	Cellulosic Fire		Hydrocarbon Fire	
	A	E_A	A	E_A
outer cold section	400	70000	600	68000
inner hot section	1200	54000	1200	54000

Table 5.4 Kinetic parameters for WR Phenolic laminate in a hydrocarbon fire

	A	E_A
outer cold section	600	60000
inner hot section	1200	58000

Table 5.5 Thermophysical Data of Pitt-Char (length=100cm)

m_0	m_c	$k_r(10°C)$	$k_r(1050°C)$	$C_p(10°C)$	$C_p(1050°C)$
3.89	*1.5*	*0.3*	*0.05*	*1380*	*1000*
C_{pg}	ϕ	E_{max}	n	A	E_A
2000	-6×10^5	*3.33*	*0.2*	*2000*	*52000*

Table 5.6 Thermophysical Data of Reinforced Pitt-Char (length=100cm)

m_0	m_c	$k_r(10°C)$	$k_r(1050°C)$	$C_p(10°C)$	$C_p(1050°C)$
6.51	*4.35*	*0.3*	*0.16*	*1300*	*900*
C_{pg}	ϕ	E_{max}	n	A	E_A
2000	-6×10^5	*1.56*	*0.2*	*2000*	*52000*

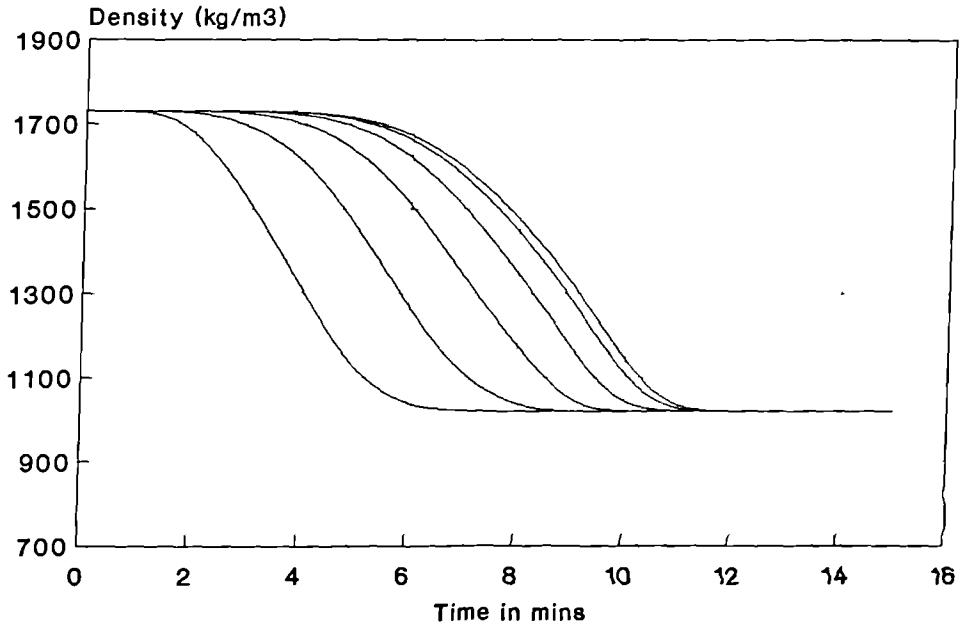

Fig.5.3 The Mass Loss Rate at
A = 800/s, Ea = 58000 J/mol

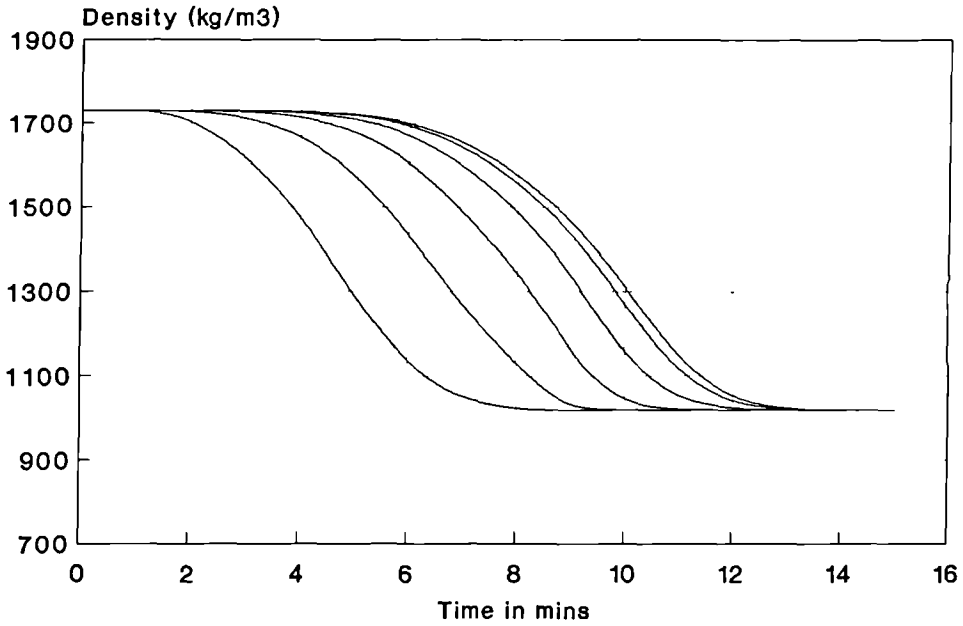

Fig.5.4 The Mass Loss Rate at
A = 400/s, Ea = 58000 J/mol

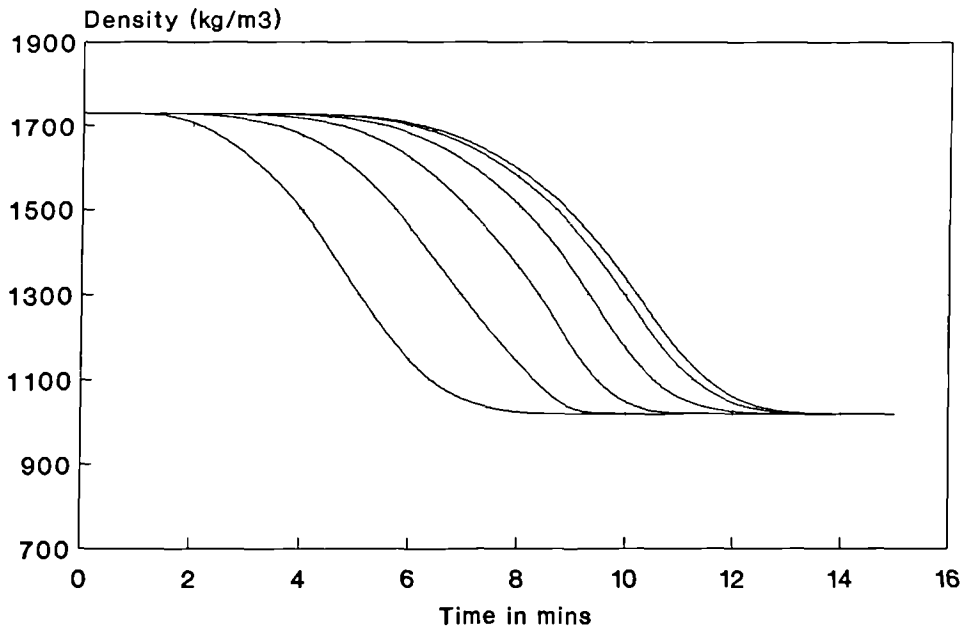

Fig.5.5 The Mass Loss Rate at
A = 800/s, Ea = 62000 J/mol

CHAPTER 6

Fire Test Results and The Verification of Numerical Modelling

A description of the fire test facilities and the procedures used is given in a supplement at the end of this thesis.

6.1 'Traditional' Fire Resistant Panels

To validate the accuracy of the numerical modelling and to determine the fire performance of different materials, a number of standard fire resistance tests were carried out for the materials which were described in Chapter 5. The 'simulated fire' tests were, and will continue to be, the principal means of affirmation. Panels with different thicknesses and moisture contents have been tested under the condition in which the temperature of a gas-fired furnace was controlled to follow the BS476 cellulosic time-temperature curve[1.1]. The computer program which controls the furnace uses a continuous PID three term closed control loop system. The three terms are Proportional, Integral and Derivative. By acting on an error signal E(t), which is the difference between the instantaneously required temperature and the measured furnace temperature, the PID method will achieve continuous control with a good accuracy[6.1].

The panels, most of them with an area of 300×300mm^2, were clamped in a vertical position across an aperture in the door of the furnace with one side exposed to the furnace environment, and open to the ambient air on the other

side. The ambient air temperature in the general vicinity of the test construction fell into the interval of 5°C to 40°C specified by the standard[1.1]. The temperatures of the exposed and unexposed sides of the panels and furnace were recorded on hard disc every 20 seconds by the computer. The readings on the centre of the exposed and unexposed sides were adopted to simulate the one-dimensional heat transfer behaviour. According to BS476:part 20, there are two fire resistance criteria for insulation failure based on the measured temperatures on the unexposed face[1.1]. One criterion is that the mean unexposed face temperature should not increase by more than 140°C above its initial value. Another one is that the temperature recorded at any position on the unexposed face should not exceed 180°C above the initial mean unexposed face temperature. Because only the temperature at the centre of unexposed face, which is the highest temperature on the surface, was measured, the second criterion was adopted as an indication of material performance.

The thermal model was verified in two parts, separating the influence of two sets of important parameters, namely the parameters describing conduction in the panel and the parameters describing heat transfer from the furnace to the specimen by convection and radiation. First, the heat conduction in the panel was examined by applying the measured hot face temperatures as the hot side boundary condition for the numerical simulation (first method specified in section 2.4). Secondly, the heat transfer rate from the furnace to the specimen was calculated on the basis of the furnace temperature or the standard curve and the assumed heat transfer parameters. In the numerical modelling, the cross-section of each panel was subdivided to give six equally spaced nodal points. Some typical results using the thermal properties quoted in Chapter 5 are

presented below.

Specimen 1. *Mineral Wool Sheet*

A Pilkington rockwool sheet with a thickness of 25mm was tested in the furnace. The measured temperature profile is shown in Fig.6.1 (page 108). According to the previous definition, the insulation failure time for this sheet is 15 minutes. The recorded hot face temperatures were employed as prescribed boundary conditions in numerical analysis. The cold face temperature of sheet was calculated by both finite difference(FDM) and finite element methods(FEM). The description of finite element method will be given in Chapter 8 later. Fig.6.1 shows that the numerical results have a quite good agreement with the experimental results.

Specimen 2. *Calcium-Silicate Board*

The fire test results for this material are shown in Fig.6.2 and insulation failure time is now 9.68 minutes. Using the BS476 cellulosic temperature curve as the furnace temperature, the cold face temperature history of a calcium silicate board was again computed by FDM and FEM. The thickness of panel was 12mm and the density of material was 949 kg/m^3. It can be seen that the numerical results are consistent with the measured data and the adopted heat transfer coefficients from the fire to the specimen are appropriate (Fig.6.2).

Specimens 3-6. *Four Plasterboards*

The proposed moisture model was verified by testing four plasterboards with different thickness and moisture contents. The data for these panels are summarised in Table 5.2 and their insulation failure times are shown in Table 6.1.

Table 6.1 Insulation Failure Time for Plasterboard Specimens

Sample	Thickness (mm)	Moisture Content (% by weight)	**Insulation Time (mins)**
1a	12.5	17.5	**25**
2b	15.0	20.2	**32.4**
3c	25.0	19.4	**76**
4c	25.0	6.4	**45**

By comparison with the results from calc, the insulation time is extended considerably due to the moisture effect. The 'dwell' of temperature rising on the unexposed face of the samples can be easily seen from the water loss plateau in Figs.6.3 to 6.6.

In the finite difference calculations, the boundary condition on the exposed side of samples was prescribed by the measured temperature. The computed

temperature history on the unexposed side was then compared to the measured results (Figs.6.3 to 6.6). It can be concluded that the simulation of the moisture effect is quite successful in these cases. This demonstrates that the influence of different percentages of moisture on the fire resistance can be predicted accurately.

At the same times the selection of the associated thermophysical properties is also validated by these specimens. The reason for the small deviation between the calculated and measured data over 230°C on unexposed face is probably because some small cracks begin to appear on the exposed side of plasterboard at that temperature. Then the prerequisite of a continuum for the validity of equation (2.1) no longer exists.

The modelling of the heat transfer from the fire compartment to the specimen was also verified by plasterboard 3c. The selections of heat transfer parameters to simulate the heat transmission from furnace to specimen are specified in section 2.4. The computational temperature history of the exposed and unexposed faces are compared with experimental results in Fig.6.7. A good agreement is again noted.

Specimen 7. *Plasterboard and Calcium-Silicate Sandwich Panel*

The verification of the modelling for a multi-layer panel was carried out for this case. A Wallboard plasterboard, thickness 12.5mm with 6.4% moisture content, was combined with a calcium-silicate board, thickness 6mm in the dry state. The

insulation failure time is now 26 minutes. Identical thermal properties-temperature relationships as used in previous calculations were also applied in this case. The actual furnace temperature history was used as the exposed side boundary condition and the heat transfer parameters were the same as those in previous examples. Fig.6.8 shows that the numerical prediction gives a reasonable agreement with the measured result. The discrepancy might be caused by the assumption of perfect contact at the interface between two material layers.

Specimens 8-10. *Three Concrete Panels*

Three normal concrete panels, as described in the last chapter, were also tested. They have three different thicknesses namely 53mm, 77mm and 102mm respectively. The moisture content of the concrete was 0.9% by weight after oven drying. The corresponding insulation times were extrapolated as 42, 77 and 120 minutes. The measured temperature on the exposed side was also applied as the boundary condition in the numerical analysis. Excellent agreement was obtained when the numerical predictions were compared with the test data, as illustrated in Figs.6.9 to 6.11.

Specimen 11. *Salford Voidfill Panel with thin steel sheets*

In this sample, the combination of hygroscopic core material and impervious skins is investigated. The core material was Salford Voidfill No. 7D. Its density was

325kg/m^3 and its moisture content was 7.02%. Two thin (0.7mm) steel sheets were used as the faces of the sandwich panel during fire testing. The insulation time was extrapolated as 230 minutes. An excellent fire resistance time was therefore obtained.

The numerical calculations showed that the heat resistance of the thin metal sheets could be neglected. Nevertheless, the emissivity of these steel sheets should be adopted as actual surface emissivity of sandwich panel on the unexposed side. The measured furnace temperature was used as boundary condition on exposed side. The calculated cold face temperature development shows a reasonable agreement with experimental result (Fig.6.12).

An imperfection in this testing arrangement was that the periphery of the panel was not insulated. The moisture might escape more easily from the edges of this relatively small sample compared with large scale samples. Therefore, the magnitude of the thermal conductivity which was derived from this test might over-estimate the value that would be appropriate for an actual full scale panel.

6.2 WR Glass-fibre Reinforced Polyester Laminates

The polyester and woven roving glass-fibre laminate was made with thermocouples (K type) embedded inside the central region in order to measure the temperature profile history across the cross-section of the laminate, as shown schematically in

Fig.4.1. The resin which was used for the baseline testing was Crystic® 489 PA unsaturated polyester resin which based on isophthalic acid and supplied by Scott Bader Company Ltd. The reinforcement was Owens Corning E-glass-fibre woven roving at 600 gsm for the laminate. Since full-scale testing is very expensive, model-scale testing has again been developed for material characterisation tests of the type required for this investigation. The polyester laminates were made using a hand lay-up technique and cured at room temperature.

Series of both simulated cellulosic and hydrocarbon fire tests have been carried out. Since, in the small furnace that was used for these tests, it is impossible to achieve the initial rapid rate of temperature increase needed for hydrocarbon fire simulation, the furnace was first pre-heated to 900°C. During this heating period, the blanking panel was in place with a dummy piece of material covering the window opening. Immediately after switching off the furnace, the dummy piece of panel was removed and replaced by the test piece and the furnace was switched on again. A point on the hydrocarbon time-temperature curve was then attained within a few seconds.

The size of each panel was 380×380mm^2 with an area 250×250mm^2 exposed to the furnace. In the cellulosic fire tests, the average thickness of the panels was 5.9mm and the polyester resin content was 31% by weight. In the hydrocarbon fire tests, the average thickness of the panels was 6mm and the resin content was 33% by weight. The density of the resin was 1130 kg m^3 and that of the fibre glass was 2560kg/m^3. The catalyst for the resin was 1.5% by weight of Catalyst M. The number of glass plies in all of the panels was 13. Due to the scatter of

experimental data on a sample-to-sample basis, for both series of fire tests, several samples with the same configuration were tested and the average test results were compared with the analytical results. Normally the measured deviation among the samples was within 10% if there was no local delamination. The general trend of the temperature history, most noticeable on the unexposed side, was that, at the beginning of test, the temperature increased at a moderate rate. When the material started to decompose, the rate of temperature rise was slowed down due to the energy absorbed in pyrolysis. However, after the cracks appeared in the char and char was consumed, the temperature increased rapidly again (see Figs.6.13 and 6.14)

The cellulosic fire test lasted for about 40 minutes whereas, in a hydrocarbon fire, the 6mm thick panel can only survive for about 15 minutes. The time to insulation failure in a cellulosic fire was 7.8 minutes, while, in a hydrocarbon fire it was 5.3 minutes. This shows that, if thin GRP panels are used alone, they are insufficient to supply a satisfactory performance in terms of heat insulation under fire condition. Therefore, a good practice is to combine them with low density fire resistant core material in a sandwich construction. For this reason the single panel tests were sustained well beyond insulation failure until the cold face temperature reached about 400°C.

In the finite difference analysis of these tests, eight mesh nodes across the thickness of panel were used. The measured temperature-time history on the exposed was used as the hot face boundary condition.

Several points of interest were discovered in the course of the numerical

investigation. The first one is that the second term of the right side of equation (4.6) can be ignored. The physical meaning of this term depends on the direction of the flowing volatile. The main part of the volatile flows outward and has a cooling effect on the exposed side of panel while the inward flowing component enhances the heat flow to the inside. It was found that the net effect can be neglected by comparison with the powerful incident heat flux that was used in the furnace tests. It seems that the endothermic pyrolysis and poor conductivity of the char play a much more important role than internal convection. The second point is that the accuracy of results will be improved if the influence of thermal expansion is included into the model. The expansion will increase the thickness of panel and this has an obviously beneficial effect on the heat insulation of the panel. The thermal expansion coefficient was chosen as 5×10^{-4} (1/°C) for the glass-reinforced polyester panels considered here. This figure is obviously much larger then the value within the normal temperature range. When this effect is included in the finite difference analysis, the spatial interval Δx in the panel changes with temperature.

The reduction of resin density given by equation (4.3) can be seen from Figs.6.15 and 6.16 for both fire tests. Evidently that there are different mass loss rates for the inner hot part and the outer cold part of the panel. This coincides with the experimental observation of the two-peak shape of mass loss rate[6.2], and the final amount of remaining mass in the tested samples generally agrees with the numerical predictions.

The comparisons of the predicted and measured temperature profile histories for both series of fire tests are shown in Figs.6.13 and 6.14. The dashed lines

represent the transient temperature given by the numerical analysis for the same spatial location as the thermocouples. The agreement between them is reasonably good.

In order to gain further confidence in the numerical modelling, an additional verification test was designed using same basic materials but with a different resin content and thickness. For this test the resin content was increased to 42% by weight and the number of glass plies was 16. The final thickness of panel was measured as 8.8mm. A hydrocarbon fire test was carried out and the time to insulation failure was found to have increased to 7 minutes. As shown in Fig.6.17, good correlation between theory and experiment was again obtained by using the same thermal properties as previously.

Bearing in mind the rather steep thermal gradient inside the relatively thin laminate tested, the calculated results gave a quite good correlation with experimental measurements. It appears that the fire resistance of a GR polyester laminate in a standard fire test can be predicted well by the proposed computational treatment.

There are, nevertheless, some discrepancies between the calculated and measured results and these might have been caused by following factors. First, the numerical model does not account for all of the physical processes which occur within the material. For example, both the heat exchange between the volatile and solid material and the char shrinkage are partly neglected. Some processes, for instance moisture evaporation, were included in an implicit way (the value of decomposition heat contains some energy needed for moisture

evaporation). Secondly, there are some stochastic variations that effect the heat transfer and which are difficult to control such as the delamination and cracking in the material and the positions of the thermocouples relative to these effects. Delamination is also an important feature associated with the fire resistance of GRP laminates. However, for polyester laminate, it may be not so crucial as it is for phenolic laminate with a high moisture content. But it should, nevertheless, be mentioned as one possible reason for the discrepancies in Figs.6.14 and 6.17. Thirdly, most input data of the thermal properties were deduced on an empirical basis. It is well known that the value of the thermal properties plays a crucial role in the numerical simulation of heat transfer and, unfortunately, there are considerable practical difficulties in the explicit determination of material parameters at elevated temperature. Besides, some parts of the limited published data can not be used directly due to differences in the sample's preparation, test assembly and heat loading level. Hopefully, the need for such data will encourage more work to be carried out in this area. As more accurate property values become available, ever better results may be given by the proposed models.

An additional sandwich panel was tested with aim of achieving H120 fire resistance (H120 means the fire resistance time is 120 minutes under hydrocarbon fire test condition). It comprised two polyester laminate skins and a new Vermiculux core. This new Vermiculux is an 'improved' version of the calcium silicate board product by Cape Boards Ltd. Vermiculux readily absorbs water and this can significantly extend the measured fire resistance. In order to limit its influence, the 60mm thick Vermiculux panel was dried to constant weight ($504Kg/m^3$) at 110°C before the fire test. Nevertheless, it was found that 11.3%

of chemical bonded water was still held in the material. The polyester laminates consisted of 12 layers of glass with 67% glass content by weight. The thickness of the hot face skin was 6.4mm and the cold face skin was 6.2mm.

The fire test was conducted by another Ph.D student, David Dewhurst. The test result gave a fire resistance time of about 180 minutes which is comfortably in excess of the H120 target. The computational simulation was carried out by this author. The theoretical treatment included the model for polyester laminate, multi-layer configuration and moisture content. Excellent correlation between the theory and experiment was again obtained (Fig.6.18).

6.3 WR Glass-fibre Reinforced Phenolic Laminates

Two phenolic laminate specimens designated I and II, with thicknesses of 12.6mm and 11.7mm respectively, were tested under the hydrocarbon fire regime. The specimens were laid up by hand and subjected to 5 hours post cure at 80°C. In the numerical model, nine mesh nodes across the thickness of each laminate were used. It is assumed that, at 200°C, each node will split into two separated points in order to simulate delamination. Each time-temperature curve (except that at the outside surface) will then split into two as well, as shown in Fig.6.19. Due to the random position of the thermocouples relative to the position of the interstices in the thickness as well as spatially, the analytical result is considered to be acceptable if the measured temperature falls within the interval between the two disjointed curves.

The measured and calculated transient temperature distributions in laminate I are shown in Fig.4.3 and Fig.6.19, respectively. The comparisons of them are shown in Figs.6.20 and 6.21. The broken curves in the figures represent the transient temperatures measured by the thermocouples and the solid curves are the temperatures given by numerical simulation. It can be seen that the insulation time was increased to 30 minutes due to the delamination and the computational results gave a reasonable agreement with the test results.

The reduction of resin density given by equation (4.3) is shown in Fig.6.22 for different locations within the laminate. Due to the limitation of the test facility used, it was not possible to monitor the instantaneous amount of mass in the laminate. Nevertheless, the final amount of remaining mass of the specimen was measured, and it generally agreed with the numerical result.

In order to obtain further confidence in the numerical modelling, an additional validation was carried out for laminate II with a thickness of 11.7mm. Unfortunately, only the [illegible] at locations 1, 5 and 6(Fig.4.2) gave [illegible] temperature readings. This time the insulation time was found to be 28 minutes due to the thickness being slightly reduced. Fig.6.23 shows a good agreement between the numerical and measured results by using the same above quoted thermal properties that were used for laminate I.

These comparisons proved that delamination is an important phenomenon which is related to the fire resistance of phenolic laminate with a high moisture content and which must be considered in the analysis model if a reasonable result is to be obtained. A valid explanation has also been given for the somewhat bewildering

outcome of the temperature measurements obtained when testing the phenolic-woven roving glass laminate. It is evident that the fire resistance of GR phenolic laminate in a standard hydrocarbon fire test can be predicted by the proposed analytical treatment. The causes of the discrepancies are quite similar with those in polyester laminate and will not be repeated.

6.4 Glass-Reinforced Plastic Pipes

For pipe problems, the one-dimensional model in polar coordinate has been verified by the fire test results for Ameron glass-reinforced epoxy pipes and BP phenolic pipes with different thicknesses. These pipes with a length of 0.5-0.8m and with the two ends blocked by ceramic fibre were placed inside the large furnace, which can simulate the hydrocarbon fire without preheating. For hydrocarbon fire testing, the hydrocarbon time-temperature curve (Eq.2.20) was followed for an initial five minutes, then the gas supply was cut off. This is to simulate the start of a fire and the deluge response of the firewater system.

The outer and inner surface temperatures of the pipes were measured during the test. The temperature inside the pipe is probably the best way to monitor pipe performance under fire. The two dry Ameron pipes which were tested were a 3" 2000M pipe with an average thickness 5.7mm and a 4" 2000M pipe with an average thickness of 5.4mm. The corresponding times for the inner temperature to reach 200°C were 3.2 minutes for the 3" pipe in a cellulosic fire test and 1.7 minutes for the 4" pipe in a hydrocarbon fire test respectively (Figs.6.24 and 6.25).

The thermal properties which were used in calculation were specified in section 5.3. The measured temperatures on the outer surface was applied as a known boundary condition. The comparisons of calculated and measured temperatures on the inner surface for two pipes are shown in Figs.6.24 and 6.25. A good correlation between both results is obtained.

Furthermore, three unprotected BP pipes were tested under hydrocarbon fire with average thicknesses of 5.6mm, 7.7mm and 9.5mm respectively. The inside diameter approximately was 75.8mm and density of the GRP was 1900kg/m3. The corresponding times for the inside temperature to reach 200°C were 1.86, 2.75 and 3.5 minutes respectively. The thermal properties which were used in the computation were also specified in section 5.3. The measured temperature history on the outer surface was adopted as an essential boundary condition. The comparisons of calculated and measured temperatures on the inner surface for three different pipes are shown in Figs.6.26 to 6.28. The dashed lines represent the transient temperature given by the numerical analysis. A good agreement between calculated and measured results is again obtained.

Although, in order to keep the solution stable and to give good accuracy, the time step Δt is chosen as 0.1 sec, the whole running time is less than 1 minute on a PC486.

There are some deviations between the calculated and measured temperatures, especially during the cooling stage. These might be caused by the following factors. First, the numerical model does not precisely and explicitly account for all of the physical processes which occur within the material, such as the

combustion of the volatiles and micro-cracks. Secondly, most of the input data of thermal properties of material are given on an empirical basis and did not fully account for the difference between the heating up and cooling down stages. However, the results demonstrated that an appropriate set of data can produce a consistent result for GRP pipes with different thicknesses.

After an initial five minutes fire impingement, either natural or forced cooling by air was then commenced. It was noted that the pipe continued to smoulder or burn during cooling and that this resulted in continuing damage to the pipe. When the pipe had cooled sufficiently to be handled, its ability to hold water was investigated. All the above type pipes failed to hold water under pressure after fire testing. This revealed that the operable survival of unprotected thin GRP pipes under the furnace hydrocarbon fire condition for more than 5 minutes is unlikely. Therefore, an additional protection is needed and this can be achieved by one of following methods: a coating of fire-retardant intumescent material, mineral or ceramic wool wrapping, or by filling the pipe with stagnant or flowing water. These methods have proved that they can considerably reduce the damage to GRP pipes under fire as shown in next section typically for the intumescent coatings.

6.5 GRP Pipes with Intumescent Coatings

Two Ameron 4" epoxy pipes with the intumescent coating Pitt-Char and reinforced Pitt-Char were tested under a hydrocarbon fire. The Pitt-Char is also

an epoxy based material which is sometimes reinforced with glass fibre. The average thickness of un-reinforced coating was 7.5mm and reinforced coating was 11.5mm. These straight pipes with a length of 0.7m and the two ends blocked by ceramic fibre, were placed inside the gas-fire furnace which followed the hydrocarbon temperature-time regime(Eq.(2.20).

The outer and inner surface temperatures of the pipes were measured during the tests(Fig6.29 and 6.30). It can be seen that the temperature increase in the inner surface of GRP pipes was significantly delayed in comparison with the fire test result on the unprotected GRP pipe (Fig.6.25).

Although the reinforced coating is thicker than the un-reinforced coating, both of them gave the similar results. This is because, although the reinforcement enhanced the integrity and adhesion of the intumescent char, it also impeded the swelling of intumescence.

The adopted thermophysical and kinetic data for intumescent coatings were listed in section 5.3. The exponent n = 0.2 (see Eq.(4.18)) indicates that the expansion occurred early in the outgassing stage which is consistent with the experimental observations. The comparison between the measured and calculated temperature profiles on the inner surface of pipe shows that a good agreement is obtained (Figs. 6.29 and 6.30).

A relatively simple approach was developed to simulate the temperature history of GRP pipes with intumescent coatings under the standard hydrocarbon fire condition. The famous intumescent material Pitt-Char was chosen which normally

expanded 2-4 times the original thickness. The favourable correlation was obtained between the experimental and theoretical results. For different intumescent systems, it is anticipated that only the thermophysical parameters required adjusting in the modelling.

6.5 Conclusions

All above-mentioned numerical calculations were completed in a few minutes by a PC 486. The computational time is short and the cost is low. The convergence of the numerical results was proved to be satisfactory for mesh refinement and shorter time-steps. It can be concluded that the numerical results based on the proposed thermal models provided a favourable simulation of the fire resistance of panels and pipes and the cost for the numerical prediction is insignificant.

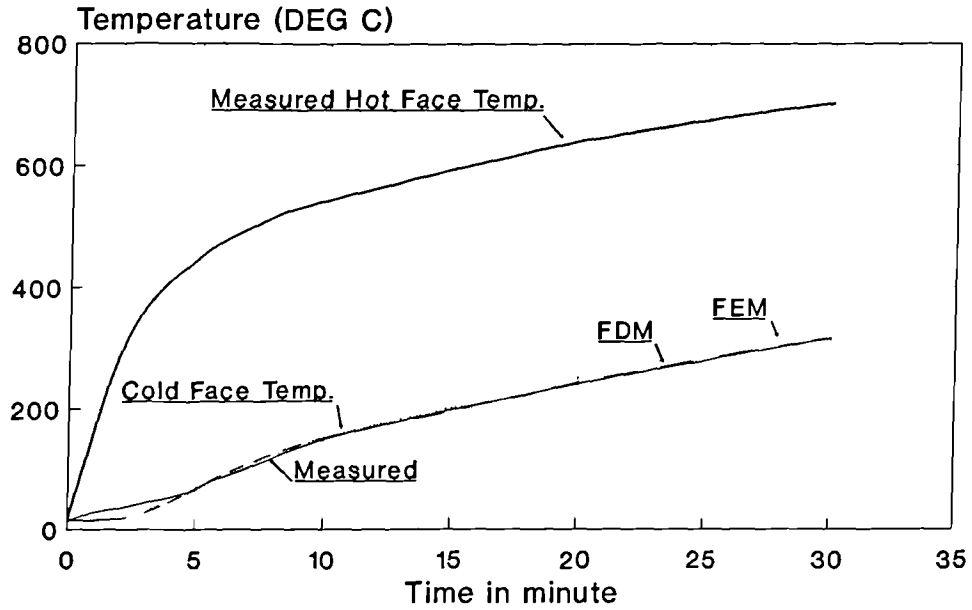

Fig.6.1 Fire Test of Mineral Wool Sheet
The thickness of sheet is 25mm

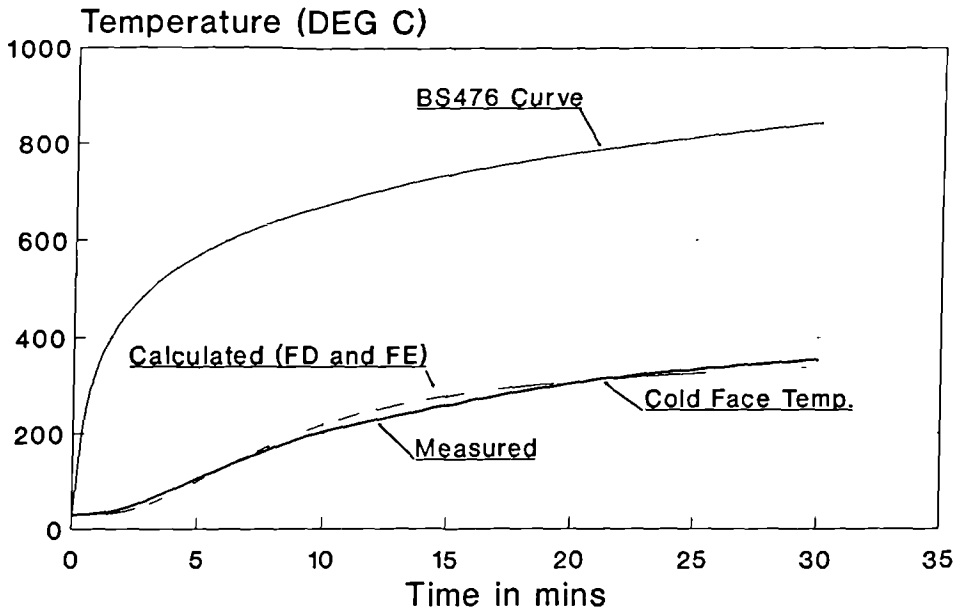

Fig.6.2 Calcium-Silicate Board (12mm)
BS476 Fire Boundary Condition

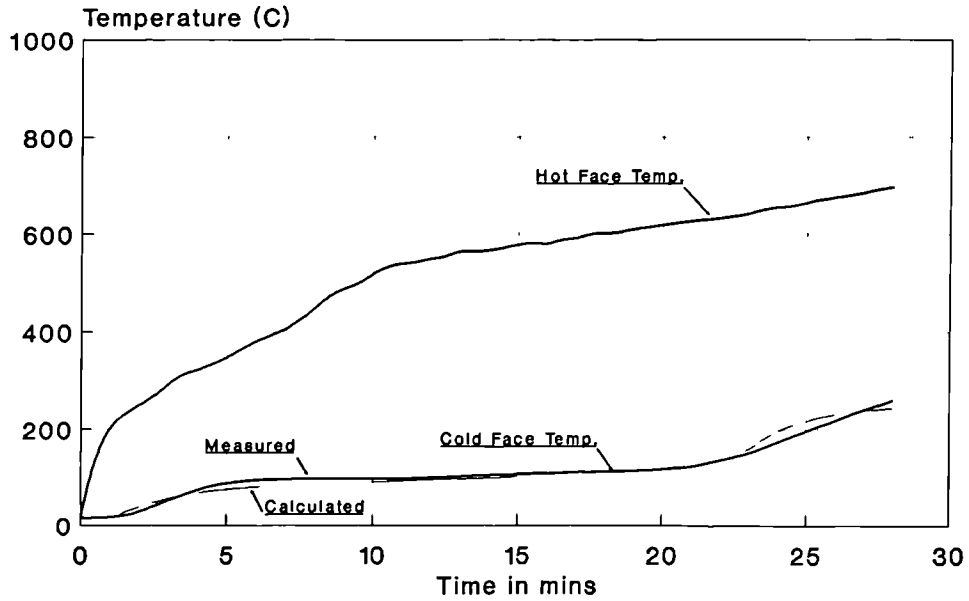

Fig.6.3 Fire Test of Plasterboard 1a
thickness 12.5mm, moisture content 17.5%
Computational and Experimental Results

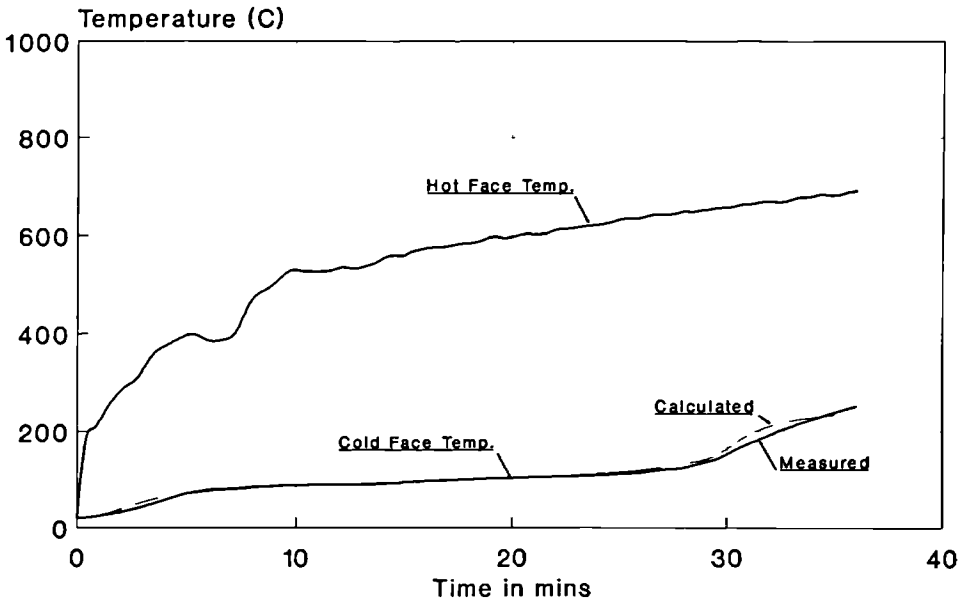

Fig.6.4 Fire Test of Plasterboard 2b
thickness 15mm, moisture content 20.2%
Computational and Experimental Results

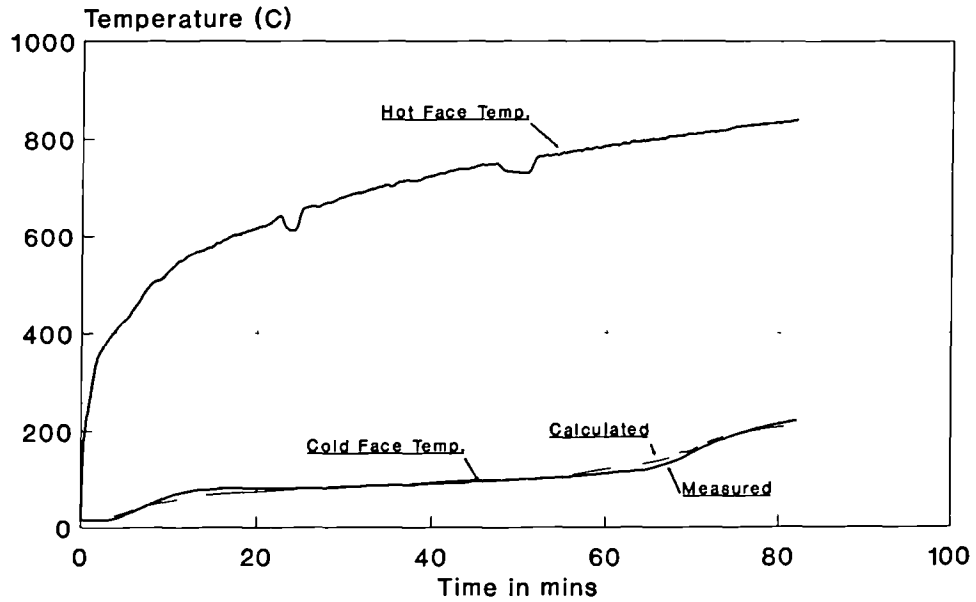

Fig.6.5 Fire Test of Plasterboard 3c
thickness 25mm, moisture content 19.35%
computational and experimental results

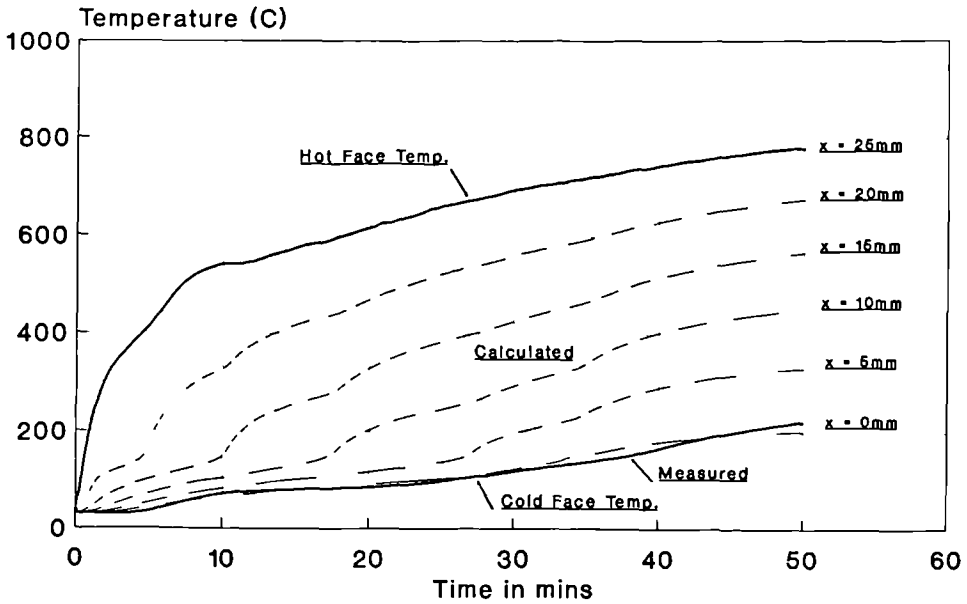

Fig.6.6 Fire Test of Plasterboard 4c
thickness 25mm, moisture content 6.36%
Computational and Experimental Results

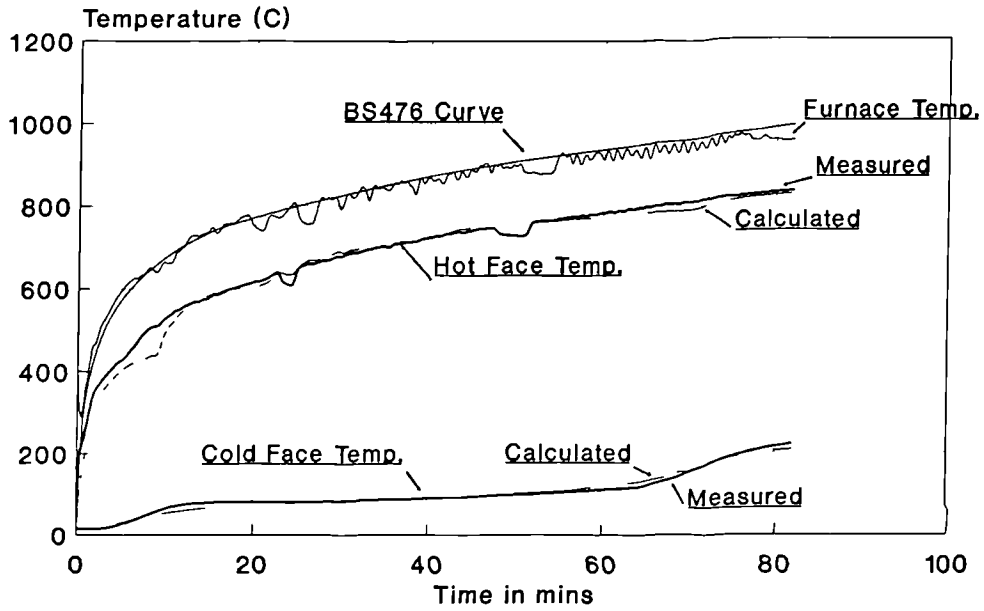

Fig.6.7 Fire Test of Plasterboard 3
fire boundary modelling

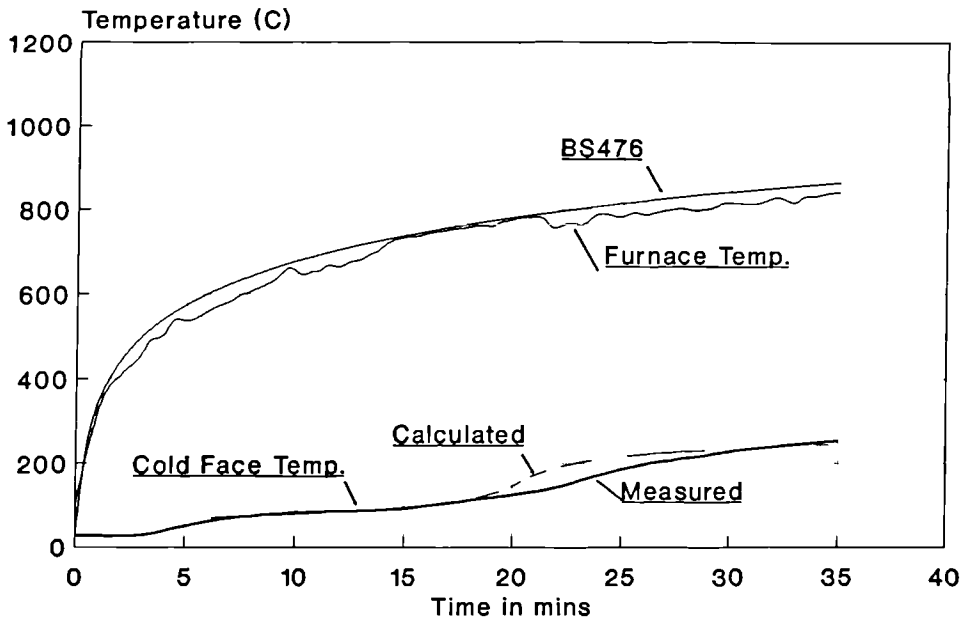

Fig.6.8 Fire Test of Multi-layer Panel
Plasterboard and Calsium-Silicate Board

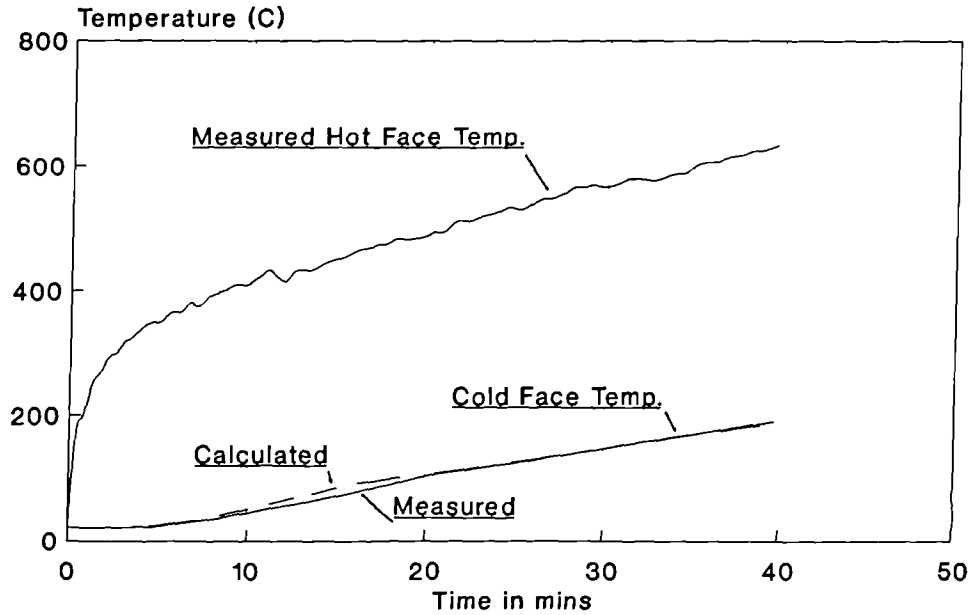

Fig.6.9 Fire Test of Concrete Panel 1
Thickness of panel is 53mm

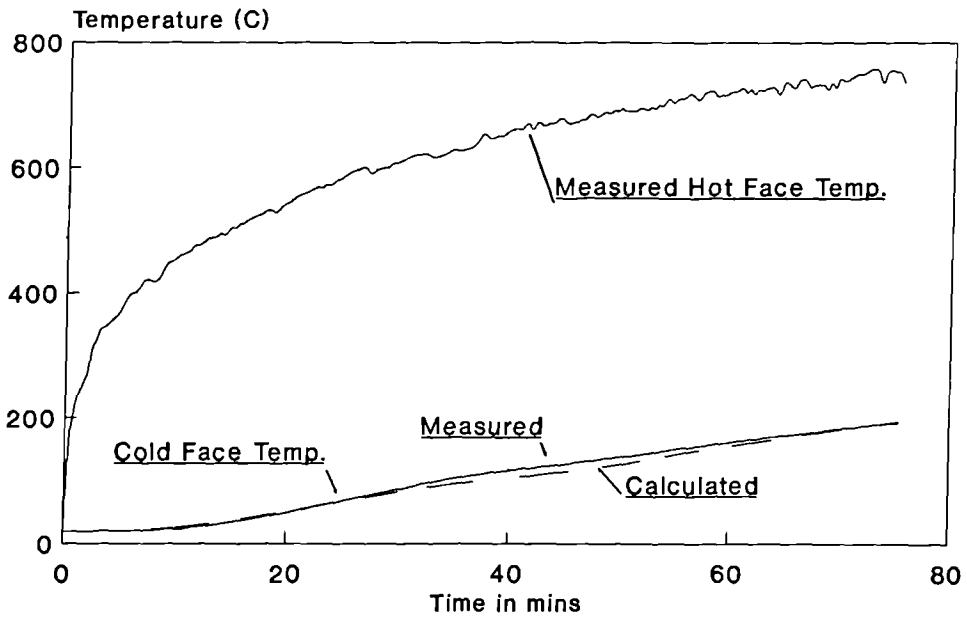

Fig.6.10 Fire Test of Concrete Panel 2
Thickness of panel is 77mm

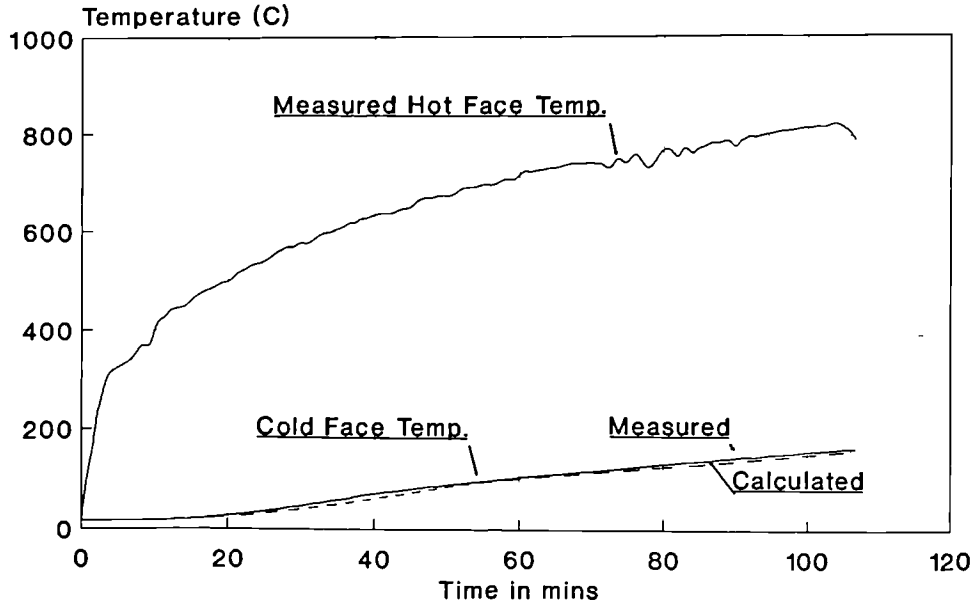

Fig.6.11 Fire Test of Concrete Panel 3
Thickness of panel is 102mm

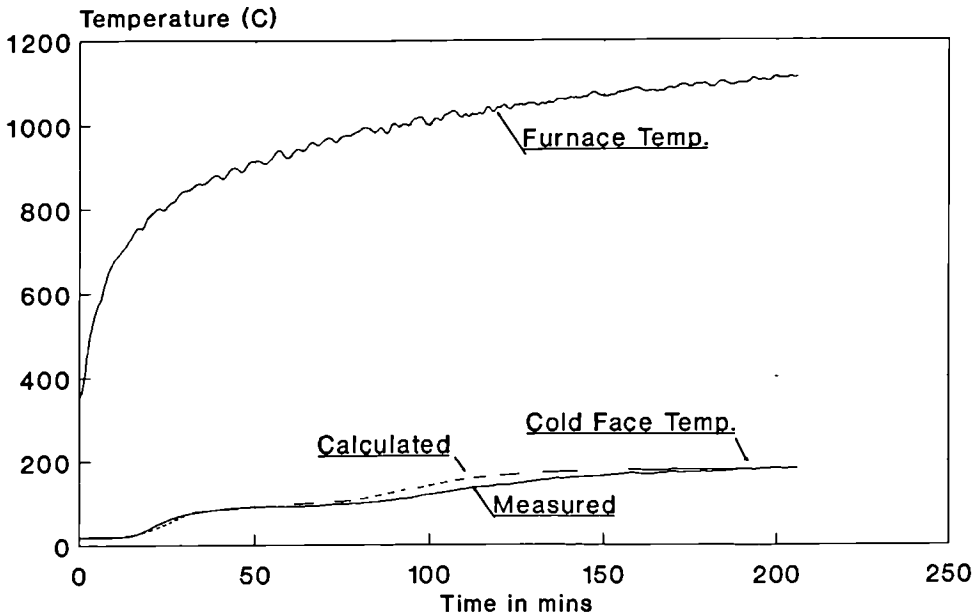

Fig.6.12 Salford Voidfill Panel No.7D
Thickness of panel is 50mm

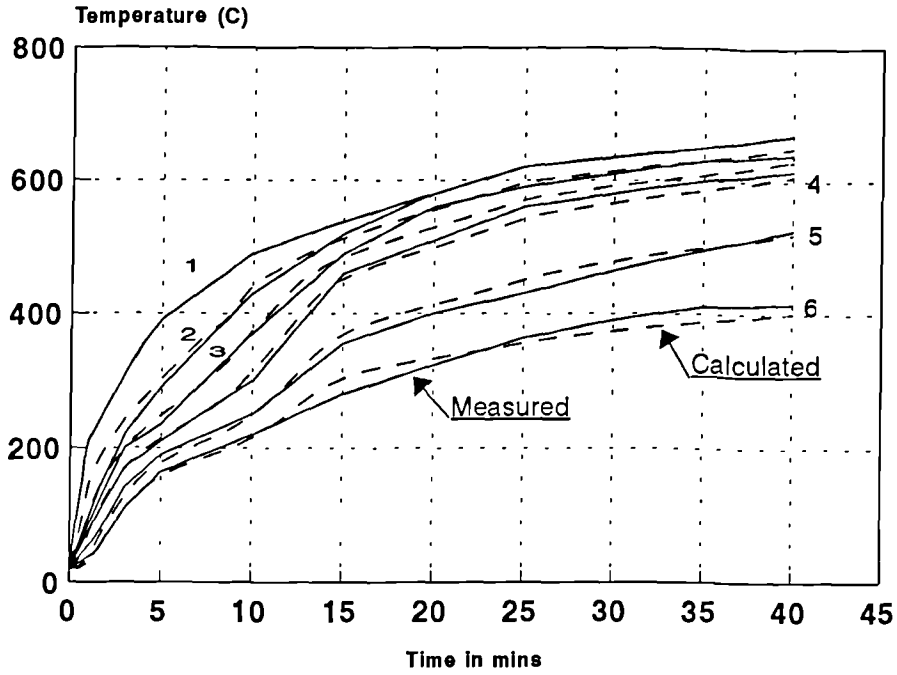

Fig.6.13 The Comparison of Time-Temperature Profile Between the Measured and Calculated Results
WR Polyester Laminate (5.9mm), Cellulosic Fire Test

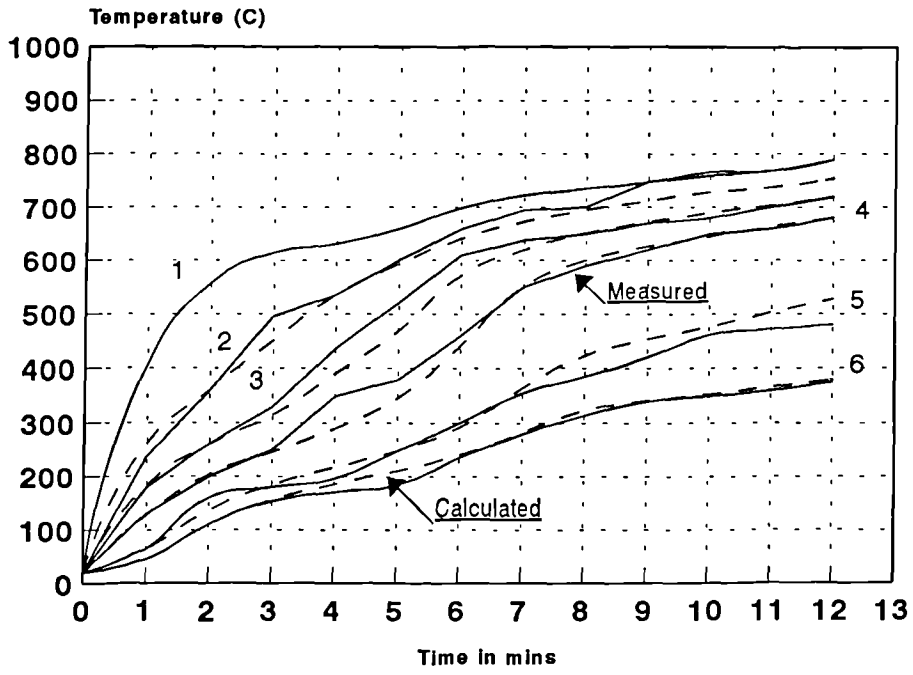

Fig.6.14 The Comparison of Numerical and Measured Results
WR Polyester Laminate (6mm), Hydrocarbon Fire Test

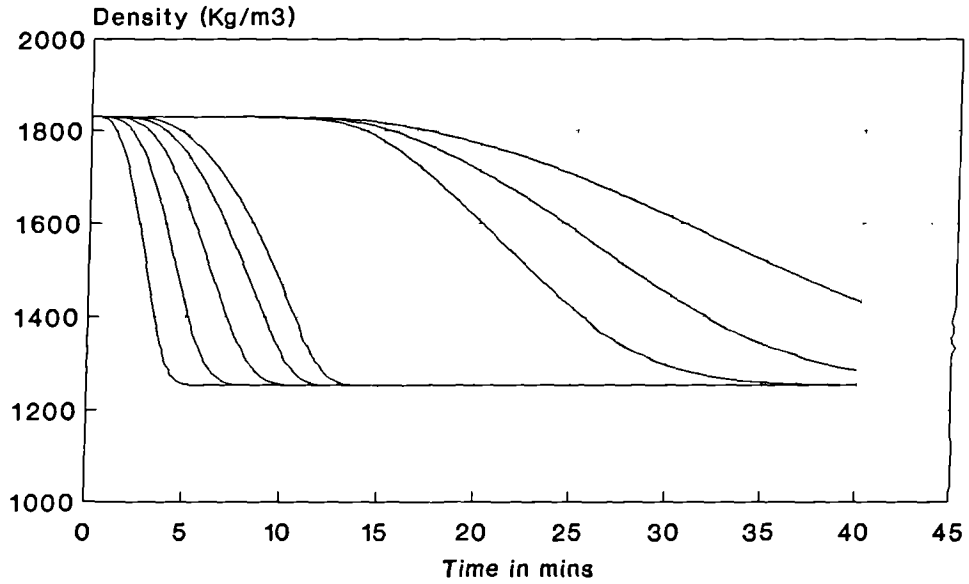

Fig.6.15 The Mass Loss Rate at Different Locations of WR Polyester Laminate
Numerical Simulation for Cellulosic Fire

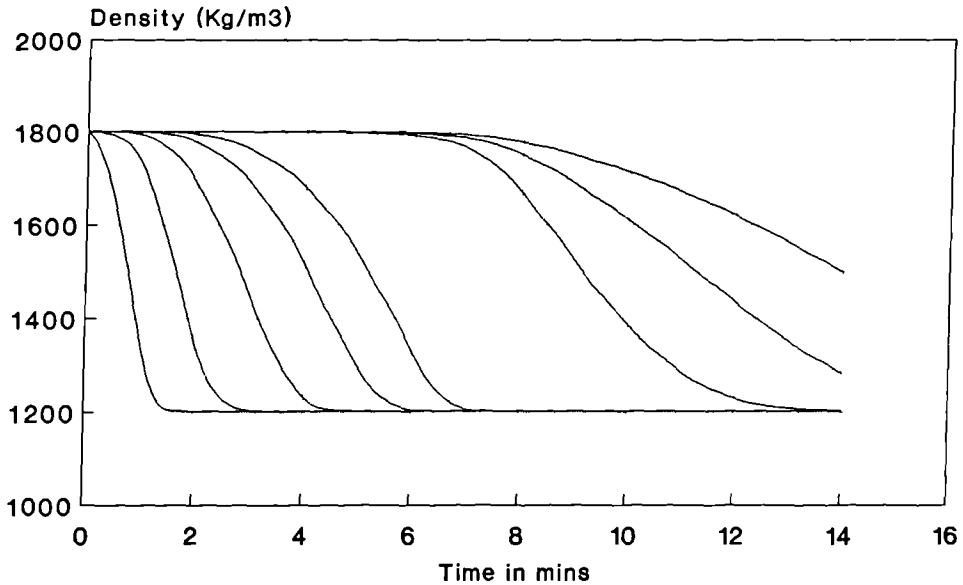

Fig.6.16 The Mass Loss Rate at Different Locations of WR Polyester Laminate
Numerical Simulation, Hydrocarbon Fire

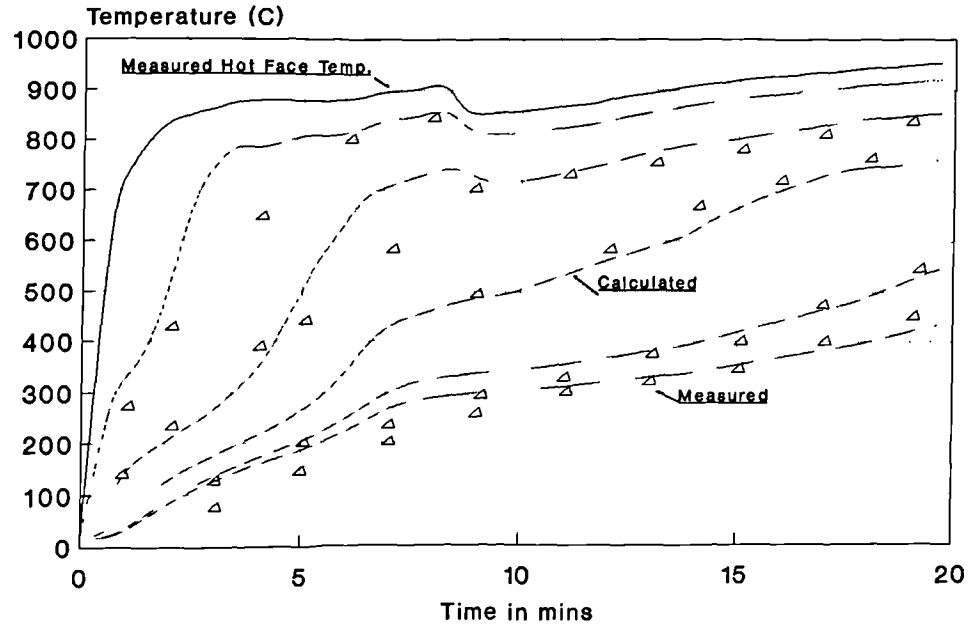

Fig.6.17 Hydrocarbon Fire Test of
WR Polyester Laminate (8.8mm, 42% resin)

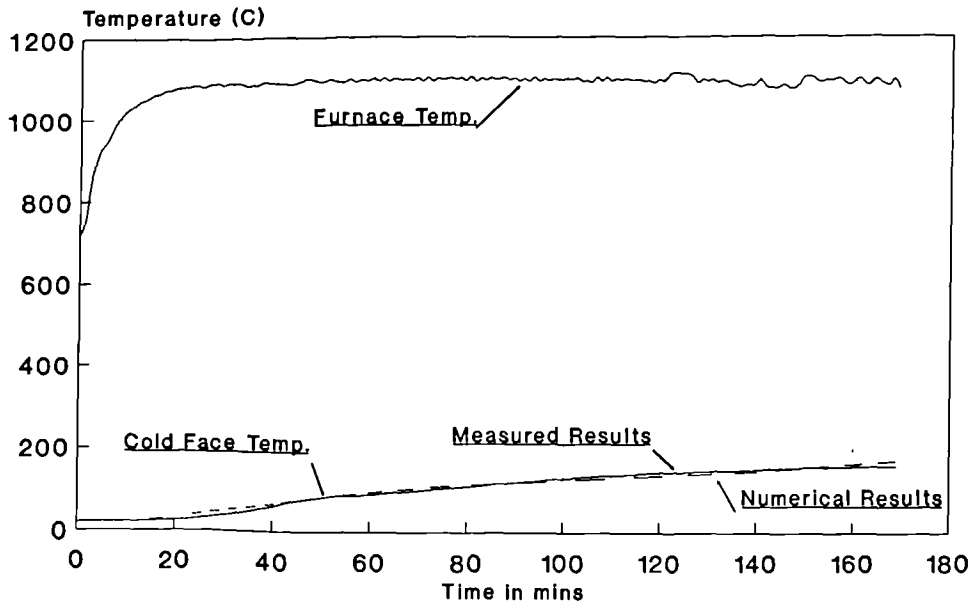

Fig.6.18 Vermiculux (60mm) with two GR
Polyester Skins (6.4mm,6.2mm)
Hydrocarbon Fire Test

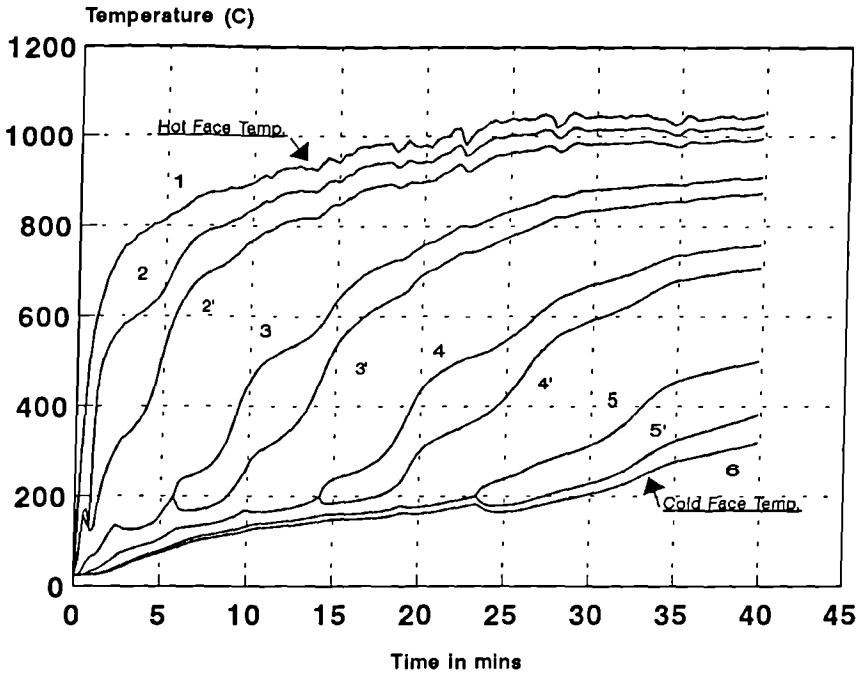

Fig.6.19 Computational Time-Temperature Profile of WR Phenolic Laminate I (12.6mm) in Hydrocarbon Fire Test

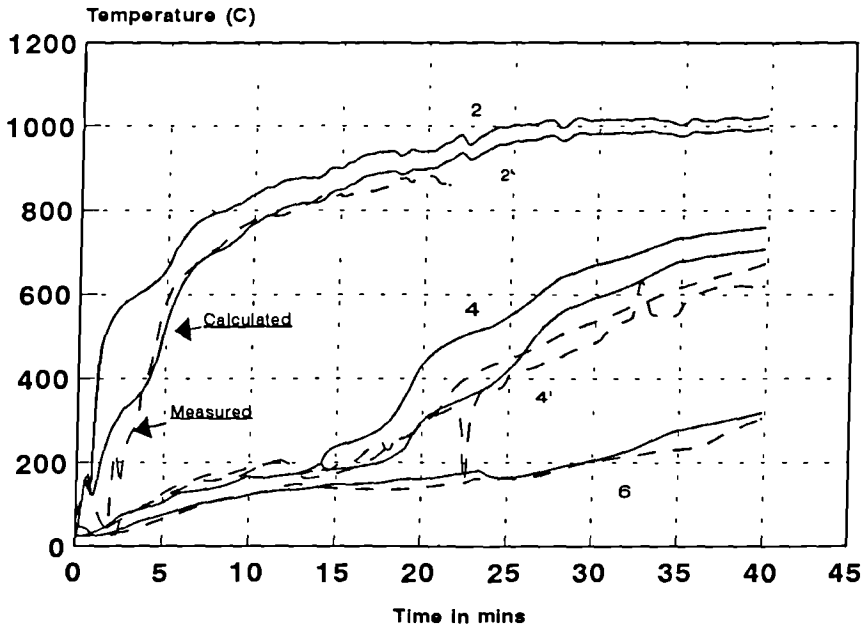

Fig.6.20 Comparison of Numerical and Measured Temperature Profile Hydrocarbon Fire Test of WR Phenolic Laminate I (12.6mm)

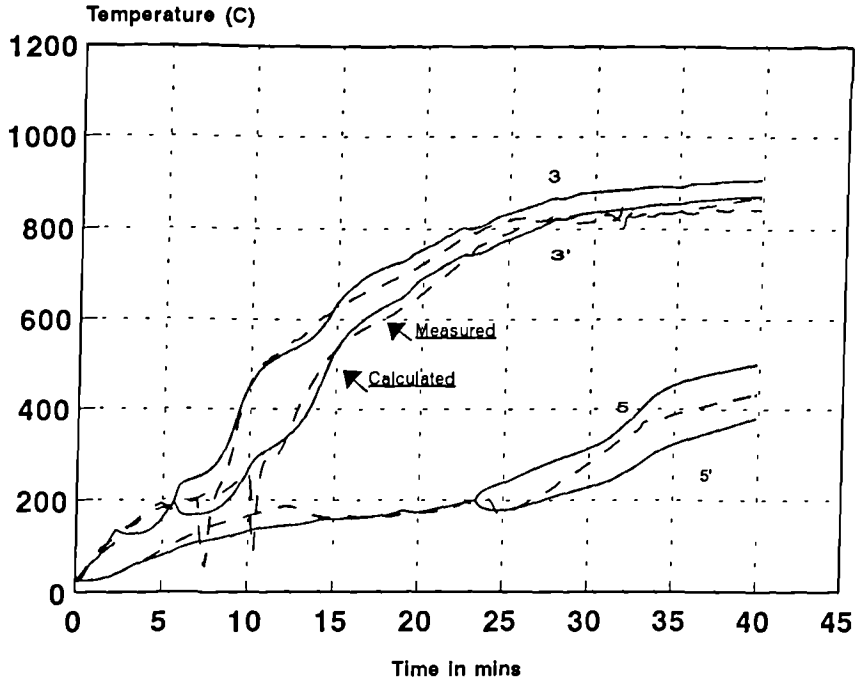

Fig.6.21 Comparison of Numerical and Measured Temperature Profile Hydrocarbon Fire Test of WR Phenolic Laminate I (12.6mm)

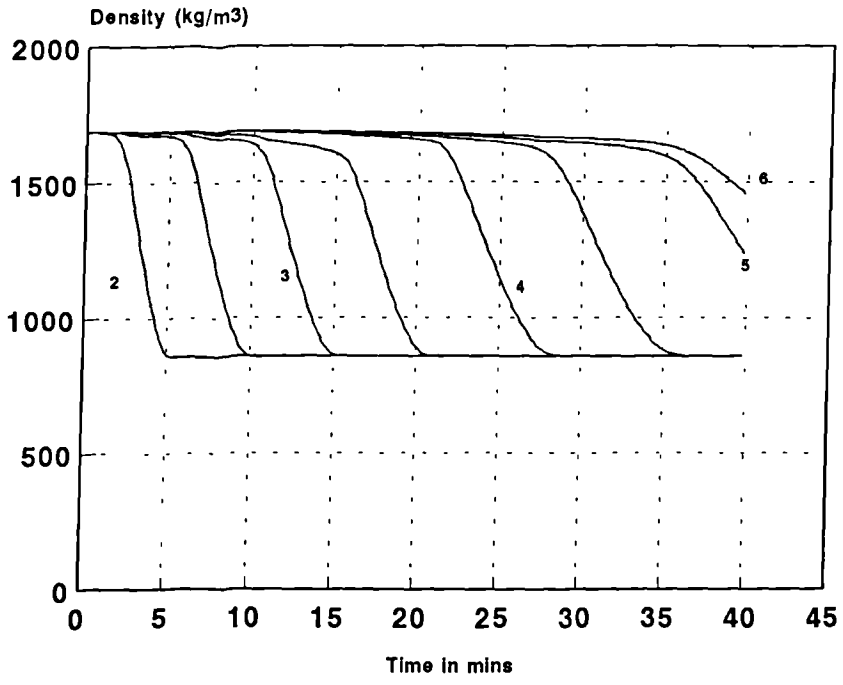

Fig.6.22 Declining Density at Each Location of WR Phenolic Laminate I, Numerical Simulation

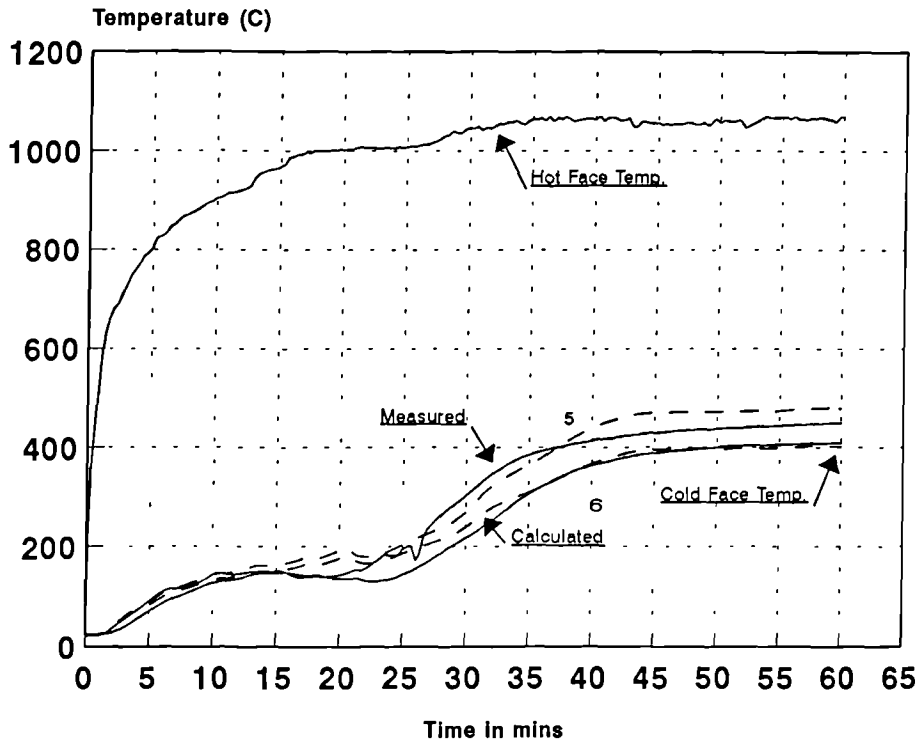

Fig.6.23 The Comparison of Numerical and Measured Temperature Profile WR Phenolic Laminate II (11.7mm) in a Hydrocarbon Fire Test

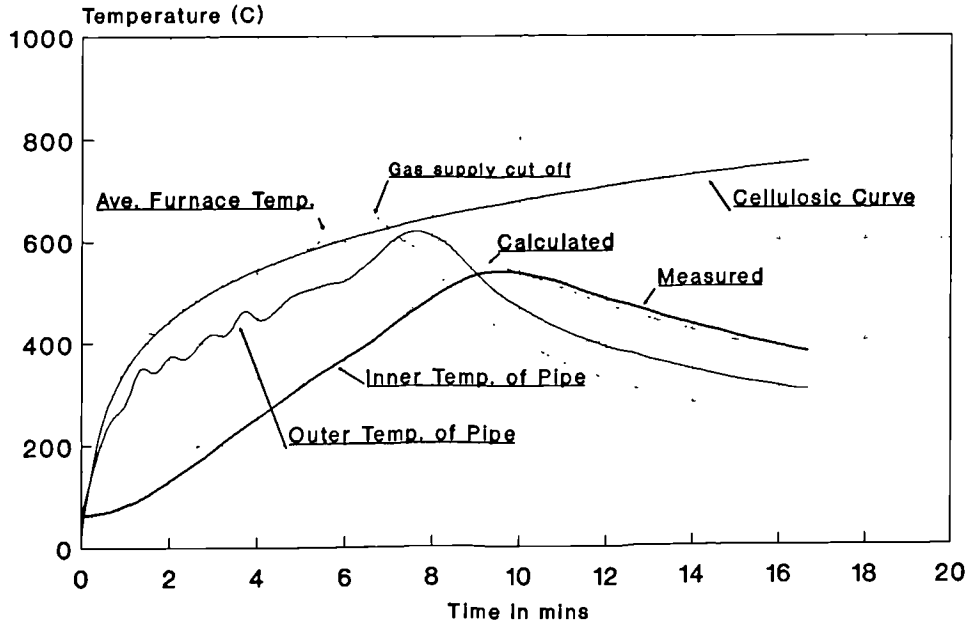

Fig.6.24 Ameron 2000M 3" Epoxy Pipe
Cellulosic Fire Test

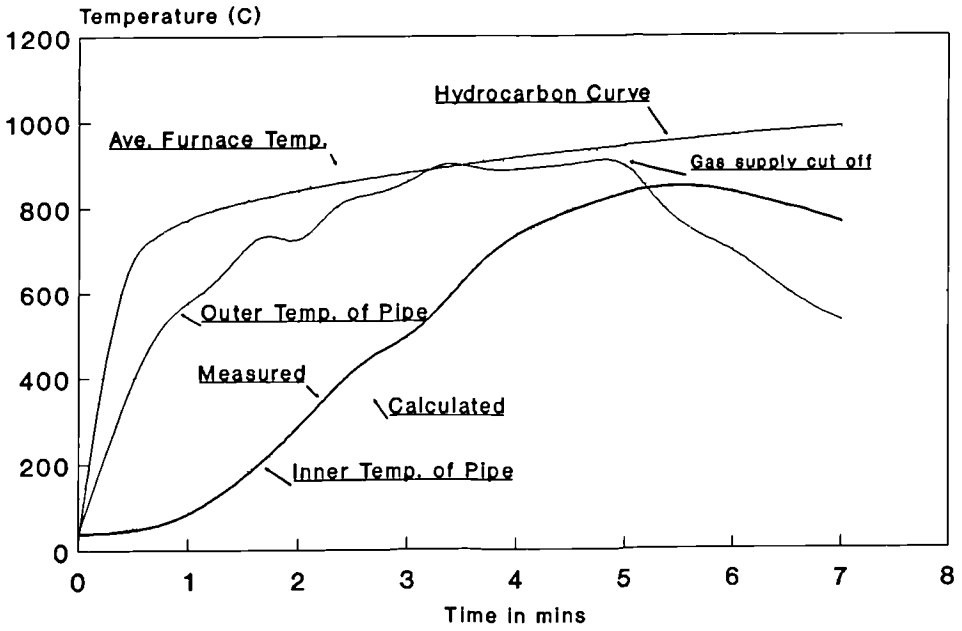

Fig.6.25 Ameron 2000M 4" Epoxy Pipe
Hydrocarbon Fire Test

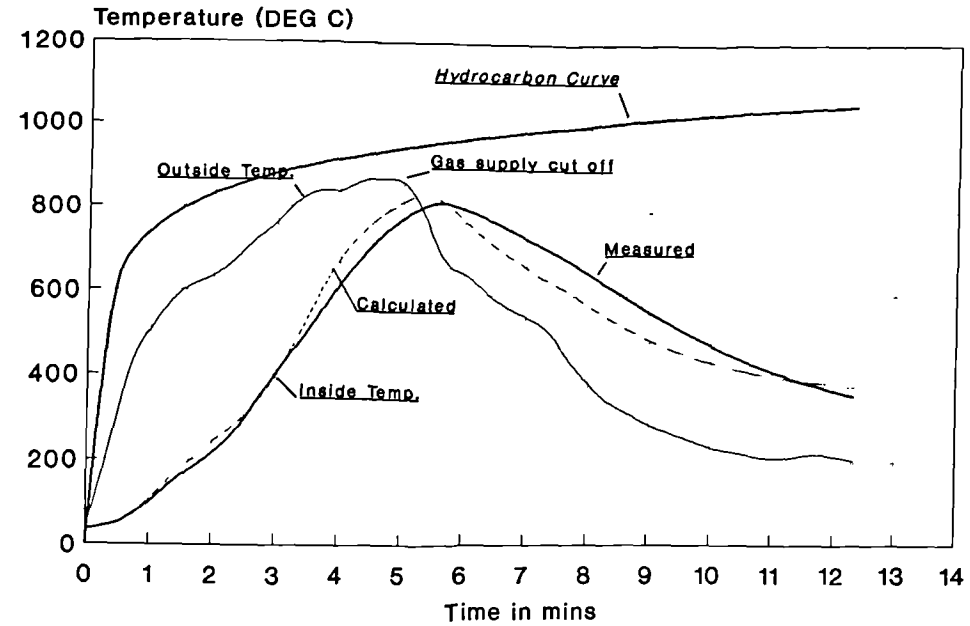

Fig.6.26 BP Phenolic Pipe, Hydrocarbon Fire Test, Thickness of Pipe is 5.6mm

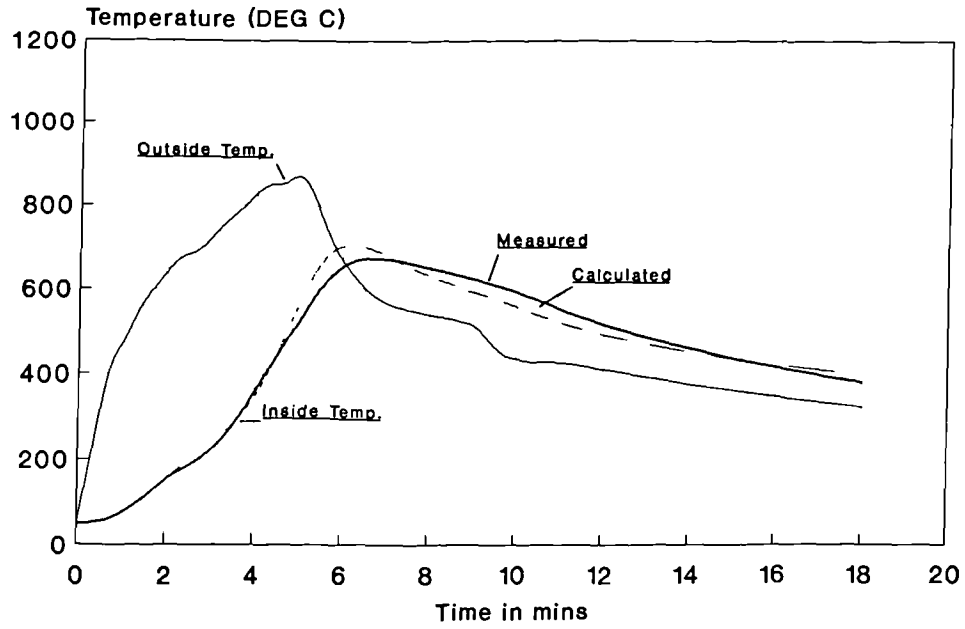

Fig.6.27 BP Phenolic Pipe, Hydrocarbon Fire Test, Thickness of Pipe is 7.7mm

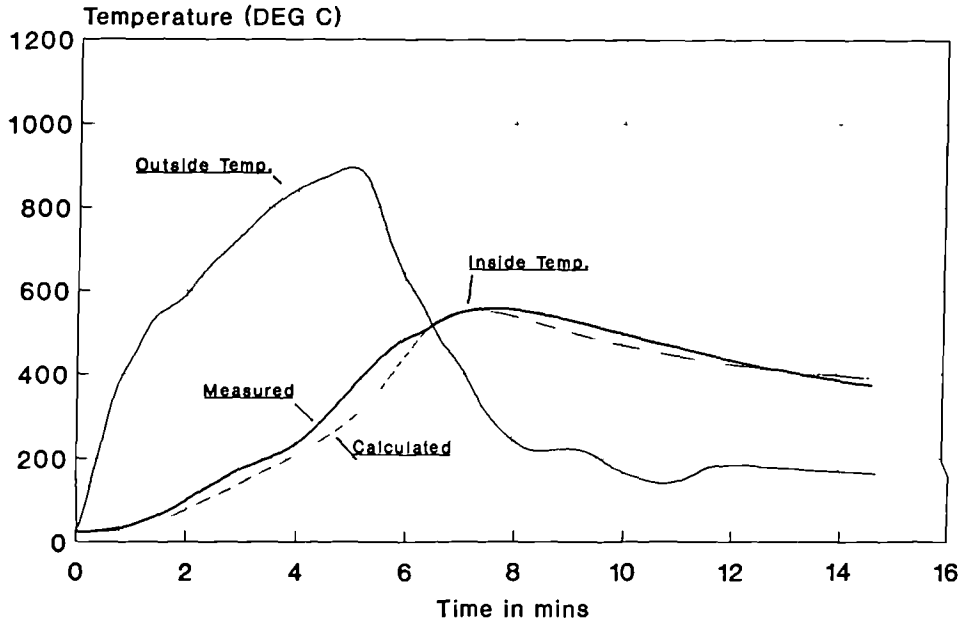

Fig.6.28 BP Phenolic Pipe, Hydrocarbon Fire Test, Thickness of Pipe is 9.5mm

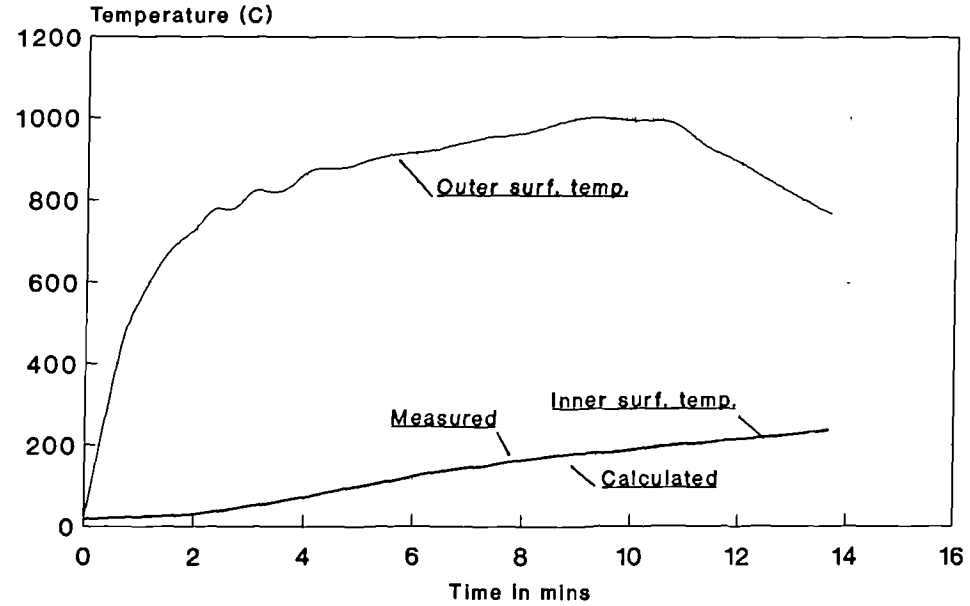

Fig.6.29 Ameron 4" 2000M Epoxy Pipe with
Intumescent Pitt-Char (7.5mm)
Hydrocarbon Fire Test and Computation

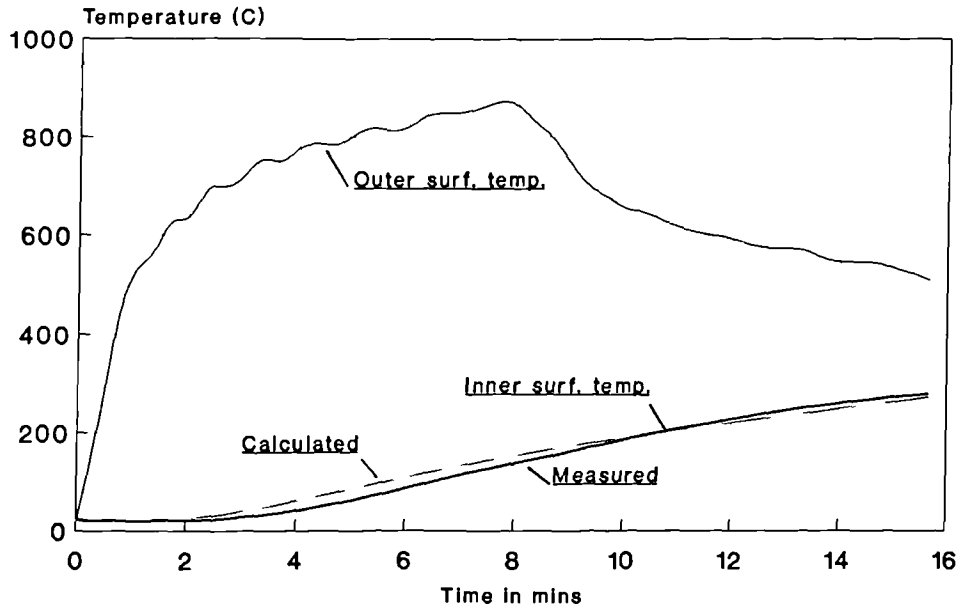

Fig.6.30 Ameron 4" 2000M Epoxy Pipe with
Reinforced Pitt-Char (11.5mm)
Hydrocarbon Fire Test and Computation

CHAPTER 7

Computer Program Development for FDM

Although, numerical heat transfer calculations can be performed by general commercial packages, this would not meet the requirements of this study. The first point is that calculations using such general purpose programmes will take a considerable amount labour owing to the size of these programmes. Another point is that if we want to study the particular behaviour of materials under fire, such as moisture effect and decomposition of material, none of these programmes have the required facilities, nor are the source codes available to be modified. In general, the existing commercial software packages have not included efficient fire - material models which usually tend to lag behind those used for research purposes. It is therefore necessary to create an effective and reliable program that can be executed within a PC environment, enabling a large number of calculations to be made in a convenient way for this study.

Based on the finite difference formulae described before, a Numerical Temperature Analysis Program - **NTAP** has been developed using the FORTRAN language for one-dimensional analysis of heat transfer in either Cartesian or polar coordinates, and two-dimensional analysis in polar coordinates. The results obtained by using the program are the temperature profile of a particular element of construction (panel, multi-layer panel or pipe) in a hostile

thermal environments of a specified intensity and time duration. **NTAP** is designed to operate on a personal computer, although it can be executed on other small computers or main frames. To make **NTAP** user friendly and efficient, a simple data input by a pull-down menu management system and run-time screen display have been established. In order to achieve this, the routines and graphics facilities from the FTN77 (University of Salford) run-time library were used. A high resolution graphics monitor with VGA screen type was assumed and a mouse driver is required to make selections from the menus of the program.

The main menu is shown across the top of the screen when the program is running. It contains the following items: **Configuration, Heat Source, Properties, Settings** and **Options.** The menu option **Configuration** is used to specify the geometric dimensions of the element and the number of material layers. The **Heat Source** selection is used to define the nature and duration of the thermal impact which causes the structure to be heated. Five types of exposed side boundary conditions are available, which included most of the possible types of fire exposure. These are:

1). Cellulosic temperature-time curve[1.1];
2). Hydrocarbon temperature-time curve[1.1];
3). Actual furnace temperature-time history as recorded during a test;
4). Heat flux loading; It includes radiative and convective heat flux in unit of KW/m^2. The jet fire may be included in this category.
5). Actual exposed side surface temperature history.

The **Properties** selection is used to define the thermal and physical properties of the materials. If the thermal conductivity and specific heat are temperature-dependent, their relationship can be supplied to the program. These values are adjusted according to the temperature and moisture content as the program is running. Some default data for commonly used materials are held in the program.

An additional property library of further materials is to be included in a database. The **Settings** option is used to adjust or alter the parameters used in the modelling. The last menu item, **Options**, is used to command the program to do a general task such as to quit the execution, display the previous results, re-run the problem after alteration of the data and to start the new run. The detailed explanation of how to use the menu system is given in a user's manual.

The initial time-step is set by the user based on the requirement for accuracy. Firstly, this time-step is checked by program for the stability requirement. If the time-step does not meet the requirement, the program automatically reduces the time-step to half of its previous value until it meets this requirement.
In the principle, there is no limitation on the minimum thickness of the elements.

Sometimes the user may wish to run a similar problem many times. Typing in almost same data repeatedly from menu selection could be tedious. The program provides a solution to this in that the input data can be read from an existing data file which can also be edited.

When the user runs **NTAP**, the curves of the numerical solutions are instantaneously displayed on the screen. The experimental data can also be shown on the screen at the same time for comparison. The data and graphic

results are also written to an output file and can be printed to provide a permanent record. As with other finite difference packages, the program predicts the temperature at every node and time step. Output of the nodal temperatures can be done at a specified time interval. It is considered that the resulting program is both stable and user-friendly.

The verifications of the performance of these computer programmes were carried out during every stage of development. The details have already been described in the previous chapters.

CHAPTER 8

Heat Transfer Calculation Using FEM

8.1 Introduction

In last two decades, another powerful numerical method - the Finite Element Method (FEM), developed originally for the solution of structural problems, has been applied to the solution of heat transfer problems[8.1, 8.2 and 3.1]. For problems with complex geometries, the FEM has the potential to offer some advantages over the FDM in the solution of heat conduction problems. Also, the requirement for thermal-structural analysis raises a strong argument for using finite element methods because they permit the use of a common discretization for the thermal and mechanical analysis of structures. In this approach, either the variational principles or, preferably, the Galerkin method is used to transform the heat conduction problem to a set of algebraic equations. Then the transient temperature field is obtained by the solution of these algebraic equations.

In this study, a two-dimensional finite element model and computer program in Cartesian coordinates have been developed to analyze the heat transfer problems of elements of construction exposed to fire.

Since the principles of FEM for heat transfer problems are well known[8.1], the details of its formulations will not be repeated here. A concise description of the function of the developed FE program is presented in section 8.2, and a representative problem is solved in sections 8.3 and 8.4 to show the capability of FEM and the treatment of boundary conditions and moisture content.

8.2 Finite Element Computer Program Development

The developed 2-D FE program has a *number of features that make it suitable* for the required purpose. The object structures may contain several materials with thermal properties which vary with temperature. The heat transmission in the enclosed voids by radiation and convection can be simulated as described in section 3.3. Various boundary conditions can also be conveniently specified.

The traditional use of the enthalpy concept in the FE formulation[3.2] was abandoned in our program. It is believed that the introduction of enthalpy in the formulation is not a necessity and may cause unnecessary complexity in the programming and application.

In the present version of the program, two-dimensional four-noded rectangular and three-noded triangular elements are used. By input of the main geometry data, the generation of the finite element mesh has been automated. Graphic output is available; ie, a display of the colour contours of temperature distribution during the calculation process is provided. This provides a quick check for both

the element mesh and temperature profile.

Although this is a two-dimensional program, it can also deal with one-dimensional problems. First, the check for one dimensional modelling was carried out. The results given by the program for mineral wool and calcium-silicate panels are quite consistent with the results which were given by fire tests and finite difference modelling (see Figs.6.1 and 6.2).

8.3 Test Example:
Composite Concrete/Steel Deck Slab Exposed to Fire

For two-dimensional modelling, a series of careful standard fire tests for composite deck slabs, conducted by P.W.Haar et al[8.3], were utilised to verify the validity of the numerical analysis. The experimental arrangement used by Harr is described in a supplement at the end of the thesis. The time-dependant temperature distribution in the cross-section of composite concrete/steel deck slabs exposed to standard fire condition was calculated. Furthermore, the effects of temperature-dependent thermal properties of material, moisture content and boundary condition have all received a detailed study.

The composite concrete/steel deck slabs normally span in one direction, in which profiled steel sheeting acts as a permanent formwork and as reinforcement to the concrete placed on top, as shown in Fig.8.1. A rapid increase in the use of this form of construction in the UK has occurred since 1980. This is due in part to the possibility of demonstrating adequate fire resistance without the necessity of any added fire protection. The overall slab depth is usually 100 to 150mm, with

spans ranging from 2.5 to 4.0m. The steel sheet, with thickness between 0.7 and 1.5mm, is galvanised for durability. A number of fire tests have been conducted carefully with the primary object of verification of the numerical models[8.3,8.4]. Unlike some other test reports, sufficient information was provided for the numerical analysis to be replicated. Although R. Hamerlinck, L. Twilt and J. Stark have already published a finite difference comparison for part of these results[8.5], there is scope for refinement of their theoretical evaluations, particularly with respect the treatment of the influence of the moisture content of the concrete. In reference [8.6], a brief mention was given to the numerical calculation for a similar problem. Nevertheless, it did not take into account the effect of moisture which means that the over-predicted temperatures in concrete were displayed.

The finite element meshes for the analysis of floor decks using the Holorib and Prins profiles are shown in Figs.8.2 to 8.4, where both rectangular and triangular elements are used. Because of the periodic nature of this form of construction, only part of cross-section was used in the calculation. It was shown by measurements made during testing [8.4] that the heat transfer in the longitudinal direction of slab can be neglected. It follows that the temperature distribution is not significantly influenced by the presence of any additional reinforcement in the form of longitudinal bars or mesh.

The elements are assigned thermal properties of the materials which depend on the average nodal temperature. These thermal properties are specified at a number of temperature levels and are assumed to vary linearly between these. Owing to the rapid temperature rise specified in standard fire conditions, a rather

short time step is needed as the analysis proceeds. An explicit direct time integration approach is therefore appropriate.

8.3.1. Boundary Conditions

In the tests, the slabs were positioned on the top of fire compartment with their bottom face exposed to the fire. This represents a more severe situation than the alternative with the fire burning above the floor. The temperature development in the fire compartment was controlled to follow the ISO 834 standard time-temperature curve as shown in Fig.8.5. A corresponding measured temperature development in the fire compartment is used to generate an appropriate boundary condition in the numerical modelling.

Both the radiative and convective heat transfer rates on the exposed and unexposed sides can be described by equation(2.5). At the unexposed side of the slab, a general formula for the free convection heat transfer coefficient in horizontal plates is used, namely[8.4]

$$h(T) = 1.52 \cdot (T_a - T)^{1/3} \qquad (8.1)$$

This is the simplified form of equation (2.15) for the current case. Alternatively, only a constant value of h (8 W/m°C) was used in [8.5]. The configuration factor F is 1 and emissivity of E is assumed to be 0.8 here.

At the exposed side of the slab, although the heat transfer coefficient h and the

resultant emissivity E are supposed to be constant, a distinction needs to be made between the lower flange, upper flange and web because the heat transmission to upper flange and web is partially obstructed. After first making reasonable assumptions, these parameters were adjusted in order to improve the fit with the test results. The values used in the analyses quoted later are summarised in Tables 8.1 and 8.2.

Table 8.1. Super Holorib Specimens

Specimen	1,8 (lf)	1,8 (uf,wb)	11 (lf)	11(uf,wb)
h	25	15	25	10
EF	0.2	0.08	0.52	0.12

Table 8.2. Prins PSV Specimens

Specimen	6(lf)	6(uf)	6(wb)	12(lf)	12(uf)	12(wb)
h	25	20	20	25	10	20
EF	0.2	0.12	0.14	0.52	0.14	0.38

Specimen 1 is Super Holorib 51/Hb=70mm (Fig.8.3) with the steel deck in place and Specimen 11 is similar but without the steel deck. Specimen 8 is Super Holorib 51/Hb=90mm (Fig.8.4) with the steel deck. Specimen 6 is Prins PSV 73/Hb=70mm (Fig.8.2) with the steel deck and Specimen 12 is without steel deck.

In the above tables, 'lf' refers to lower flange, 'uf' refers to upper flange and 'wb' denotes web.

8.3.2. Moisture Effects

The concrete slabs were made using normal-weight concrete B25. Although they were subjected to a long period of natural and forced drying, they still contained about 3% moisture content on the day of test. The levels of moisture content for each specimen derived from the test report[8.3] are given in Table 8.3.

Table 8.3. Moisture Content of Test Specimens

Specimen	1	11	6	12	8
Moisture Content[1]	2.8	3.0	3.6	2.9	3.67

[1] mass percentage of dry weight

It is well known that the heat transfer in moist materials is influenced significantly by the moisture content. A same simple engineering approach is used as described in Chapter 5. Although the distribution of moisture throughout the slab profile is not necessarily uniform, it is assumed to be so in the current numerical modelling.

According to this model, the moisture evaporation is assumed to take place during a temperature interval, 100°C to 130°C. $\Lambda = 1.5$ in equation (5.2) is found

to give a satisfactory correlation with the experimental results for the cases considered here.

Difficulties associated with numerical instabilities due to the abrupt variations in C_p were overcome by choosing a gentle change occurring over the 30°C temperature interval in a way shown schematically in Fig.8.16.

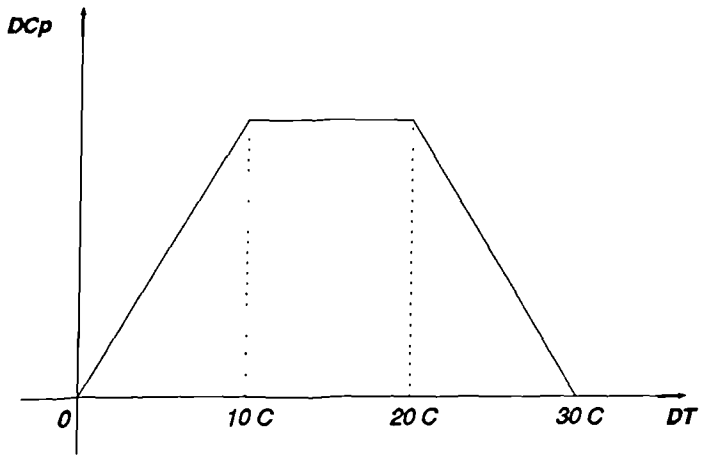

Fig.8.16 The variation of DC_p in a temperature interval

This was adopted solely to provide enhanced numerical stability and convergence characteristics in the numerical calculations. The total energy which was needed to evaporate the moisture was, in fact, not altered.

The thermal conductivity of concrete will be also influenced by the moisture content. This will be discussed in the next subsection.

8.3.3. Thermal Properties of Materials

Since the thickness of the steel sheet forming the deck profile is small and its thermal conductivity is high, the heat capacity and conduction resistance of the steel deck may be neglected. Nevertheless, the emissivity of the galvanized steel sheet has to be taken into account on the exposed side of specimens 1, 6 and 8. This is the reason that the resultant emissivities on the exposed sides of specimens 1, 6 and 8 are lower than those for specimens 11 and 12 (see Tables 8.1 and 8.2).

The effective thermal conductivity of moist concrete will display an apparent increase when the concrete is heated. Then the following relation between conductivity and temperature shown in Table 8.4 is used for normal-weight concrete (density = 2350 kg/m^3) with a moisture content around 3%. It may be noted that the highest conductivity is at a temperature of 100°C.

Table 8.4. Thermal conductivity of concrete

Temperature (°C)	0	100	200	895	1200
Conductivity (W/m°C)	2.0	3.0	1.6	0.85	0.85

The specific heat for totally dried concrete is 900 J/kg°C at 0°C, and 1300 J/kg°C at 1200°C. The actual specific heat of concrete with moisture content is calculated by equation (5.3). The value of the final specific heat and conductivity given by this procedure are consistent generally with the recommendations of the

ECCS[2.5].

8.4 Numerical Results and Comparisons

Numerical calculations were carried out for the five specimens mentioned above using the finite element meshes shown in Figs.8.2 to 8.4. In order to obtain coincidence between the positions of the thermocouples and element nodes, there are slightly dimensional variations between the meshes for slabs with and without the steel deck.

The comparisons of the observed and calculated time-temperature curves for selected points are presented in Figs. 8.6 to 8.15. The 'No.' on the graphs denotes 'Node Number' in the finite element mesh (see Figs.8.2 to 8.4). The calculated results show good agreement with the test results. The calculation time is just a few minutes with a PC 486 with time-step $\Delta t=2$ sec.

The calculations for specimen 8 provide a particularly good confirmation of the accuracy of the modelling. The shape of cross-section of specimen 8 is similar to that of specimen 1, except that the concrete depth is increased to 90mm. All input data for the numerical calculation for specimen 8 was therefore a copy of that for specimen 1 except for the mesh generation and moisture content. An excellent prediction was again obtained. This compares favourable with the 16 minute error in predicted insulation time found in[8.4].

In spite of the high thermal conductivity that was assigned to moist concrete at a

temperature around 100°C, the calculated temperature rise is still delayed in this range as shown in Fig.8.10 and 14. This probably because the heat transmission by diffusion of moisture was not fully considered. Nevertheless, the present analysis gives better correlation with the test results than was obtained by the authors of reference [8.4]. The total extra energy needed for vaporizing water therefore seems to be correctly estimated.

Some discrepancies between the observed and calculated results occur on the *exposed side* of slabs with steel sheets during the initial and final stage of testing. In the initial stage, the relatively slow rise of measured temperature was probably caused by the congestion of steam *(Figs.8.8, 8.9, 8.12 and 8.13) while, in* the final stage of the tests, the rapid rise of measured temperature might be a consequence of debonding of the steel sheet (Fig.8.13). Cracks appearing in concrete towards the end of fire testing also enhance the heat transmission in the slabs.

The numerical results presented above show that an accurate prediction of the temperature development in a composite concrete/steel deck slab exposed to fire is available. Its use requires the determination of a number of parameters, namely, the moisture content and its distribution, the energy needed for evaporation, the value of the thermal conductivity under the influence of moisture, and the actual heat input from the fire compartment.

For a prescribed time-temperature development, the parameters that determine the radiative and convective heat loading from the fire compartment to the exposed side of test sample differ from case to case. With the extremely

complicated turbulence of hot gas inside the test furnace, it is difficult to give the accurate values of them in advance. The comparisons give here suggest that the values of both the emissivity of the fire compartment and the heat transfer coefficient (Eq.(2.5)) are high at the start of the test when the temperature is increasing rapidly. They then decrease as the rate of temperature increase decreases. On the other hand, the galvanized steel sheet shows low emissivities for low temperatures. When the temperature exceeds 400°C, however, the zinc layer melts and surface blackens with the result that its emissivity increases. For the combination of these two effects, a constant resultant emissivity appears to provide a reasonable assumption for the radiative heat exchange between the steel sheet and the fire compartment. For the concrete slabs alone, specimens 11 and 12, although a constant value was chosen for simplicity, the numerical results will be improved if variable emissivity is used (Fig.8.10).

The use of a high thermal conductivity for moist concrete around 100°C gives a good predictive of the behaviour as the moisture evaporates. An accurate value of the extra energy needed for vaporization is also important.

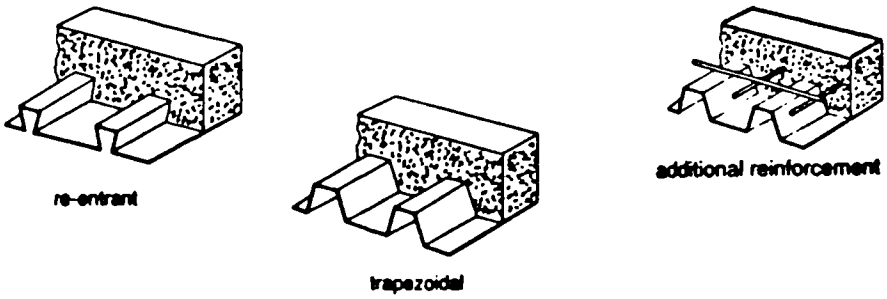

Fig.8.1 Typical composite concrete/steel deck slabs [8.2]

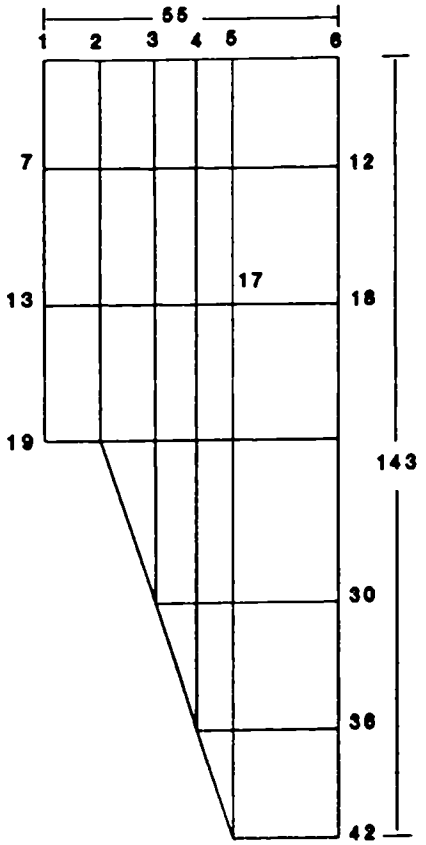

Fig.8.2 Finite element mesh for Prins PSV 73

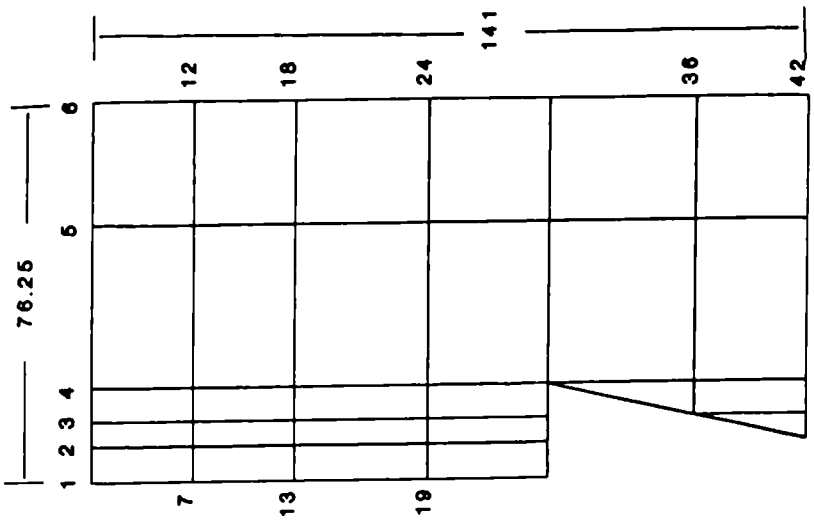

Fig.8.4 Finite element mesh for Super Holorib 51 with 90mm concrete

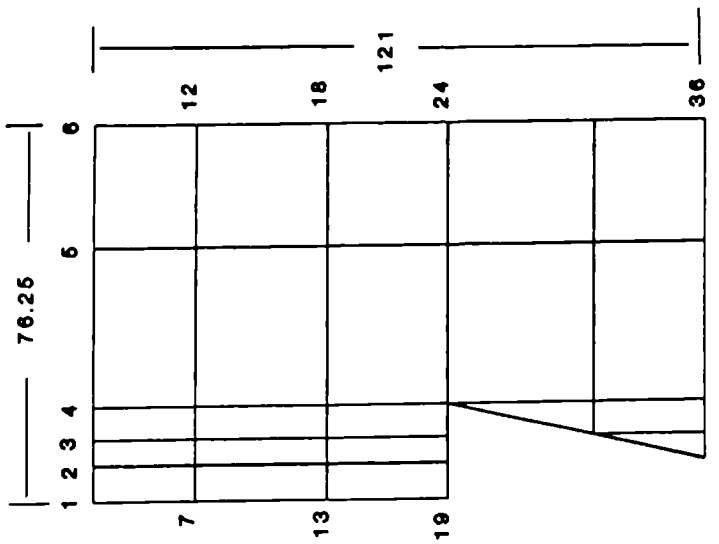

Fig.8.3 Finite element mesh for Super Holorib 51 with 70mm concrete

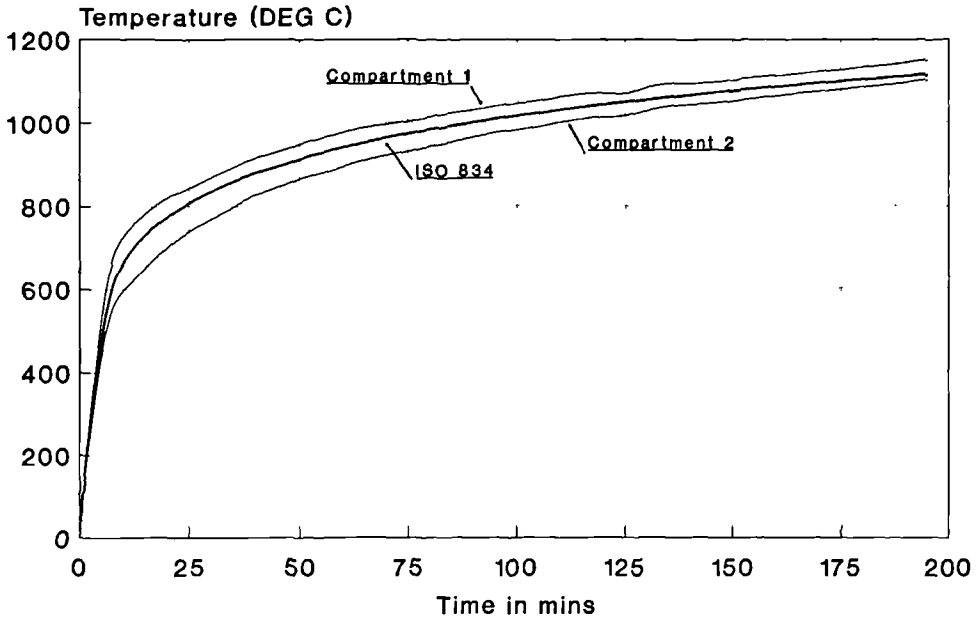

Fig.8.5 The Measured Temperature in Fire Test Compartment [8.2]

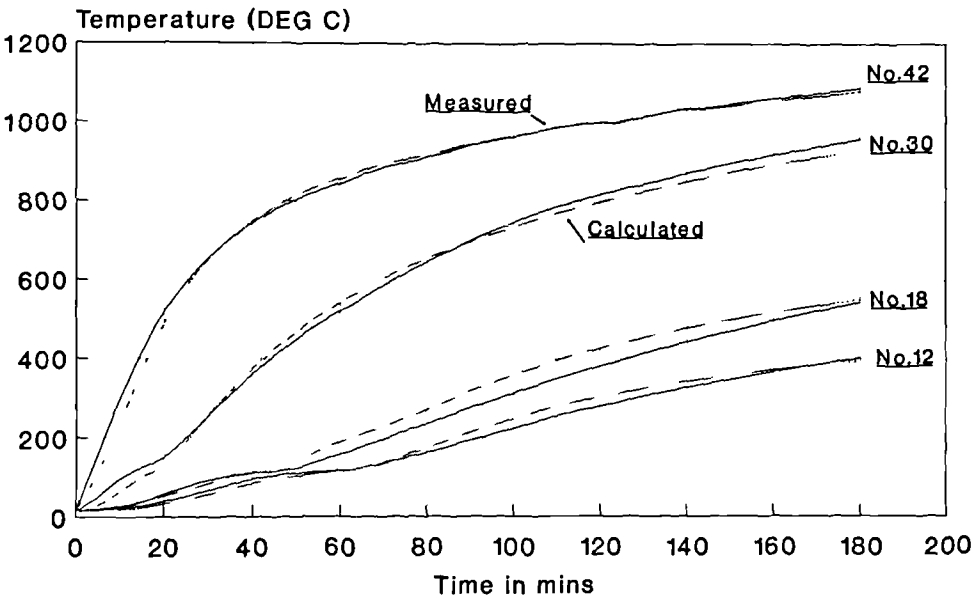

Fig.8.6 The Comparison of Calculated and Measured Temperature Distribution Prins PSV 73 (without steel sheet)

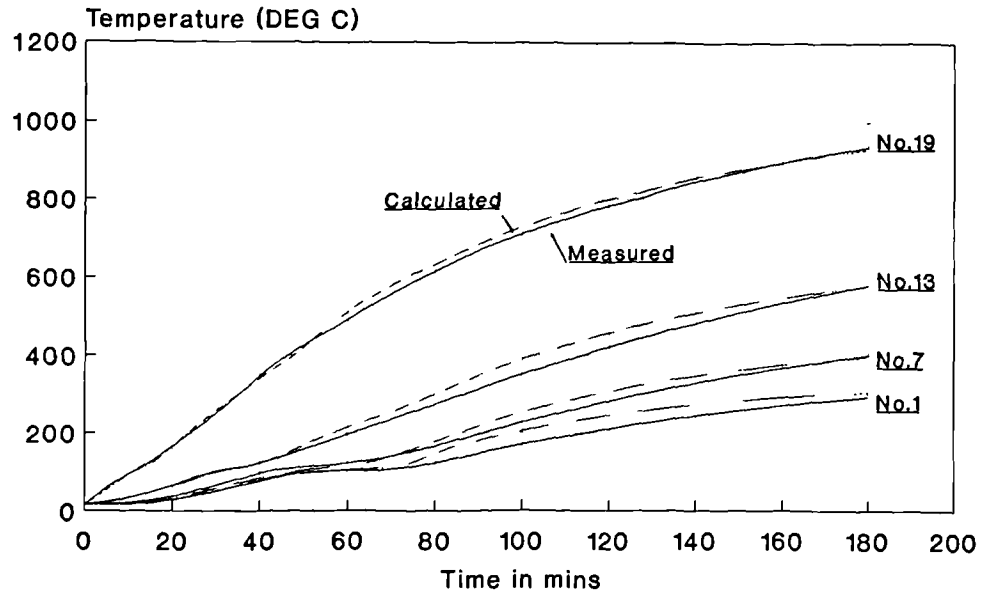

Fig.8.7 The Comparison of Calculated and Measured Temperature Distribution Prins PSV 73 (without steel sheet)

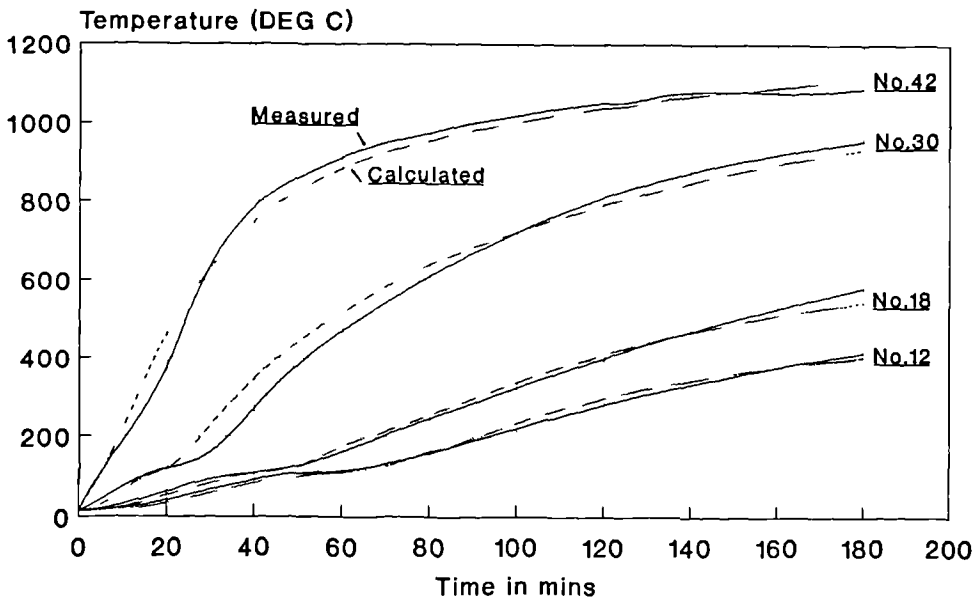

Fig.8.8 The Comparison of Calculated and Measured Temperature Distribution Prins PSV 73 (with steel sheet)

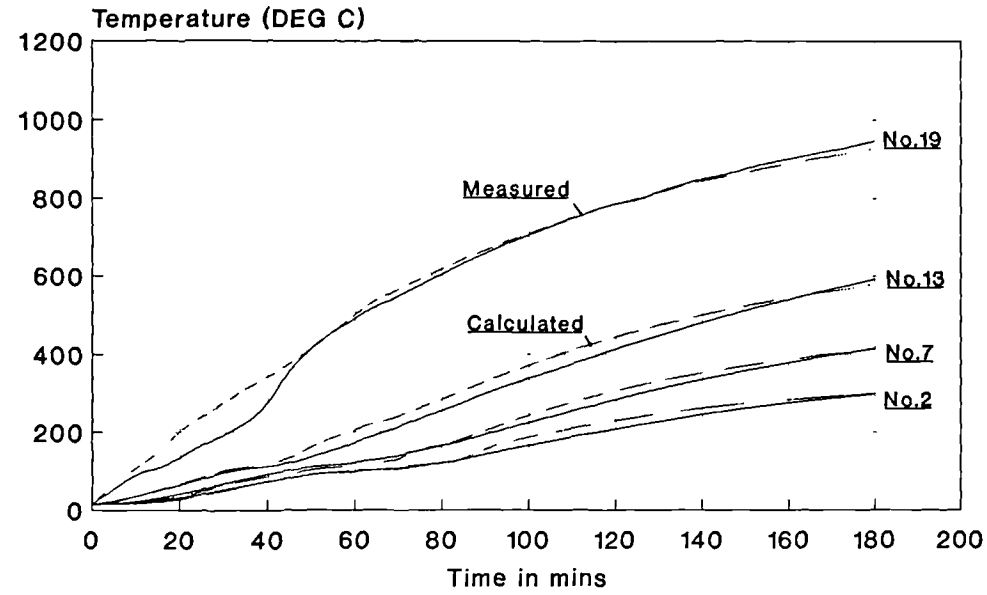

Fig.8.9 The Comparison of Calculated and Measured Temperature Distribution Prins PSV 73 (with steel sheet)

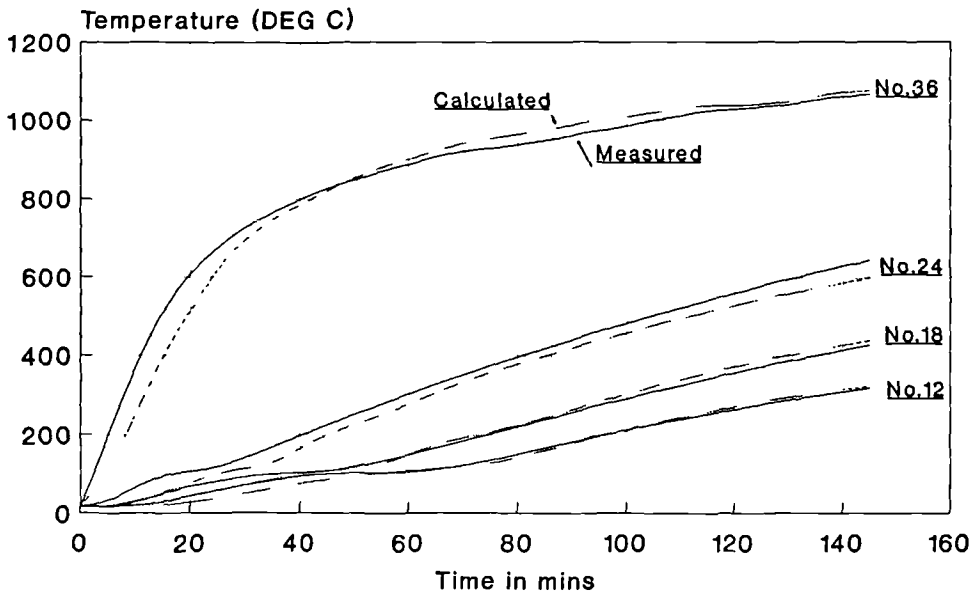

Fig.8.10 The Comparison of Calculated and Measured Temperature Distribution Holorib 51/HB=70mm (without steel sheet)

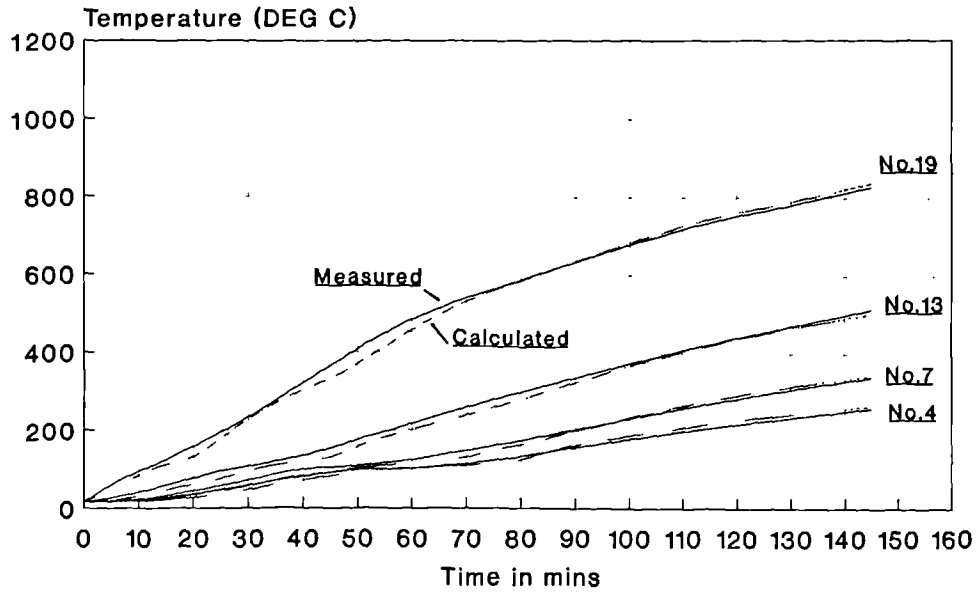

Fig.8.11 The Comparison of Calculated and Measured Temperature Distribution Holorib 51/Hb=70mm (without steel sheet

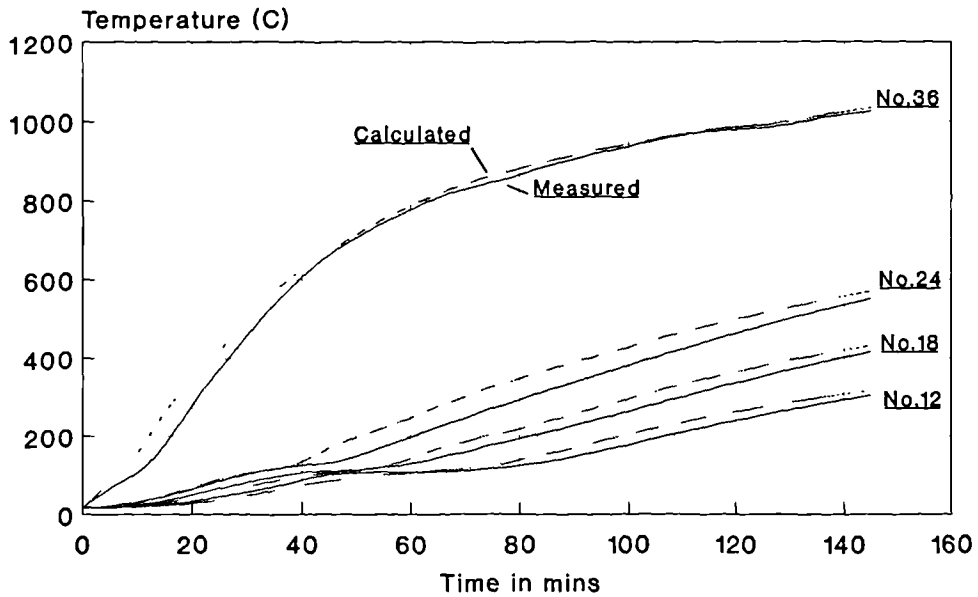

Fig.8.12 The Comparison of Calculated and Measured Temperature Distribution Holorib 51/Hb=70mm (with steel sheet)

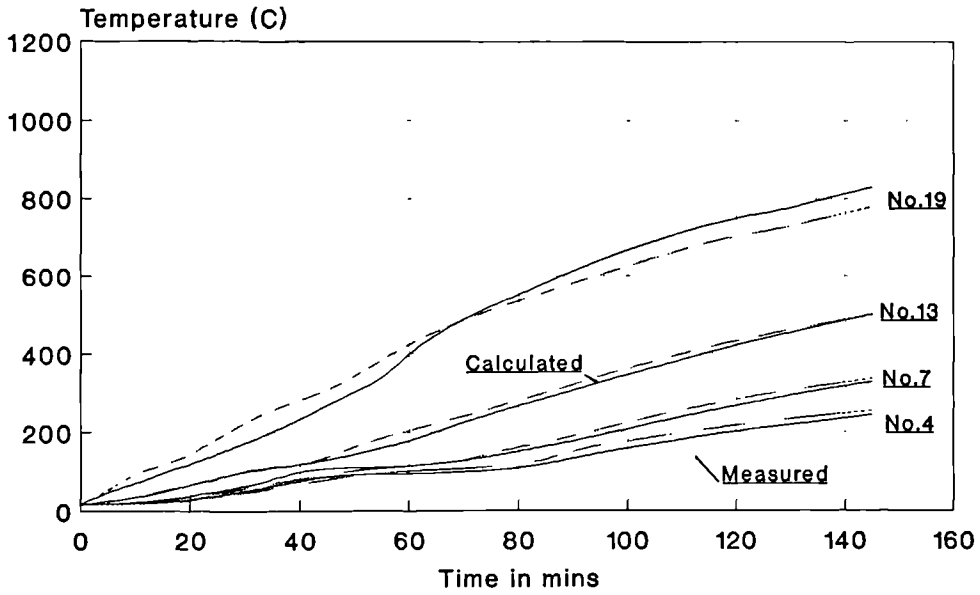

Fig.8.13 The Comparison of Calculated and Measured Temperature Distribution Holorib 51/Hb=70mm (with steel sheet)

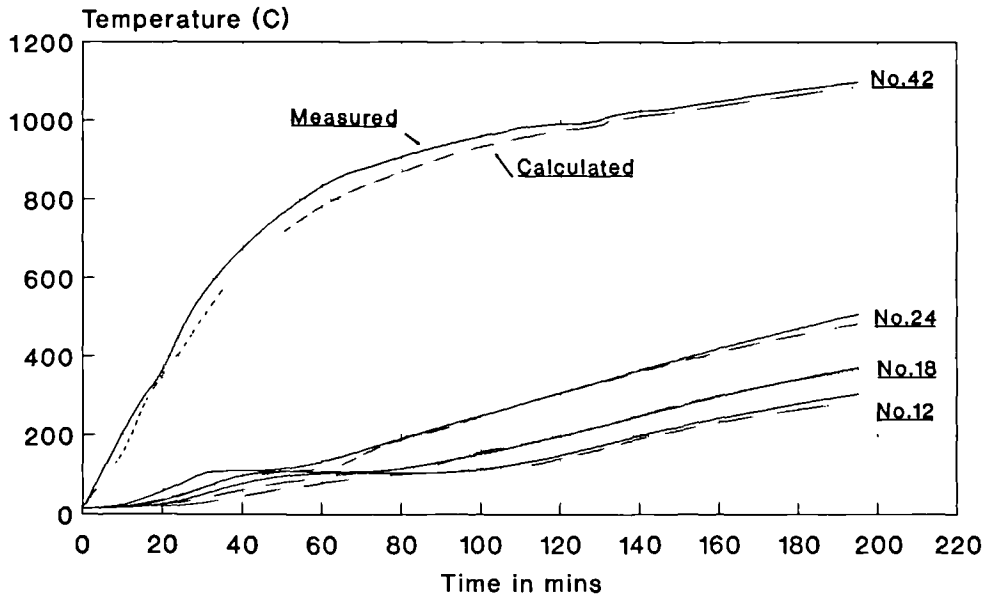

Fig.8.14 The Comparison of Calculated and Measured Temperature Distribution Holorib 51/Hb=90mm (with steel sheet)

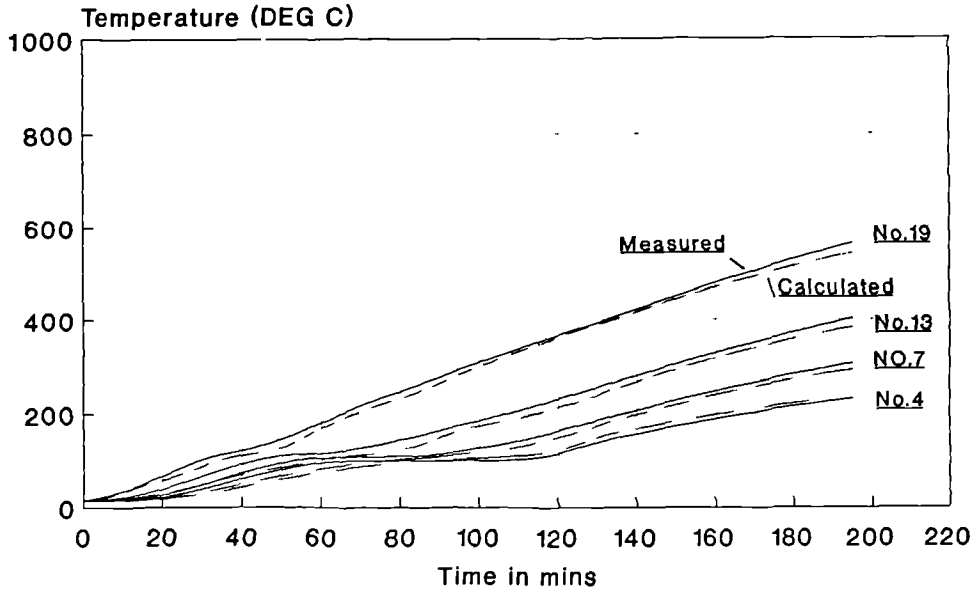

Fig.8.15 The Comparison of Calculated and Measured Temperature Distribution Holorib 51/Hb=90mm (with steel sheet)

CHAPTER 9

Experimental and Computational Approaches

In the past, considerable research has been done and considerable advances have been made in the determination of the fire resistance of components of construction. Nevertheless, there *is still a lack of appropriate* regulations and design codes concerning the use of some composite materials such as GRP. Moreover, one of the major recommendations which was strongly endorsed by the Lord Cullen report[9.1] on the Piper Alpha disaster, which occurred on 6 July 1989 and claimed 167 lives, was that the industry should move away from a prescriptive, mechanistic approach to safety requirements, to those of a goal-setting nature which ensure an adequate response. Then the one major problem often confronted by designers and product developers is: **" which is the best and cost-effective way to satisfy such guidance? "**

Currently, there are two fundamental ways to investigate the fire performance of a structure, namely experimental and computational approaches. Both the advantages and disadvantages of experimental and computational approaches are discussed in this chapter. The main conclusion is that the best strategy to carry on the optimisation of design for fire critical applications, is to obtain *synergy* between the experimental and theoretical approaches. In fact, both approaches are complementary to each other in nature.

9.1 Fire Resistance Tests

Although fire tests for materials and structures could include consideration of the following aspects: fire resistance, fire propagation, heat release and smoke release rate; fire resistance is the main concern of this thesis. As stated above, the primary objective of the fire resistance test method is to determine the length of time that an assembly of construction will satisfy certain criteria related to its intended function under exposure to the test conditions. The fire resistance test is used basically for three purposes:

- to be able to claim fire resistance for a given construction and hence to have it accepted by the regulatory bodies
- to assist with the development of new products and systems
- to establish the essential parameters to predict the fire behaviour of elements of a structure.

Furthermore, fire resistance tests can be divided into the following categories: full-scale standard tests, small-scale 'standard' tests and whole structure tests.

The required fire resistance rating is assigned by the building codes for various portions of the assembly, depending on its relative significance to the overall structural stability or the importance of it retains its function. The size of the element for a full-scale standard test, for example for a vertical separating element according to BS476:part 20[1.1], should be a full sized element of building construction or if it exceeds the size that can be accommodated by the furnace, the minimum size of element exposed to the heating conditions in the

furnace should be 3m high by 3m wide. These tests therefore require considerable facilities, manpower, and material to conduct and thus they can be expensive. The testing costs for a large research program can be appreciable since many samples may be needed to evaluate alternative protection materials with various thicknesses and construction details. Another problem is that the number of existing furnaces which meet the size requirement is also limited. However, the fire resistance rating is a basic property for which all products in the market are tested, and it gives the user or specifier the first criterion for selecting a suitable product.

The indicative small-scale test, which replicates the particular test specifications but on a smaller sample, provides an alternative scheme for fire testing. It is usually preferred for the research activities involved in developing a fundamental understanding of the behaviour of a component and is the procedure used in this thesis. Obviously this test method greatly reduces the costs and time. This enables sensible assessments and indications for actual fire performance to be made which is very useful in the development of a new material or in the comparative evaluation of existing materials. It can also provide the data for the calibration and validation of theoretical models.

Although the standard tests have their limitations, such as the consideration that the applied thermal procedure may not represent an actual fire, they certainly establish the points of comparison for the overall risk and behaviour, and provide a measure of the relative performance of structures and materials within the capabilities of fire testing furnaces. Therefore, they are the prescriptive testing which is required in many countries. Full-scale tests can also supply the

information necessary for the development of reliable small-scale tests.

Once the confidence has been established in the design of a structure on the basis of material and element fire tests, a whole-scale compartment test might be needed to prove its performance conclusively with the provision of realistic fire conditions. Sometimes, realistic dimensions are important in evaluating certain effects, for example, the effects of continuity in continuous beams or of the degree of fixity in beam-to-column connections, the effects of static loads on structural elements exposed fire and the effects of specimen dimensions. In any case, it is the real fire attack that has to be anticipated and to be withstood by fire protecting structure. A whole-scale experiment may be the only resort for some very complicated and critical cases, and most engineers have more confidence in the results of such tests.

In these tests, the treatment of fire as a load condition requires that the fire type, location, geometry, intensity and heat flow characteristics be defined. It is clear that the design of this sort of experimental arrangement, which is a true representation of the actual hazard, is by itself a fairly difficult process. It will depend on the actual circumstances and requirements, and may require an empirical approach to be designed by fire experts. Obviously, to test the whole structure under realistic fire condition is also overwhelming costly.

Fire tests can also be classified according to the type of fire that they represent. Typical examples are cellulosic furnace fire tests, cellulosic room fire tests, hydrocarbon furnace fire tests, hydrocarbon jet fire tests and pool fire tests. Except for the furnace tests, there are no well established individual standards for

these tests.

Every fire test, if reproducible, is satisfactory for its own configuration and scenario. However, it is unrealistic to expect that one small-scale test will completely describe the fire risks of the real world. This problem exists even in large-scale tests are used. Yet, properly interpreted small-scale tests offer the most practical and economically reasonable method of evaluation the fire behaviour of materials. Therefore, problems have arisen in using the results from specific tests to predict fire behaviour in the unlimited configurations found in the real world.

9.2 Computational Approach

The ever increasing cost of fire tests is contrasted to the failing costs of computer software and hardware. The time scale associated with the running of a computer programme can be significantly less than the time required to set up and execute a fire test of the same problem. In addition, an advantage of a computational analysis is that it enables the performance of a passive fire insulation material to be assessed for applications which may deviate significantly from those modelled in the standard tests. Numerical analysis can offer greater flexibility in the choice of geometries, sizes, materials and boundary conditions, then as a consequence, increasing the opportunities for flexibility in design. It gives the designer more control over the performance of the system and a considerable reduction in the need for involved fire tests. The modelling of

different possible alternatives by computational technique is of great help during the planning stage.

The prime objective in passive fire protection is to reduce the temperature rise in the components during the fire. The computational thermal models allow the prediction of the temperature increase throughout a structure subject to a heat flux. The constructional design can then be easily established for a range of required thermal insulation at an appropriate thickness for particular heat loads and fire durations.

Nevertheless, it is useful to be aware of the drawbacks and limitations of the computational method. The limitations of the computational approach are that some processes are not easily modelled and that the accuracy of a model depends on the assumptions and approximations made in formulating it and in the material properties adopted. In detail, the applicability of the thermal model is dependent upon following factors:

a. A precise representation of the heat loading with time.
b. Thermal properties and pyrolysis data, including the:
    1. Thermal conductivities of the material at various temperatures (and moisture contents).
    2. Specific heat capacities of the material at various temperatures.
    3. Emissivity of the surfaces at various temperatures.
    4. Kinetic parameters A and E_A, as defined in Chapter 4.
c. Energy losses or gains associated with chemical reactions or changes of state that may occur to materials at elevated temperature.

If these requirements are fulfilled, then the performance of a particular element of construction subjected to a fire test will not be difficult to determine by a computational approach.

Over the last two decades, research bodies in many countries have studied the behaviour of construction elements in real fires and in fire resistance tests, and thus obtained data on the effect of high temperatures on the properties of material. This has consequently paved the way for the possibility of computing fire resistance as part of the normal design process. Many national and international committees are now engaged in refining procedures which can be adopted by professional bodies, code preparing organizations and regulatory authorities. Given the common research effort, the tendency to replace some fire tests with fire-safety engineering calculations is now being accepted at official and legal levels. For instance, the European Convention for Constructional Steelwork published its European Technical Notes on a calculation method to determine the fire resistance of centrally loaded composite steel concrete columns exposed to the standard fire[2.5], and the 1992 Eurocodes contain clearly separate chapters on structural fire design where calculation procedures are accepted[9.2]. An American Concrete Institute Committee 216 even offered the following revising statement to ACI 216R-81 'Guide for Determining the Fire Endurance of Concrete Element' [9.3]: " *As shown in the previous sections of this Report, performing such (fire endurance) tests is not necessary for a large number of concrete elements. Information on their fire endurance can be derived by the application of calculation procedures based on heat flow studies and structural analyses, and on the knowledge of the behaviour of concrete and steel at elevated temperatures, rather than by fire test.*"

Nevertheless, the evaluation of the fire behaviour of components of construction under real fire condition is a complex process. Risk depends not only on the intrinsic properties of the material but also on the amount of material, its configuration, and its exposure. Risk also depends critically on the environment and usage. Research in numerical modelling has the potential to provide a more fundamental understanding of heat transfer and fire resistance problems. In principle, numerical modelling offers a rigorous framework because all the interacting processes, if known and capable of accurate quantitative description, can be included.

In order to obtain the desired level of accuracy and predictability, the fire test arrangements also need improvement in order to provide more precise data to verify and elaborate the numerical models. The harmonization of standard test methods for different countries is also demanded. Efforts should be made to standardize the construction of test furnace such as to dimension, materials used, fuel, burner and exhaust arrangement, aiming at reducing the differences between the various furnaces.

Looking ahead, the development of rigorous and intelligent computational tools incorporating fire parameters to complement or replace the furnace tests will be continuously pursued, with the aim of maturing the simplified design guidance to meet the requirement of stipulations and even the prediction of the durability in *real fire scenarios*. This is believed to be of considerable long-term value to the industry.

CHAPTER 10

Summary and Conclusions

10.1 Present Study

Major fires usually cause severe structural damage, even in areas remote to the fire area. Fire could lead to partial or total collapse of an industrial installation or domestic building resulting in loss of life, property and/or environmental pollution, as happened in the North Sea Piper Alpha disaster. Considerations should then be given in the design of the structure and its protection in order to minimize the effects of these events. Preventive measures have historically been, and will continue to be, the most effective approach in reducing the probability of spread of a fire and the resultant consequences of the conflagration.

The industries have long relied on prior experience to provide 'expert judgment' for evaluating fire hazards. This has worked reasonably well for traditional materials used in the traditional manner, but when new materials are used or old materials are used in new ways, hazards may be developed which are difficult to anticipate if there is a lack of suitable analytical methodology. It is desirable that the fire safety of products, including those using advanced composite materials, should be treated by the same good engineering practices as are used for the determination of strength and performance.

The determination of the temperature distributions in the components of construction, due to fire, is critical for the valuation of the passive fire protection required in the construction. This thesis presents a methodology to study such events, which involves a combination of theoretical, numerical and experimental approaches.

The design of building elements for a prescribed level of fire safety can be made based on established engineering principles. Prediction of their fire endurance can also be derived by the application of analytical procedures, rather then by fire tests only. The complexity of the governing equations generally allows analytical solutions to be obtained only for very simple cases, making it necessary to use numerical techniques for most problems of practical interest. With the expansion of the capability of personal computer and using computer codes, this approach is becoming increasingly more practical. The growing need to optimize fire protection systems has made it imperative to simulate the relevant thermal transport phenomena numerically, since experimentation is usually too involved and expensive. There has been a phenomenal increase in the use of computational methods for heat transfer problems, as a result of their low cost, remarkable speed, detailed and complete information. However, available analytical and experimental results are of considerable importance in checking the accuracy and validity of numerical results.

In the principle, the computational thermal models developed in this thesis can be used for the design of the loadbearing and non-loadbearing elements of construction for prescribed level of fire safety. However, for loadbearing components, their deflection should be included in the calculation, provided that

the mechanical properties of the material at elevated temperature are known.

General speaking, there are three obstacles to the numerical heat transfer analysis for an element of construction subject to fire. The first problem is to determine the heat exchange between the outer surface of the element and the fire environment. This includes the determination of the heat loading from the fire and environment, the heat loss from the structure, the view factor and the emissivity. The next question concerns that the inadequate information on the thermal properties of material at elevated temperatures. The third problem is the shortage of knowledge of the various processes that affect the heat transfer during exposure to fire, such as moisture migration and material decomposition.

All of these problems and their influences have been investigated in this study. Simulated cellulosic and hydrocarbon fire tests have been conducted for various materials and configurations. Emphasis was laid on the development and verification of one and two-dimensional finite difference and finite element thermal models.

With the advances in material science, sandwich construction is increasing its application in fire resistant structures. In Chapter 2, the explicit finite difference formulations for multi-layer panels were derived. The spatial intervals for FD analysis of the different material layers could be unequal. The realistic boundary conditions on the exposed and unexposed sides of the panel have been formulated from the normally established physical equations. The heat transfer coefficient for convection and resultant emissivity for radiation are the decisive factors within the formula.

A similar treatment for the multi-layer pipes was described in Chapter 3. It also includes the two-dimensional finite difference formulations for pipes and the treatment of internal heat exchange.

One of the major concerns of the architect and engineer using materials incorporating plastics resin in the construction industry is the problem associated with fire. In Chapter 4, a blend of experimental, theoretical and numerical techniques was used to exploit predictive capabilities for the thermal response of fire resistant polymer composites. The approach included the correlation of thermophysical properties as function of temperature and stage of decomposition. These correlations are then used in a one-dimensional numerical model, with a formulation based on major physical and chemical processes occurring in a decomposing and expanding polymer composite. The initial attention was focused on the performance of GRP laminates and pipes. The various factors which influence the heat transmission were investigated in detail.

One discovery as a consequence of fire tests on GRP laminates is that the effect of internal convection may be neglected due to the poorer contact between the liberated gas and the fragments of the carbonaceous char.

Another finding is that the interlayer delamination is an important factor which affects the fire resistance of woven roving glass-fibre/phenolic laminates. A new model for delamination in a phenolic laminate was therefore proposed, and a good agreement was then obtained between the theoretical prediction and experimental measurement.

Depending on the type of problem under consideration, either the heat absorbed or the heat released by combustible materials in a fire environment may be critical respectively. When the flashover point of a fire in a construction is considered, the heat generated by the combustion of the volatiles should be known. Conversely, if the fire resistance of a component in a standard furnace test is simulated, the amount of absorbed heat for decomposition is important. In fact, both the heat absorbed and heat released are two key factors in the progress of a fire. They will determine the probability of ignition, fire spread and sustaining, and the decay of a fire.

The characteristics of the intrinsic thermal properties and the kinetic parameters of pyrolysis on heat transfer were discussed in Chapter 5. The values of these parameters which were used in the numerical modelling were listed. The significant influence of moisture content on thermal conductivity and specific heat capacity was investigated in considerable detail. A new treatment for the moisture influence on heat transmission was then proposed and the experimental confirmation was given.

Chapter 6 provided the experimental verification of the theoretical analysis and numerical calculation for various 'traditional' and innovative composite materials. The dimensions and constitution of the specimens were described and the comparisons of numerical and experimental results were performed.

On the basis of the developed models, a number of use-friendly finite difference computer programmes were written. The description of these programmes was outlined in Chapter 7. These programmes are capable of evaluating the

temperature distribution history of various construction components under fire impingement. Pre- and post-processors were integrated into the programmes which allow fast and use-friendly input/output operations. The programmes provide a convenient tool for the validation of innovative theoretical models and, at same time, a valuable means for fire safety design.

Heat transfer analysis may be expected to be able to model realistic environmental boundary conditions, to represent complicated geometry and to analyze a variety of materials. Of the two, the finite element method is believed to be superior to the use of finite difference methods. In Chapter 8, a two-dimensional finite element model for the heat transfer problem was accomplished. The verification of its performance was carried out by means of a practical example: namely a composite concrete/ steel deck slab exposed to fire using data from tests conducted by other researchers. An excellent agreement was obtained between the computational results(which incorporated the proposed model for moisture effects) and the experimental measurements.

In Chapter 9, the general issues about the role of experimental and computational approaches in fire safety study and design were highlighted.

The following main conclusions can be drawn from this work:

1. In order to address the fire resistance problem effectively, the optimal approach is the combination of experimental and computational schemes.

2. Due to the aforementioned advantages of numerical modelling, the

influence of each parameter on heat transmission can be more readily assessed by computer. This enables both the controlling authorities and designers to arrive at solutions which represent the optimum level of protection commensurate with the risk.

3. The discussion about the relative merits of computational analysis and experimental investigation is not aimed at recommending computation to the exclusion of experiment. Both of them have their own place. The sequence of fire testing should be in an ordered progression leading from small scale laboratory testing, then gradually increasing in scale and complexity.

4. In the development of the computational models, it should be born in mind that they should easy to apply. The simplest model can be accepted which has the ability to predict the thermal behaviour with an acceptable accuracy and which minimizes the number of variables in the model.

5. With the provision of the requisite parameters, it is possible to provide an accurate temperature distribution for elements of construction subjected to a specified fire environment. The thermal properties of insulating materials can be evaluated by comparisons with the results obtained from the necessary fire tests and computer simulations. Once confidence is obtained, the computational programme can analyse and optimise the passive fire protection of any profile for any boundary condition and fire exposure. It can also assist and guide the experimental work.

6. The explicit finite difference method was proven to be a simple and effective method to solve the heat conduction problem in elements of construction .

7. A number of successful comparisons between numerical analysis and test results have been obtained in this study, and additional insight into the heat transmission mechanism on a variety of elements of construction has been offered. Based on the results of this thesis, two scientific papers have been presented in distinguished international forums[5.18,10.1], and a further three papers are going to be published[10.2-4].

8. With the consideration of the moisture content, although the presence of moisture will raise the apparent thermal conductivity of the material, the energy needed to drive off the water, which could be either physically or chemically trapped in the material, is of considerable significance. Then the time needed to elevate the temperature on the unexposed side of a component heated until the insulation criterion is exceeded is extended significantly and this is of great benefit for its fire resistance.

9. Although the delamination in woven roving glass-fibre/phenolic laminate at high temperature will be beneficial for heat insulation, it may be unwelcome since it will wreck the structural integrity and reduce the mechanical strength. In order to avoid this, some property improvements should be made for phenolic resin to relieve this effect.

10. Whereas the development of scaled down bench mark tests will not totally

eliminate the need for full scale testing, it will allow quick and low cost screening of candidate materials. The laboratory-scale technique which was employed in this study is suitable for calibrating the theoretical models.

11. Most previous tests were not initially designed to provide an analytical basis for computing, and consequently difficulties have been experienced in completely correlating the calculated and the experimentally obtained performance. The standard fire test methods should be improved by establishing the precise properties of the materials being subjected to the test and by applying additional data to the mathematical model, which will then facilitate interpolation and extrapolation of these data. It will also be of great help for the wide acceptability of the analytical approach[10.5].

12. With the advent of computers in design offices and their use for normal design purposes, it is inevitable that similar techniques should be considered for fire design. The completion of this thesis is expected to form a necessary step towards this end. The computation of the fire resistance of some types of elements of construction has become a reality and it is only a matter of time before these methods will be widely used by the industry.

10.2 Future Development

Standard fire resistance tests and their computational simulation play an important role

in fire engineering. Both the temperature of a fire and its heat flux should be considered before making a fire safety judgment because there is no accepted correlation existing between the temperature of a fire and its heat flux falling on the surface of a structure. Unfortunately, the existing inventory of various fire resistance standards have a serious deficiency at this point. The temperature in a fire testing furnace is usually controlled in accordance with these standards. However, defining temperature-time characteristics is necessary but not sufficient as the sole characteristic for determining the thermal loading for a construction element exposed to a fire, as shown in Eq.(2.5). For a prescribed temperature-time curve, the convection and radiation heat transfer from the fire to a specimen can vary considerable from one furnace to another[10.5,10.6]. Ideally, it would be preferable to control furnaces to regulate the total heat irradiation received at the surface of the test specimen. Unfortunately, there are serious instrumental difficulties inherent in such a scheme.

Accordingly, an important development will be concerned with the instrument improvement which can precisely measure of heat flux received by the structural element under test. If this does not work, alternatively, the following proposal might be worth exploring. The idea is that with the use of numerical techniques and the measurement of the temperature profile on a thermally stable sample whose properties are well known, the irradiation provided by the furnace might be computed by the methods described in this thesis. The main advantage of such data is to enable an accurate assessment to be made of heat transmission from the fire to the construction. This would allow furnace test results to be correlated to a standard heat impingement. In the long term, uniformity in the method of controlling exposure conditions for different fire test environments

needs to be pursued.

Other further subjects could be:

1). Additional experimental verification of pipe modelling. Tests on more pipes and their joints are needed to check the numerical programme. These should also include two-dimensional heat loading and pipes filled with stagnant and flowing water.

2). Extra verification of moisture modelling with large hygroscopic panels with impervious skins. The interrelation between bench-scale and full-scale fire test methods is also needed to be further investigated.

3). The assumption of perfect contact between the interface of two material layers may cause some errors, as shown in Specimen 7 in Chapter 6. Although considerable amounts of theoretical and experimental work have been done on the prediction thermal contact resistance, it appears that the reliable results for practical use are still those that have been determined experimentally[5.19]. Based on experimental results, an empirical formula might be added to the existing numerical modelling.

4). Continued development work on the three-dimensional model and programme will permit the analysis of the problems with more complicated configurations, such as joints and concrete with spalling. Identifying the most effective numerical procedure to solve the corresponding nonlinear equations is also demanded.

5). More accurate thermophysical properties of various materials are required. The nonlinear regression method might be useful to tune these properties from experimental data[10.7-8]. Some data, for the instance heat release rate of combustible materials, might be procured through some special instruments, such as the cone calorimeter[10.9].

6). For decomposing materials, a study of the effects of the assumption of local-thermal equilibrium and internal convection on the overall response might be needed. More work could be carried out to verify the extended model for other materials, such as timber.

7). As was outlined previously, one main drawback in the all existing fire resistance standards is that all of them specified the severity of fire in terms of temperature. Actually, the fire severity does not solely depend on the temperature of the fire. The more important parameter is how much heat flux is irradiated onto the surface of the structure. The determination of the emissivity and heat transfer coefficients for standard and actual fire environments should be further explored.

9). The determination of the mechanical responses of structural element under fire impingement is also very important in many situations. The interrelated influence of thermal and mechanical behaviours should be considered at this stage. As the temperature field and the mechanical properties of the material at elevated temperature are known, the mechanical behaviour of the structure can be determined by using commercially available finite element packages.

List of Main References

[1.1] BS476:Part 20: Fire Tests on Building Materials and Structures. British Standards Institution, 1987 and AMD 6487, April 1990.

[1.2] International Organization for Standardization: International Standard ISO 834, First edition, 1975.

[1.3] Babrauskas, V., and Williamson, R.B.: The Historical Basis of Fire Resistance Testing -Part I., Fire Technology, 14,184-194, 1980.

[1.4] Babrauskas, V., and Williamson: The Historical Basis of Fire Resistance Testing -Part II., Fire Technology, 14,304-316, 1980.

[2.1] Croft, D.R. and Lilley, D.G.: Heat Transfer Calculations Using Finite Difference Equations, Appl. Sci. Publ., London, 1977.

[2.2] Orivuori, S.: Efficient Method for Solution of Nonlinear Heat Conduction Problems, Int. J. Num. Meth. Eng.,14,1461-76,1979.

[2.3] Wrobel, L.C.: A Novel Boundary Element Formulation for Nonlinear Transient Heat Conduction, Numerical Method in Thermal Problems, Ed. R.W.Lewis and K. Morgan, vol V.,1987.

[2.4] Holman, J.P.: Heat Transfer, 7th Edition, McGraw-Hill Publishing Company, 1990.

[2.5] European Convention for Constructional Steelwork: Calculation of the Fire Resistance of Centrally Loaded Composite Steel-Concrete Exposed to the Standard Fire. First Edition, 1988.

[2.6] Thring, M.W.: The Science of Flames and Furnaces, second edition, Chapman & Hall LTD, 1962.

[2.7] Incropera, F.P. and De Witt, D.P.: Findamentals of Heat and Mass Transfer, third edition, John Wiley & Sons, 1990.

[2.8] Fletcher, J.D. and Williems, A: Emissivities of Ceramic Fibre Linings for High-temperature Furnaces, J. of the Institute Energy, p377-380, V57, 1984.

[3.1] Ozisik, M.N.: Heat Transfer, McGraw-Hill, New York, 1985.

[3.2] Sterner, E. and Wickstrom, U.: TASEF - Temperature Analysis of Structures Exposed to Fire, Swedish National Testing Institute, SP Report 1990:05.

[3.3] McAdams, W. H.: Heat Transmission, McGraw-Hill Book Company, 1954.

[3.4] Siegel,R. and Howell, J.R.: Thermal Radiation Heat Transfer, third edition, Hemisphere Publishing Corporation,1992.

[4.1] Bamford, C.H., Crank, J. and Malan, D.H.,The Combustion of Wood, Part 1, Cambridge Phil, Soc. Proc., Vol.42, p166-182, 1946.

[4.2] Matsumoto,T., Fujiwara,T. and Kondo,J.: Nonsteady Thermal Decomposition of Plastics, Twelfth Symposium (International) on Combustion, The Combustion Institute , p515-521, 1969.

[4.3] Kung, H.C.: A Mathematical Model of Wood Pyrolysis, Combustion and Flame, Vol 18, p185-195, 1972.

[4.4] Griffis,C.A., Masumura, R.A. and Chang, C.I.: Thermal Responspone of Graphite Expoxy Composite Subjected to Rapid Heating, J. of Composite Materials, Vol 15, p427-442, 1981

[4.5] Kanury,A. M. and Holve,D.J.: Transient Conduction with Pyrolysis (Approximate Solutions for Charring of Wood Slabs), J. of Heat Transfer, Vol.104,p338-343, 1982.

[4.6] Henderson,J.B., Wiebelt,J.A, and Tant,M.R.: A Model for the Thermal Response of Polymer Composite Materials with Experimental Verification, J. of Composite Materials, Vol.19, p579-595, 1985.

[4.7] Fredlund, B.: Modelling of Heat and Mass Transfer in Wood Structures During Fire, Fire Safety Journal, Vol.20,039-69,1993.

[4.8] Henderson,J.B. and Wiecek,T.E.: A Mathematical Model to Predict the Thermal Response of Decomposing, Expanding Polymer Composites, J. of Composite Materials, Vol.21,P373-393, 1987.

[4.9] Milke J.A. and Vizzini A.J.: Thermal Response of Fire-Exposed Composite, J. of Composites Technology & Research, Vol 13, No 3, p145-151,1991

[4.10] Cagliostro, D.E. et al.: Intumescent Coating Modeling, J. Fire & Flammability, vol 6,205-221,1975

[4.11] Anderson, C.E. and Wauters, D.K.: A thermodynamic Heat Transfer Model for Intumescent Systems, Int. J. Engng. Sci.,vol.22, no.7, 881-889,1984

[4.12] Anderson, C.E., *et al* : Intumescent Reaction Mechanisms, J. of Fire Sciences, Vol.3, PT:3,p161-194,1985.

[4.13] Buckmaster, J.: A Model for Intumescent Paints, Int. J. Engng. Sci., vol.24, no 3,263-276,1986.

[4.14] Zverev,V.G., *et al* : The Heat Transfer Mechanism and Fire Insulation Properties of Some Intumescent Materials, Intern. J. Polymeric Mater.,Vol.20,p91-99, 1993.

[4.15] Ferdlund, B: A Model for Heat and Mass Transfer in Timber Structures During Fire, Report LUTVDG/(TVBB-1003), Dept. of Fire Safety Engineering, Lund University, SWEDEN, 1988.

[4.16] Roberts, A.F.: Problems Associated With the Theoretical Analysis

of The Burning of Wood, p893-903, Thirteen Symposium (International) On Combustion, the Combustion Institute, Pittsburgh, 1971.

[4.17] Kung, H-C, and Kalelkar, A. S.: On the Heat of Reaction in Wood Pyrolysis, Vol 20, p91-103, Combustion and Flame, 1973.

[4.18] Hume,J: Assessing the Fire Performance Characteristics of GRP Composites, Material and Design Against Fire, International Conference, IMechE 1992-7, London, 27-28 Oct.,1992.

[4.19] Thon, H., et al: Use of Glass Fibre Reinforced Plastic (GRP) Pipes in the Fire Water System Offshore, Proc. of the 10th Int. Conf. on OMAE., 1991.

[5.1] Harmathy, T.Z.: Properties of Building Materials: Bases for Fire Safety Design, Design of Structures Against Fire, edited by R.D. Anchor, J.L.Malhotra and J.A. Purkiss, Elsevier Applied Science Publishers,1986.

[5.2] Parrott, J.E. and Audrey D.S: Thermal Conductivity of Solid. Pion Limited 1975.

[5.3] D.P.H. Hasselman, et al: Effective Thermal Conductivity of Uniaxial Composite With cylindrically Orthotropic Carbon Fibers and Interfacial Thermal Barrier, J. of Composite Materials, P637-646, Vol.27, No.6, 1993.

[5.4] Pilkington, Offshore and Marine Insulation Manual.

[5.5] Cape Boards Limited: Cape Boards, the Fire Protection Handbook. 1987.

[5.6] Harmathy, T.Z.: Effect of Moisture on the Fire endurance of Building Elements, Sixty-seventh Annual Meeting Papers, ASTM Special Technical Publication No.385,p74-95,1965.

[5.7] Sullivan, P.J.E., Terro, M.J. and Morris,W.A.: Critical Review of

Fire-Dedicated Thermal and Structural Computer Programs, J. Applied Fire science, Vol.3(2), p113-135,1993-94.

[5.8] Lie, T.T. and Celikkol, B.: Method to Calculate the Fire Resistance of Circular Reinforced Concrete Columns, ACI Materials Journal, p84-92,Jan-Feb, 1991.

[5.9] Huang, C.L.D, Ahmed, G.N. and Fenton, D.L.: Responses of Concrete Wall to Fire, Int. J. Heat Mass Transfer 34,649-661, 1991.

[5.10] Sahota, M.S. and Pagni, P.J.: Heat and Mass Transfer in Porous Media Subject to Fires, Int. J. Heat Mass Transfer,22,1069-1081(1979)

[5.11] K. Ödeen: Fire Resistance of Prestressed Concrete Double T Units, Acta Polytechnica Scandinavica, Ci 48,Stockholm, 1968.

[5.12] Hamerlinck R., Twilt L. and Stark J.: A Numerical Model for Fire-Exposed composite Steel/Concrete Slabs. Tenth International Specialty Conference on Cold-formed Steel Structures, St. Louis, Missouri, U.S.A., October 23-24,1990.

[5.13] Drysdale, D: An Introduction to Fire Dynamics, John Wiley and Sons, 1985.

[5.14] Redland Plasterboard Limited: Redland Plasterboard, Redland Drywall Manual 1990.

[5.15] Mehaffey, J.R., et al: A Model for Predicting Heat Transfer through Gypsum-Board/Wood-Stud Walls Exposed to Fire, Fire and Materials, p297-305, Vol.19, 1994.

[5.16] Jakob, M.: Heat Transfer, Vol.1, Chapman and Hall, London. ١٩٤٩

[5.17] Harmathy, T.Z.: Properties of Building Materials at Elevated Temeratures, DBR paper No. 1080, Division of Building Research, National Research Council Canada.

[5.18] Davies,J.M., Hakmi, R. and Wang,H.B.: Numerical Temperature Analysis of Hygroscopic Panels Exposed to Fire, p1624-1635, Numerical Methods in Thermal Problems, Vol. VIII Part 2, Proceedings of the Eighth International Conference Held in Swansea, July 12-16th, 1993. Pineridge Press, UK.

[5.19] Hollaway L.:Glass Reinforced Plastics in Construction, Surrey University Press, 1978.

[5.20] PATHOS Manual: Palm Computing's Analysis of Thermal Hazards on Offshore Structures. Palm computing Limited, Dec 1991.

[5.21] Madorsky, S. L.: Thermal Degradation of Organic Polymers. Interscience Publishers, John Wiley & Sons,Inc., 1964.

[6.1] Davies, J.M., McNicholas J.B., Dr. Hakmi R. and Hong-Bo Wang: Cost Effective Use of Fibre Reinforced Composites Offshore, Final Report, Marinetech North West Programme, Phase 2. 191

[6.2] Ellen G. Brehob and Anil Kulkarni: Time-dependent Mass Loss Rate Behaviour of Wall Materials Under External Radiation, Fire and Materials, Vol.17,249-254,1993.

[8.1] K.H. Huebner: The Finite Element Method for Engineers, Wiley, 1975.

[8.2] Becker, J., Bizri, H. and Bresler, B.: FIRES-T - A Computer Program for the Fire Response of Structures - Thermal, Report No. UCB FRG 74-1, Dept. of Civil Engineering, University of California, Berkeley, 1974.

[8.3] P.W. van de Haar, et al: The thermal Behaviour of Fire-Exposed Composite Steel/Concrete Slabs, Test Report, TNO report, BI-90-113, June 1990.

[8.4] Ralph Hamerlinck: The Behaviour of Fire Exposed Composite Steel/Concrete Slabs, Doctoral thesis, Eidenhoven University of Technology, 1991.

[8.5] Hamerliack,R., Twilt, L. and Stark, J.: A Numerical Model for Fire-Exposed Composite Steel/Concrete Slabs, Tenth International Specialty Conference on Cold-formed Steel Structures, St.Louis, Missouri, U.S.A., October,1990.

[8.6] Cooke,G.M.E., Lawson, R.M. and Newman, G.M.: Fire Resistance of Composite Deck Slabs, The Structural Engineer, Page 253-267, Vol 66,No.16, August 1988.

[9.1] The Hon. Lord Cullen: The Public Inquiry into the Piper Alpha Disaster, HMSO, London, November 1990.

[9.2] Commission of the European Community: Eurocodes - Part 10, Structural Fire Design. First Draft, Brussels-Luxembourg, 1990,

[9.3] ACI Committee 216: Guide for Determining the Fire Endurance of Concrete Elements (ACI 216R-81) (Revised 1987), Committee Action, ACI Material Journal, p101-103,Jan-Feb,1989.

[10.1] Davies, J M and Wang, H B: Numerical Temperature Calculation for Composite Deck Slabs Exposed to Fire, Advanced Computational Methods in Heat Transfer III, P331-338, Proceedings of the Third International Conference, Southampton, 22nd-24th, Aug., 1994.

[10.2] Wang, H B and Davies, J M : A Numerical and Experimental Heat Transfer Study of GRP Panels Subjected to Standard Cellulose and Hydrocarbon Fire Tests, to be published.

[10.3] Davies, J M and Wang, H B: Glass-Reinforced Phenolic Laminate Subjected to Hydrocarbon Fire Test - A Numerical and Experimental Heat Transfer Study, to be published.

[10.4] Wang, H B and Davies, J M: Computational Temperature Analysis of Glass-Reinforced Plastic Pipes Exposed to Fire, to be published.

[10.5] Malhotra, H.L.: Design of fire-Resisting Structures, Surrey

University Press, 1982.

[10.6] Cooke, G.M.E.: Use of Plate Thermometers for Standardising Fire Resistance Furnaces, Building Research Establishment Occasional Paper, March 1994, Uk.

[10.7] Beck, J.V.: The Optimum Analytical Design of Transient Experiments for Simultaneous Determinations of Thermal Conductivity and Specific Heat, Ph.D. Thesis, Michigan State University, 1964.

[10.8] Pfahl, R.C.,Jr.: Nonlinear Least Squares: A Method for Simultaneous Thermal Property Determination in Ablating Polymeric Materials, J. Appl. Polym. Sce. 10, p1111-1119, 1966.

[10.9] ISO: ISO 5660-1-1993, Fire Tests-Reaction to Fire, Rate of Heat Release from building Products (Cone Calorimeter Method), Geneva, Switzerland.

[S.1] Davies, J.M., Dr. Hakmi R. and McNicholas J.B.: Fire Resistant Sandwich Panels for Offshore Structures, Cost Effective Use of Fibre Reinforced Composites Offshore, CP07 Research Report, Marinetech North West Programme, Phase 1, 1991.

Supplement

DESCRIPTION OF THE FIRE TEST FACILITIES AND PROCEDURES

All the fire resistance tests (except those described in Chapter 8) included in this thesis were carried out using the No.1 (small) and No.2 (large) furnaces, in the Fire Research Laboratory, University of Salford. Both of these furnaces are natural gas-fired and are controlled by a computer programme[S.1,6.1]. During the tests, the furnace temperature and the output from the thermocouples on the samples were displayed on the computer screen in different colours. The temperature measurements were also logged onto the hard disc of the computer.

A continuous PID (Proportional, Integral and Derivative) three term closed control loop system was used to control the furnaces[S.1]. The Proportional control simply multiplies the error signal E(t) by a constant KP. The Integral control multiplies the integral of the error signal by KI, and the Derivative control generates a signal which is proportional to the time derivative of the error signal. The function of the integral control is to provide action to reduce the steady-state error, whereas the derivative control provides an anticipatory action to reduce the overshoots in the response.

The values of the three control constants KP, KD, and KI determine the behaviour of the controlled system. Because the furnace system is difficult to model, appropriate values of these constants were found experimentally. By changing these constants finer tuning of the system can be achieved.

No.1 Furnace

The No.1 furnace has an active volume of approximately 1.0 m^3 and is lined with insulating firebrick [S.1]. The furnace has a heavy door hinged on the left-hand side.

Gudgeon pins were welded onto the right-hand side of the door opening and an open rectangular metal frame fitted. This frame could accommodate test pieces up to 0.9 × 1.2 m^2 with an exposed hot face area of 0.7 × 0.9 m^2. For the reduced scale tests, the door can alternatively has small "window" opening (250 × 250 mm^2). The test pieces measuring 300 × 300 to 350 × 350 mm^2 were mounted over the "window" and the test run in the normal way (Fig.S.1). The test panels were supported at the bottom by a strip of insulating material and clamped near the top by two small pieces of calcium silicate and a bar (Fig.S.1). For measuring the temperature of the unexposed surface of the test specimens, one or two disc thermocouples have been used in the middle area of unexposed face, covered with a 2 mm × 30 mm × 30 mm insulating pad according to the specification of BS476: Part 20.

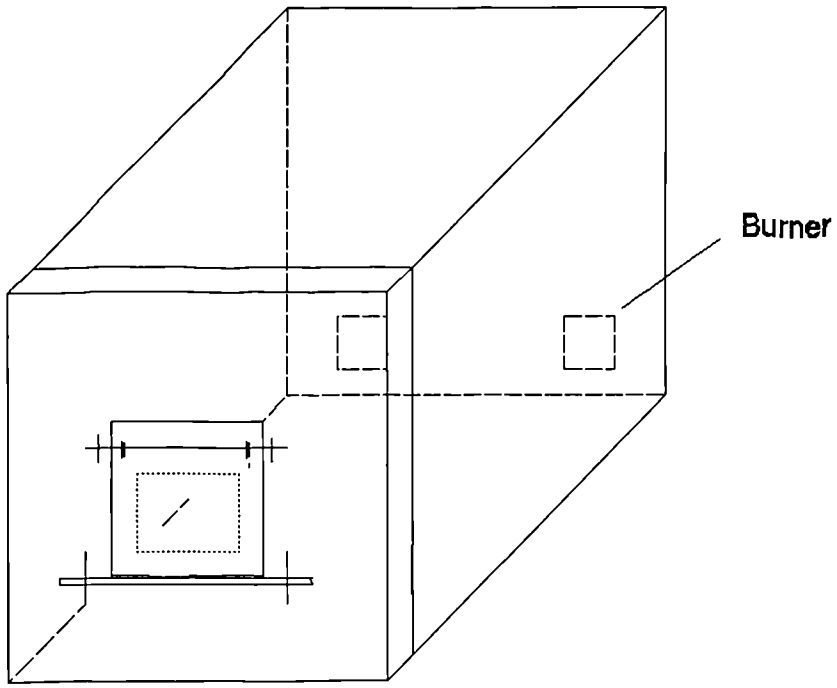

Fig.S.1 Schematic Review of No.1 Furnace and the Test Arrangement

Four furnace control thermocouples were set up in the furnace adjacent to the opening 100 mm clear of the hot face of the test panel. These were bare wire K type thermocouples meeting the BS 476 specification. The furnace has two burners with sufficient power to achieve the standard cellulosic time-temperature relationship given in BS 476: Part 20, but it had proved impossible to achieve the high initial rate of temperature increase needed for hydrocarbon fire simulation.

Pre-heating trials were carried out and eventually an acceptable procedure was devised if the hydrocarbon fire test was demanded. The procedure was that the furnace was first preheated to around 900°C and then switched off. During this heating period, a blanking panel was in place with a dummy piece of insulating material covering the window opening. Immediately after switching off the furnace, the dummy piece of material was removed and replaced by the test piece and the furnace was then switched on again. This does not create a true hydrocarbon test since, for about the first 40 seconds, the sample is subjected to a higher temperature than it specified in the standard. However, from the 40 second stage onwards, a good hydrocarbon simulation can be obtained (Fig.6.18). Since this modified test is more severe than the true test conditions it was considered to be acceptable.

No.2 Furnace

The No.2 furnace was based on a steel-frame box, clad with steel sheet and insulated with a 250 mm thickness of stack-bonded ceramic fibre(Fig.S.2,Fig.S.3)[6.1]. Lining the furnace with high quality insulation in this way allowed very rapid rates of heating to be achieved thus satisfying the hydrocarbon time-temperature requirement. Figure S.2 is a photograph of the furnace box and burner unit and Figure S.3 shows the working volume with the door open. Externally the furnace box measured 2.0m × 2.0m × 2.0m, giving an internal active volume of 1.5m × 1.5m × 1.5m (Fig.S.4 and Fig.S.5). A hinged door could be swung back through 90° to allow the testing of vertical panels in the door opening. With the door closed, pipes and other components could be tested in a fully

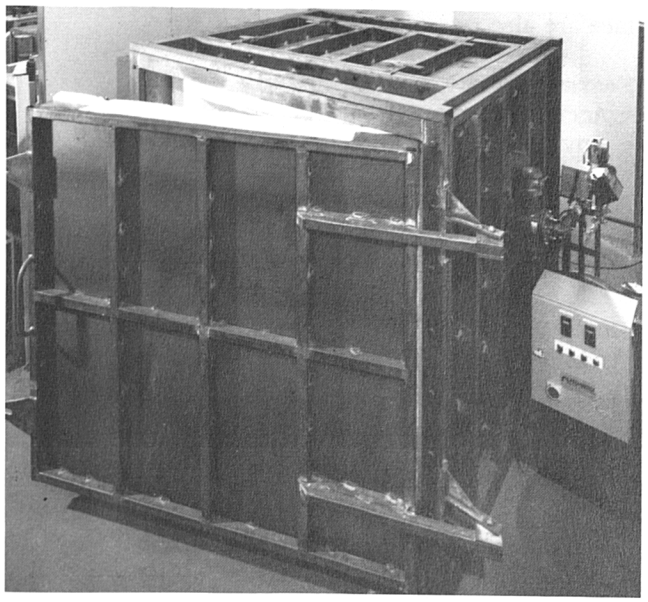

Fig.S.2 The No.2 Furnace Box and Burner Unit

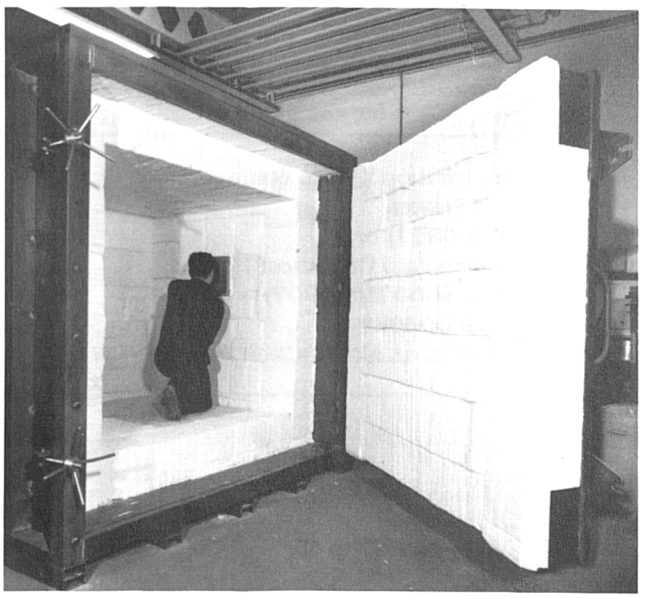

Fig.S.3 Working Volume with the Door Open of the No.2 Furnace

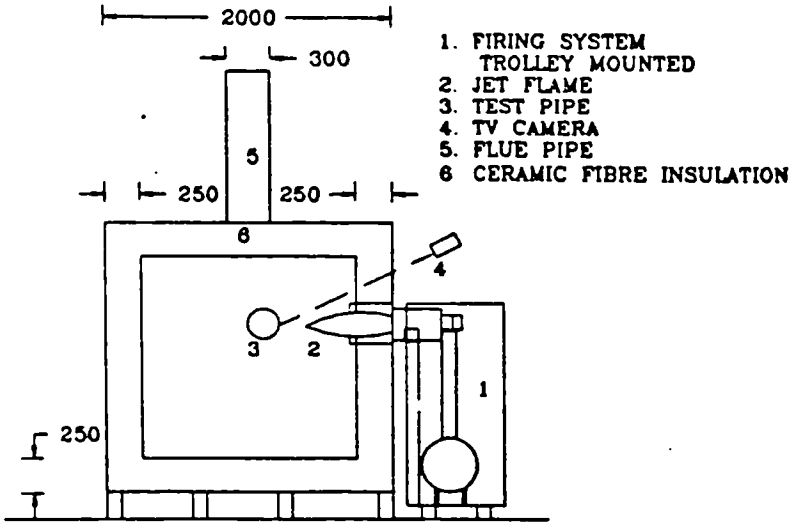

Fig.S.4 Schematic Elevation of the No.2 Furnace

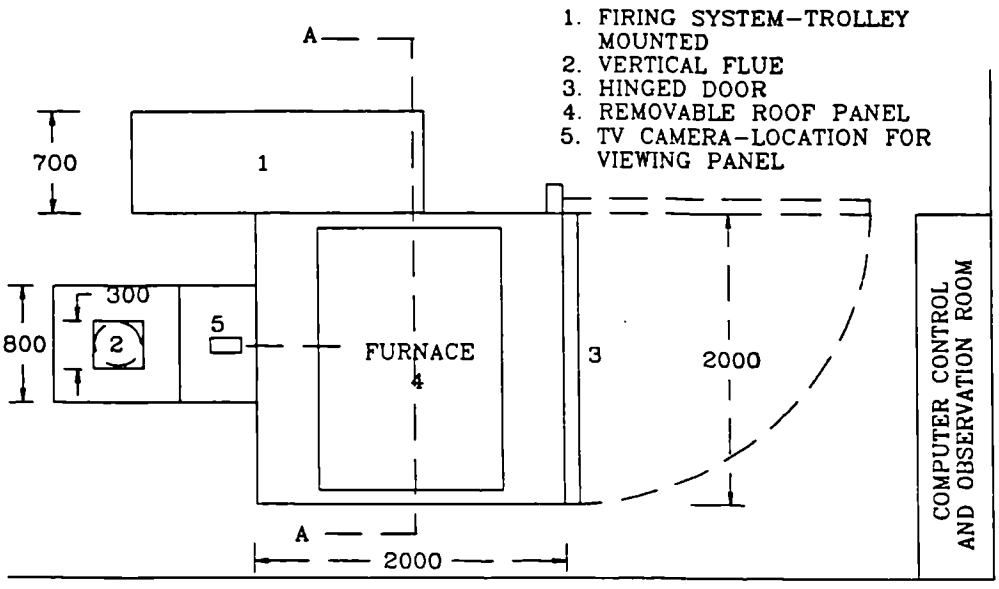

Fig.S.5 Schematic Plan of the No.2 Furnace

enclosed environment. Firing was from the side using a powerful single 15 therm burner. The flue exit was located just above the floor level, and measured 300mm × 300mm. Figure S.4 is a schematic diagram of the furnace box arrangement and Figure S.5 shows the laboratory layout which includes a separate control and viewing room. Figure S.6 shows an Ameron pipe with reinforced Pitt-Char within the furnace after an 8 minutes hydrocarbon fire test.

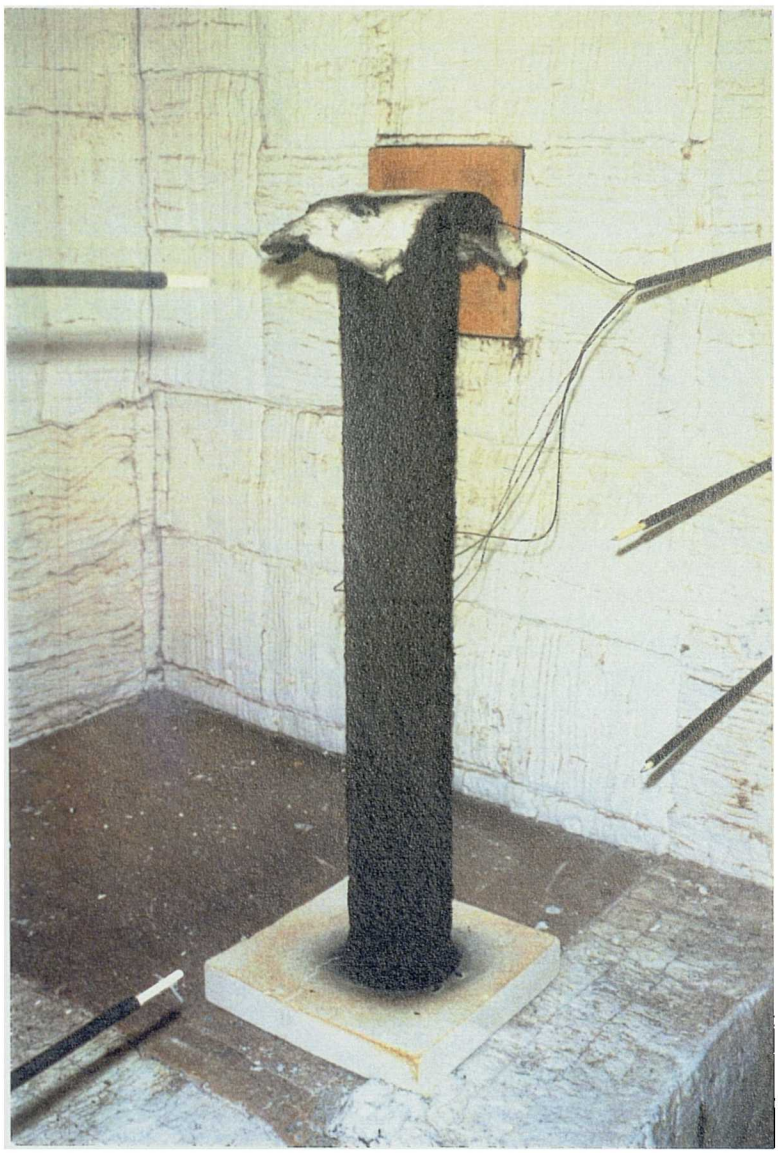

Fig.S.6 Ameron Pipe Coated with Pitt-Char after Hydrocarbon Fire Test

Haar's Experiment Arrangement

A schematic review of the test arrangement of Harr's experiments which were quoted in Chapter 8 is given in Fig.S.7 [8.3]. For each test, six unloaded test deck slabs were laid upon furnace using a temporary support in the centre of the fire compartment. The gaps between the test specimens were sealed with strips of ceramic blanket (thickness 25mm).

The slabs were not protected by means of any insulation or suspended ceiling. To ensure that the specimens would not fail during testing, additional reinforcement (ϕ8 and ϕ6) was included(Fig.S.8).

About 35 temperature measuring points were provided per specimen, spread over 3 sections: I, II and III (Fig.S.8). The thermocouples in sections I and III were used to check the longitudinal symmetry of the thermal behaviour. The thermocouples in the mid span section II were used to check the transverse symmetry of the thermal behaviour. The thermocouples were positioned with care, a supporting frame being applied to ensure that the thermocouples would not change position during pouring of of the concrete. Nevertheless, small differences between these planned positions and actual positions were observed after manufacturing of the specimens. The actual positions were used in the numerical modelling in this thesis.

① wall of aerated concrete blocks in the centre of the fire compartment.

② concrete wall closing the fire compartment

③ concrete slabs on furnace walls

④ layer of 25 mm ceramic fibre banket at vertical concrete planes.

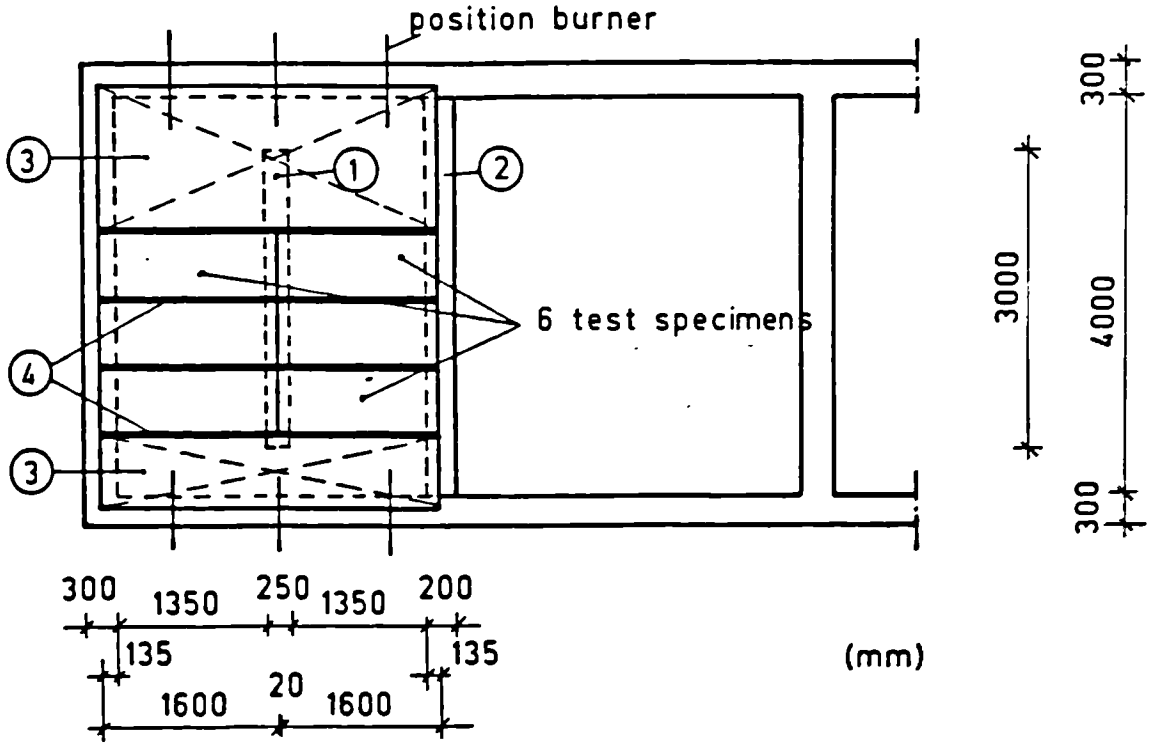

Fig.S.7 Schematic Review of the Harr's Test Arrangement [8.3]

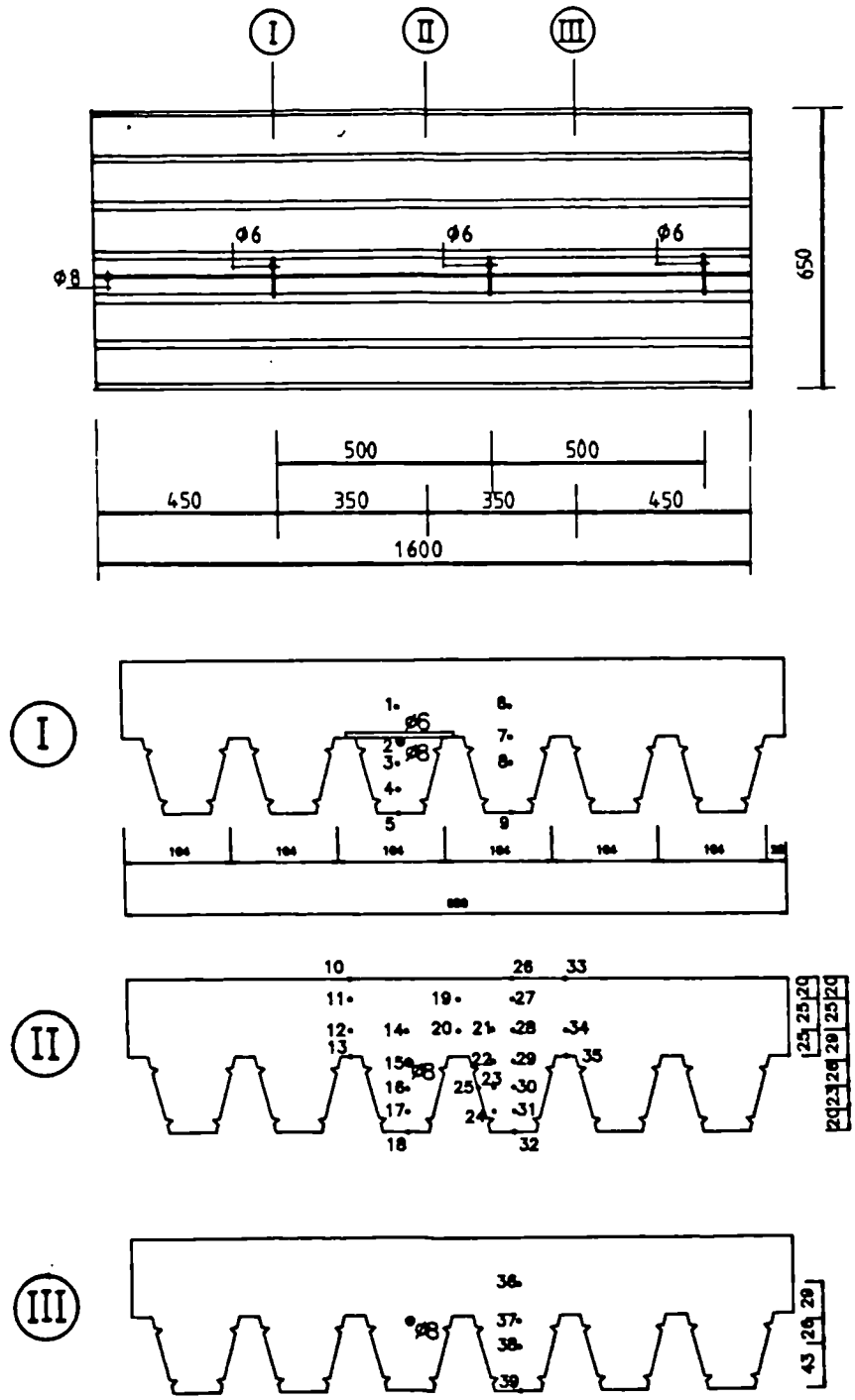

Fig.S.8 The Cross-Sections of Deck Slab and the Positions of Thermocouples (specimen 6: Prins PSV73/Hb=70mm) [8.4]